NORTHWESTERN UNIVERISTY

Innate-Like T Cells in Systemic Methicillin-Resistant *Staphylococcus aureus* Infection

A DISSERATION

SUBMITTED TO THE GRADUATE SCHOOL IN PARTIAL FULFILLMENT OF THE REQUIREMENTS

For the Degree of
DOCTOR OF PHILOSOPHY

Field of Microbiology/Immunology
Driskill Graduate Training Program in Life Sciences

BY
Samantha Genardi

EVANSTON, ILLINOIS
March 2021

Abstract

Staphylococcus aureus (SA) is a leading cause of healthcare-associated and community-acquired infection in the United States. Despite the canonical thinking that antibodies and B cells are the main drivers of protection against extracellular pathogens, T cells are now recognized as critical players in protection against SA in multiple routes of infection, as evidenced in humans and preclinical animal models. Patients with $CD4^+$ T cell HIV-mediated depletion or genetic deficiency in Th17 cell development have increased susceptibility to SA infections. In mouse models of SA infection, both $CD4^+$ T cells and $\gamma\delta$ T cells have been implicated in cytokine production and protection against SA, driven by IFN-γ and IL-17A. Additionally, $\gamma\delta$ T cell memory has been described in both humans and mice and played a protective role in a mouse model of SA skin infection.

Unconventional T cells, which are not restricted by major histocompatibility complex (MHC) class I or class II molecules, have emerged as critical players in the immune response to bacterial infections. Here I studied the roles of 2 types of unconventional T cells, natural killer T (NKT) cells and mucosal-associated invariant T (MAIT) cells, in the context of methicillin-resistant SA infection. These innate-like T cells can be activated very early during bacterial infection and secrete Th1 and Th17 cytokines. NKT cells are restricted by the MHC class I-like molecule CD1. CD1 molecules present lipid antigens to cognate T cells and have limited polymorphism relative to their MHC counterparts, making them attractive vaccine targets. MAIT cells are restricted by the MHC class Ib molecule MR1, which presents vitamin B metabolites to MAIT cells. Many bacteria, including SA, possess metabolic proteins that generate metabolites able to be recognized by MAIT cells, making MAIT cells an additional target for rational vaccine design.

To determine whether NKT cells or MAIT cells were necessary for controlling SA infection, I infected wild-type mice and mice deficient in NKT cells ($CD1d^{-/-}$) or MAIT cells ($MR1^{-/-}$) with SA. I showed that NKT cells, but not MAIT cells, were necessary for reducing bacterial burdens and controlling the amount of neutrophil influx to infected kidneys and livers early in the infection response. Using a mouse model that lacks type I NKT cells (iNKT cells) but retains type II NKT cells ($J\alpha18^{-/-}$), I further showed that type II NKT cells were sufficient to reduce bacterial burden and inflammatory infiltrate/abscess dissemination in infected kidneys in the absence of iNKT cells. Both iNKT cells and type II NKT cells required MyD88 mediated TLR activation on dendritic cells and CD1d-TCR engagement to be activated by total SA lipids and heat-killed SA (HKSA), which demonstrated that innate-mediated cytokines as well as TCR engagement were required for NKT cell activation and cytokine production to SA antigens. However, iNKT cells were dispensable for control of SA infection and became hyporesponsive to restimulation after SA infection.

Focusing on the role of type II NKT cells in SA infection, I identified a polar lipid fraction from SA containing PG and lysyl-PG species which induced CD1d-restricted MyD88-dependent IFN-γ production by type II NKT cells. Adoptively transferred type II NKT cells directly contributed to a reduction in bacterial burden in the spleen of SA-infected recipient mice. Turning to humans, SA bacteremic patients had reduced percentages of MAIT cells and iNKT cells and increased $CD4^{+}CD161^{+}$ T cells, a population enriched for type II NKT cells, in blood compared to healthy controls. Work recently published by our lab, using humanized mice expressing group 1 CD1 molecules (hCD1Tg), showed that CD1b- and CD1c-restricted T cells were expanded after SA infection and recognized PG lipids derived from SA. Together, these data demonstrate that in mice and humans, both CD1d-restricted type II NKT cells and group 1 CD1-restricted T cells are expanded and functionally active during SA bacteremia.

Acknowledgements

I want to convey my sincere thanks to my PI, Dr. Chyung-Ru Wang, for supporting me throughout the years and training me to be a thoughtful detail-oriented scientist. I would also like to thank my committee members, Drs. Alan Hauser, Pablo Penaloza-MacMaster, Bruce Bochner, and Deyu Fang, for providing guidance and scientific input at my committee meetings and beyond. I would also like to thank my collaborators at Northwestern Memorial Hospital, Drs. Yi-Hua Chen and Chao Qi, for facilitating collection of SA human blood samples and my collaborator at National Jewish Health, Dr. Evgeny Berdyshev, for isolating and purifying Staph lipids for our lab. Lastly, my heartfelt thanks go out to my lab members, past and present, for providing training, guidance, friendship, and comradery during my years in graduate school.

I also could not be where I am today without my parents and my partner Mike who have supported me throughout my scientific training. Additionally, the friendships I have made with other graduate students in the Driskill Graduate Program have been a constant source of levity and steadfastness which has made my time at Northwestern so enjoyable. I will forever be indebted to these individuals and others not mentioned here who supported me throughout my training.

Abbreviations

α-GalCer: α-galactosylceramide
APC: Antigen presenting cell
B6: C57BL/6
BCR: B cell receptor
BFA: Brefeldin A
BMDC: Bone marrow-derived dendritic cell
CD: Cluster of differentiation
CFU: Colony forming units
DAG: Diacylglycerol
DC: Dendritic cell
Dpi: Days post infection
ELISA: Enzyme-linked immunosorbent assay
ELISPOT: Enzyme-linked immunospot assay
FACS: Fluorescence activated cell sorting
Group 1 CD1: Human CD1a, CD1b, and CD1c
Group 2 CD1: Human CD1d and mouse CD1d1, CD1d2
hCD1Tg: Human CD1b and CD1c expressing transgenic mice
H&E: Hematoxylin and eosin
HKSA: Heat-killed *Staphylococcus aureus*
Hr(s): Hour(s)
IFN: Interferon
IL: Interleukin
iNKT: Invariant natural killer T
LN: Lymph node
Lysyl-PG: Lysyl-phosphatidylglycerol
KO: Knockout
MAb: Monoclonal antibody
MGDG: Monogalactosyldiacylglycerol
MFI: Mean fluorescence intensity
MHC: Major histocompatibility complex
Min: Minutes
mRNA: messenger RNA

NKT: Natural killer T

PAMPs: Pathogen associated molecular patterns

PBMC: Peripheral blood mononuclear cell

PBS: Phosphate buffered saline

PCR: polymerase chain reaction

PG: Phosphatidylglycerol

PMA: Phorbyl-12-myristate 13-acetate

PMN: Neutrophil

RT: Room temperature

RT-PCR: reverse-transcription polymerase chain reaction

SA: *Staphylococcus aureus* methicillin-resistant *Staphylococcus aureus*

SAlip: *Staphylococcus aureus* total lipid extract

TCR: T cell receptor

TET: Tetramer

Tg: Transgenic

TLR: Toll-like receptor

TNF: Tumor necrosis factor

Vβ: variable beta chain

WT: Wild-type

Table of Contents

List of Tables

List of Figures

Chapter 1

Introduction

1-1 Staphylococcus aureus

Staphylococcus aureus (SA) is a leading cause of healthcare-associated and community-acquired infection in the United States. SA causes a range of infections in humans, including skin and soft tissue infection, pneumonia, endocarditis, and bacteremia, which if left untreated, can lead to sepsis and high levels of mortality (1). In addition, SA strains with acquired resistance to methicillin and related β-lactam antibiotics make up 46% of all SA isolates tested nationally (2). Use of wide spectrum antibiotics , such as vancomycin, drive the emergence of more resistant strains such as vancomycin-intermediate and vancomycin-resistant SA (3). This escalation in antibiotic use is likely to continue as more resistant strains emerge, and thus there is a need for SA infection prevention. Traditionally, humoral immunity was thought to be the main driver of immune defense against extracellular pathogens such as SA. In recent years, T cells are now recognized as critical players in protection against SA in multiple routes of infection, as demonstrated in humans and preclinical animal models. Below I will discuss the immune response to SA infection and known mechanisms that SA employs to evade the host immune response.

1-1.1 Overview of SA pathogen

SA is a gram-positive coagulase-positive bacterium so named for its characteristic morphology of growth in gold grape-like clusters (4). SA is a common commensal bacterium, with approximately 30% of individuals in the United States colonized in the nasal passage and to lesser degrees on the skin and mucosal membranes (5). Commensal colonization with SA has been linked to passage of the bacterium from mother to infant within 1 month after birth (6). Nasal colonization with SA is a risk factor for the development of invasive infection, including SA surgical site infections and skin and soft tissue infections, in both the healthcare setting and

community setting (7). In addition, colonization with methicillin-resistant SA strains has been linked to increased complications and mortality relative to methicillin-sensitive SA strains in patients hospitalized in the ICU (8).

SA has evolved many mechanisms to evade the immune system, which presents complications when invasive colonization leads to active disease. SA has a number of cell wall associated and secreted factors that are able to inactivate, modulate, and evade immune cells. These include toxins, adhesins, immunomodulating proteins, proteases, and enzymes that target neutrophils, the main innate immune cell responsible for killing SA, as well as T cells and B cells (9). In addition to directly targeting immune cells, SA secretes factors that create a physical barrier to prevent immune cell infiltration. A characteristic outcome of SA infection is the formation of abscesses. SA secretes coagulase (Coa) and von Willebrand factor binding protein (vWbp) which activate prothrombin and cleave fibrinogen, leading to fibrin polymerization; this creates a pseudo capsule which surrounds replicating bacteria, protecting it from clearance (10). In the formation of abscesses, SA also secretes factors that directly kill infiltrating neutrophils and macrophages, leading to a ring of dead or dying cells surrounding the fibrin capsule that serve as a further deterrent for bacterial clearance (11). SA bloodstream infection can lead to sepsis, a life-threatening organ dysfunction caused by dysregulation of the host response (12). SA-driven sepsis is enhanced by secretion of clumping factor (ClfA), Coa, and vWbp, which generate fibrin deposits in the heart and lead to clotting (13). Additionally, hyperactivation of T cells by antigen-independent MHC class II crosslinking with SA-secreted superantigens leads to toxic shock syndrome, a more severe form of sepsis with increased mortality outcomes (14). Below I will review the ways in which the host immune system and this tricky pathogen compete with each other during an infection.

1-1.2 Overview of immunity against SA

1-1.2a Innate immune response to SA

Neutrophils are the first line of defense against invading SA that break the epithelial barrier (15). They are recruited to the site of infection by chemoattractants secreted by activated endothelial cells, which upregulate chemokine receptors on neutrophils; this, along with integrin expression, allows neutrophils to roll, arrest, and perform transendothelial migration from the blood into infected tissue (16). SA skin infection induces secretion of CXCL1, CXCL2, and CXCL8 by keratinocytes, which bind to CXCR2 on neutrophils, resulting in their recruitment (17). A number of factors secreted by SA act to block neutrophil activation and migration into infected tissue. These include cysteine proteases such as staphopain A (18), CHIPS (19), SA-secreted formyl peptide receptor-like-1 inhibitory protein (FLIPr) and FLIPr-like protein bind formyl peptide receptor-like-1 (FLRP1) (20, 21), and SA superantigens enterotoxin-like toxin X (SEIX) and superantigen-like 5 (SSL5) (22, 23).

Neutrophils that overcome SA inhibition to enter infected tissues act to kill SA by phagocytosis. Neutrophils bind to SA either via PAMPs or via immunoglobulins bound to PAMPs by complement, engulfing the bacteria by phagocytosis; the phagosome fuses with neutrophil granules carrying antimicrobial peptides and reactive oxygen species to kill ingested SA (15). Staphylococcal complement inhibitor (SCIN) (24), SA-derived protein A (SpA) (25-27), second binding protein of immunoglobulin (Sbi), and staphylococcal superantigen-like 7 (SSL7) (28, 29) act to inhibit complement and opsonization by neutrophils. Despite this, neutrophils can uptake SA in the absence of opsonization, showing the redundancy in mechanisms of neutrophil killing to overcome SA evasion strategies (30).

Once SA has been engulfed in neutrophil phagosomes, it has further mechanisms to evade oxidative and non-oxidative killing. SA can modify its cell membrane to increase electrostatic repulsion of neutrophil antimicrobial peptides (31, 32). Additionally, the *mprF* gene encoding lysyl-PG synthase confers resistance to cationic antimicrobial peptides by converting

negatively charged PG into lysyl-PG with the addition of positively charged L-lysine (33). SA secretion of staphylokinase and extracellular adherence proteins (Eap) inhibits neutrophil defensin, elastase, proteinase, and capthesin mediated non-oxidative killing of SA (34, 35). Oxidative killing by neutrophils is performed by reactive oxygen species (ROS) in the phagosome. SA secretes virulence factors that target multiple proteins in the ROS production pathway to reduce oxidative killing. These include SA superoxide dismutases SodM and SodA (36), Staphyloxanthine (37) methionine sulfoxide reductase proteins (38), and virulence factors under the SaeR/S two component system (39). Despite these evasion mechanisms, ROS mediated killing of SA is essential for host defense, as demonstrated in patients with chronic granulomatous disease, a genetic disorder that causes defects in NADPH oxidase; these patients have increased occurrences of SA infections (40). SA can also reside in large phagosomes, termed macropinosomes, and establish an infection in naïve mice after adoptive transfer of infected neutrophils (41). In a model of SA surgical wound infection, neutrophils containing intracellular SA were recruited to the wound via IFN-γ driven CXCL2 chemokines and led to increased bacterial burden at the wound site (42).

The final mechanism that neutrophils enact to kill SA is to undergo a terminal cell fate pathway called NETosis. This involves ROS-dependent extrusion of neutrophil extracellular traps (NETs) containing DNA coated with antimicrobial proteins (15). SA escapes NETs by secretion of the SaeR/S regulated factor nuclease (nuc) (43), which induces apoptosis of infiltrating macrophages in SA abscesses (44). Neutrophils that have successfully engulfed SA and undergo apoptosis are also inhibited from macrophage efferocytosis by SA upregulation of CD47, leading to inefficient clearance (45). It is clear from these studies that while neutrophils are key in the destruction of SA bacteria, SA has adapted many sophisticated mechanisms to circumvent this professional killer.

While neutrophils are the innate immune cell most associated with SA killing, another professional phagocyte, macrophages, are critical for control of SA infection. Ingested bacteria

are internalized into phagosomes, which fuse with lysosomes to become phagolysosomes, compartments containing antimicrobial peptides and low in pH, which is inhibitory to bacterial growth (46). SA has evolved to evade intracellular macrophage killing by selection pressure under low pH through upregulating the sensor kinase Gras (47). SA growth inside macrophages can also contribute to dissemination and evasion of neutrophil killing (48).

In addition to phagocytosing SA, macrophages and neutrophils express pathogen recognition receptors (PRRs) which play important roles in immune signaling during SA infection. Macrophages and neutrophils express TLR2 on their surface which recognize PAMPs on SA, including lipoproteins and lipotechoic acid (LTA) (49). Both TLR2 and MyD88 are critical for SA protection, as $TLR2^{-/-}$ and $MyD88^{-/-}$ mice have increased mortality after SA systemic infection (50). However, TLR2 is dispensable for SA skin infection control (51, 52). TLR2 activation leads to production of TNF-α and IL-6, which enhance neutrophil killing of SA (53). TLR2 heterodimerizes with TLR1 or TLR6 to induce downstream MyD88-dependent signaling; SA secretion of superantigen-like protein 3 (SSL3) inhibits TLR1/TLR6 heterodimerization to circumvent innate cell activation (54). In addition to TLR2, NOD2 is important for SA control; NOD2-deficient mice are more susceptible to SA systemic infection, with defects in neutrophil and macrophage phagocytosis (55). NOD2, which is expressed intracellularly in monocytes and macrophages, recognizes SA peptidoglycan in synergy with TLR2 (56). NOD2 recognition of SA α-hemolysin was critical for control of SA skin infection, enhancing SA clearance and neutrophil killing (57). In summary, neutrophils and macrophages play keys roles in immune defense against SA infection; however, SA has evolved many sophisticated mechanisms to circumvent killing by these innate immune cells.

1-1.2b B cell response to SA

Because SA is an extracellular pathogen, B cells were thought to be the primary immune cell contributing to SA protection. The primary function of B cells is to produce antibodies, which bind to bacterial antigens to neutralize and opsonize bacteria. In the case of SA infection, B cells are dispensable for control of infection. B cell genetic knockout mice (μMT) and wildtype mice had similar bacterial burdens following systemic infection with SA LS-1 strain (58). There is evidence to suggest that antibody titers in humans correlate with protection, but this evidence varies by infection site. A cohort of patients with invasive SA infections that developed anti-α-hemolysin antibodies had reduced recurrence of infection over a 12-month period relative to patients with cutaneous infections (59). Another study measuring antibody titers in SA bacteremic patients identified higher SA exotoxin antibody titers in patients that did not develop sepsis versus sepsis patients (60). A more recent study identified long-lived memory B cells reactive to conserved epitopes of SA toxins in patients who experienced SA skin and soft tissue infections. These control patients also had circulating B cells, suggesting that the healthy controls in their cohort may have been exposed to subclinical levels of SA (61).

As previously described, SA secretes virulence factors, including SpA and Sbi, that inhibit opsonization. SpA can also act as a B cell superantigen, binding to the $F(ab)_2$ region of the BCR in complex with soluble IgG to induce B cell deletion (62, 63). SA toxins can also act to generate pathogenic anti-toxin antibodies. In a model of SA cutaneous infection, mice receiving anti-Panton-Valentine leukocidin (anti-PVL) antibody treatment had increased bacterial burdens in skin following infection with PVL positive SA strains; anti-PVL inhibited neutrophil activation and antibacterial effects (64). Additionally, treatment of mice with antibodies specific for SA capsular polysaccharide and poly-N-acetyl glucosamine inhibited SA opsonization and increased bacterial burdens in SA skin and systemic infection due to binding of the two antibodies together via idiotype-anti-idiotype interaction, which prevented binding of the

antibodies to the bacterial surface (65). In summary, B cell antibody production can aide in clearance of SA infection. However, there is debate on how efficacious antibodies are at controlling SA infection, as B cells in mice are dispensable for control of some SA strains.

1-1.2c Prior vaccine designs targeting SA infections and their failures in the clinic

The majority of SA vaccines to date have focused on generating B cell antibody production against SA surface proteins and showed promise in pre-clinical animal models. In **Table 1**, I summarized a list of SA vaccines that have progressed up to phase III clinical trials and their current clinical status. Justification for generation of these vaccines and their clinical outcomes are summarized below.

Only two vaccine candidates, StaphVax and Merck V710, have progressed up to phase III clinical trials. StaphVax targeted the SA capsular polysaccharides CP5 and CP8. Preclinical animal studies demonstrated that passive immunization with purified IgG from animals immunized with a vaccine composed of CP5 and CP8 covalently linked to *Pseudomonas aeruginosa* exotoxin A protected immunized rats from SA induced endocarditis and immunized mice from SA sepsis induced mortality (66, 67). Initial efficacy testing with a prime plus boost of StaphVax in hemodialysis patients demonstrated an increase in anti-CP5 and CP8 antibody titers after vaccination (68). However, a phase III clinical trial of StaphVax in patients with end-stage renal disease showed no efficacy in preventing bacteremia in vaccinated vs. placebo patients despite generation of anti-CP antibody titers (69). Merck V710 targeted the surface protein iron surface determinant B (IsdB) of SA, an iron sequestering protein conserved across many SA strains. Pre-clinical studies demonstrated a protective effect of IsdB purified protein plus aluminum hydroxyphosphate sulfate adjuvant in vaccinated mice challenged with SA bacteremia; additionally, rhesus macaques vaccinated with IsdB generated IsdB-specific antibodies (70). However, when Merck V710 was given to cardiothoracic surgery patients in a phase III trial to test efficacy of the vaccine to prevent SA bacteremia and deep surgical wound

infection, the study was terminated early due to increased multiorgan failure and mortality in vaccinated patients vs. placebo who later developed SA infections, despite the generation of high anti-IsdB IgG titers in vaccinated individuals (71). A post-trial analysis identified that patients with low IL-2 and IL-17A serum levels preoperatively who received the vaccine were associated with higher mortality after postoperative SA infection, suggesting that T cells were critical in directing the long term protection to the IsdB vaccine (72).

Another SA vaccine, SA4Ag, targeted CP5 and CP8 plus two additional proteins, surface protein clumping factor A (ClfA) and lipoprotein manganese transporter protein C (MntC), the last of which is responsible for sequestering manganese (73). Mice immunized with a ClfA vaccine were protected from SA sepsis, with protection mediated by IL-17A producing $CD4^+$ T cells (74). Manganese is a cofactor for superoxide dismutase, which enhances SA survival in the phagolysosome by inactivating ROS (36). Despite the ability of SA4Ag to induce long-term antibody titers against CP5, CP8, and ClfA and target cellular immunity, vaccine development was suspended after a phase IIB study did not meet efficacy targets (75).

Vaccines currently in the developmental stage that have passed phase I clinical trials share targeting of SA secreted toxins. These include a multi-component vaccine, produced by the pharmaceutical company Integrated BioTherapeutics, targeting SA enterotoxins A, C1, and toxic shock syndrome toxin (TSST). A phase I clinical trial demonstrated safety in healthy patients given this vaccine (76). A second enterotoxin vaccine (STEBvax) targeting SA enterotoxin B (SEB) was safe and generated anti-SEB IgG neutralizing antibodies in vaccinated individuals (77). Lastly, a multi-component vaccine targeting SA α-toxin and PVL was safe and generated anti-rAT and anti-PVL neutralizing antibodies (78). In summary, SA vaccines to date have primarily targeted SA surface antigens or endotoxins and antibody titers and neutralization have been used as measures of efficacy. However, as has been demonstrated in vaccines that progressed up to phase III clinical trials, targeting B cell-mediated immunity alone has not been effective at inducing protective immunity against SA. In the following section, I will highlight the

role that T cells in SA infections, and how targeting cellular mediated immunity may be beneficial in future SA vaccine design.

Vaccine	Target	Phase	Infection type	Clinical outcome	citation
StaphVax	Capsular polysaccharide (CP) 5 & 8	III	Bacteremia	Augmented antibody titers, no protection after boost	(68, 69)
Merck V710	IsdB	IIB/III	Post-operative cardiothoracic surgery: bacteremia/deep sternal wound	IsdB specific antibodies; increased mortality	(71, 72)
SA4Ag	CP5, CP8, rmClfA, rrMntC	IIB	Spinal fusion surgery: bacteremia, SSI	Discontinued	(75)
N.A.	Enterotoxin A and C1, TSST	I	-	Safety completed	(76)
STEBvax	SEB	I	-	Safety, SEB IgG neutralizing antibodies	(77)
N.A.	rAT/r rLukS-PV	I	-	Safety, neutralizing antibodies	(78)

Table 1: SA vaccines in development or stopped due to low efficacy. Adapted from (79).

1-1.3 T cell response to SA infection

Despite the traditional thinking that humoral immunity is the main driver of immune defense against extracellular pathogens, T cells are now recognized as critical players in protection against SA in multiple routes of infection, as shown in humans and preclinical animal models. HIV patients with decreased $CD4^+$ T cell counts have increased susceptibility to SA bacteremia (80, 81), though whether this susceptibility is due to lack of $CD4^+$ T cells or lack of $CD4^+$ T cell help to B cell antibody production is unknown. Additionally, patients with hyper IgE syndrome who have a STAT3 mutation, resulting in an inability to develop Th17 cells, have increased susceptibility to SA skin and pulmonary infections (82). In mouse models of infection,

both $CD4^+$ T cells and γδ T cells produce cytokines and protect against SA, while a protective role for $CD8^+$ T cells has not been explored. Below I will summarize what is known about the $CD4^+$ T cell and γδ T cell response to SA, as well as discuss the role that other non-conventional T cells play in SA immunity.

1-1.3a $CD4^+$ T cells in SA infections

The earliest role for T cells in SA infection was demonstrated in 1988, with the characterization of SA superantigens enterotoxins A and B crosslinking MHC-II and the TCR to activate human $CD4^+$ T cell clones (83). Despite the ability of $CD4^+$ T cells to be activated by superantigens and cause pathogenic inflammation, they can also play protective roles in SA infection, which most groups have attributed to IFN-γ and/or IL-17A production, dependent upon the strain of SA and the infection site (84). In a murine model of SA nasal carriage, T cells and IL-17A-mediated neutrophil influx, but not B cells or γδ T cells, were required for clearance of SA (85). Additionally, mice vaccinated with a recombinant N-terminus of a *Candida* Alsp3 adhesin plus adjuvant were protected from SA bacteremia, which was mediated by IFN-γ and IL-17A producing $CD4^+$ T cells (86). IL-17A/IL-17F double knockout mice, but not IL-$17A^{-/-}$ or IL-$17F^{-/-}$ mice had increased mucocutaneous CFU following infection with SA strain 834, but displayed similar bacterial burdens to wild-type mice in the kidney after systemic infection (87).

While the majority of murine studies have focused on IL-17A production by $CD4^+$ T cells, there have been a number of studies implicating IFN-γ production by $CD4^+$ T cells as either beneficial or detrimental. $CD4^+$ memory T cells produced IFN-γ upon secondary peritonitis challenge, which enhanced recruitment of macrophages and clearance of SA (88). In contrast, mice vaccinated with irradiated SA had decreased survival upon bacteremic challenge, mediated by IFN-γ producing pathogenic $CD4^+$ T cells (89). In a model of SA surgical wound infection, IFN-γ producing $CD4^+$ T cells activated by CP8 were detrimental to clearance of SA,

by driving increased neutrophil influx and inflammation at the surgical wound site (42). In a model of SA pneumonia, $CD4^+$ T cells producing proinflammatory cytokines increased pathology and bacterial burden in the lung of SA challenged mice (90). These studies highlight the differential roles $CD4^+$ T cells can play in SA immunity.

Despite evidence that $CD4^+$ T cells can be beneficial to clearance of SA infection, SA secretes virulence factors which can kill or hyperactivate T cells. The extracellular SA toxins α-toxin and leukocidin LukDE can directly lyse T cells by binding ADAM10 and CCR5, respectively, on the T cell surface, leading to pore formation and lysis (91, 92). In addition to killing T cells, SA can hyperactivate T cells via secreted superantigens. Across strains, SA encodes 23 different superantigen genes, contained on pathogenicity islands or mobile genetic elements (84). Up to 80% of SA strains encode at least 1 superantigen gene, with the average being five or six per strain (93). Superantigens act by binding conserved structures on the MHC-II molecule and the TCR, leading to activation independent of antigen, with individual SA superantigens targeting different TCR Vβ chains. Up to 20% of the total T cell population can be activated in this manner, leading to hypersecretion of cytokines, termed cytokine storm, which can drive toxic shock syndrome, a life-threatening condition leading to organ failure and death if left untreated (93). Once a cytokine storm is induced, superantigen-activated T cells become hyporesponsive to antigenic stimulation, leading to an impaired B cell antibody response (84). However, studies demonstrating that T cells become anergic following SA superantigen activation were performed in mice without humanized MHC-II molecules, leaving the effect of superantigens on T cell anergy in the human setting in doubt (94). Despite the ability of SA superantigens to cause serious disease, the case burden of SA induced toxic shock syndrome is rare relative to the number of SA infections per year (95). Additionally, a link has been made between the ability of SA carriers to have better outcomes upon SA bacteremic infection and the generation of anti-toxin neutralizing antibodies in these patients (96). These data suggest that

superantigens can act to promote SA colonization and passive infection, leading to persistence and transmission.

SA can also direct the immune response away from protective Th1/Th17 polarization. SA peptidoglycan, found on the surface of the SA cell membrane, is recognized by monocytes and macrophages via TLR2; PBMC derived peptidoglycan-activated monocytes and macrophages were shown to polarize T cells to produce anti-inflammatory IL-10 (97). Additionally, SA phenol-soluble modulin (PSM) peptide toxin activated PBMC derived DCs to drive polarization of T regulatory cells (98). In summary, $CD4^+$ T cells protect against SA infection by polarizing to a Th1 and/or Th17 phenotype, however SA has found mechanisms to circumvent or misdirect T cell help.

1-1.3b $\gamma\delta$ T cells in SA infections

$\gamma\delta$ T cells have been well studied in SA infections, particularly in SA skin infection models. $\gamma\delta$ T cells producing IL-17A were required for control of SA bacterial burden and lesion size in a murine skin infection model (99). A more recent paper identified IL-17A producing $V\gamma4^+V\delta6^+$ $\gamma\delta$ T cells expanded in skin draining LNs and trafficked to the site of SA skin infection to control bacterial burden and neutrophil recruitment (100). Clonotypic memory $\gamma\delta$ T cells expanded in skin draining LN were also shown to protect mice after secondary SA skin infection, however this protection was mediated by IFN-γ and TNF-α production, not IL-17A production (101).

In addition to skin infection, $\gamma\delta$ T cells have been shown to contribute to SA control in other models of infection. IL-17A producing $\gamma\delta$ T cells provided protection in a model of SA surgical site infection, however protection was dependent on the ability of different SA strains to induce IL-1β production by APCs, which drove IL-17A production by $\gamma\delta$ T cells (102). In a model of SA peritonitis infection, memory $v\gamma4^+$ $\gamma\delta$ T cells contributed to enhanced IL-17A production

and bacterial burden reduction in the peritoneum following secondary challenge (103). In a murine SA pneumonia model, IL-17A producing γδ T cells were also required for bacterial burden reduction, however γδ T cell competent mice had increased lung pathology compared to γδ T cell deficient mice (104). In summary, γδ T cells show protection against multiple murine SA infection sites, and this protection is mainly mediated by IL-17A.

While there is no direct evidence for superantigen activation of γδ T cells, a few studies have demonstrated that γδ T cells proliferate in response to SA superantigen treatment. γδ T cells proliferated in rats treated with SEB and mice treated with SEA, however this proliferation was promoted by indirect activation of conventional T cells stimulated by SEA in the case of the murine model and the mechanism in the rat model was not addressed (105, 106). A study with human derived γδ T clones showed that these clones proliferated in response to SEA presented by B cells, however the binding of SEA to MHC-II and the Vγ chain has not been confirmed by crystal structure (107). In the case of SEA, mice challenged intranasally developed lung inflammation driven by IL-17A producing γδ T cells, demonstrating that superantigen-mediated γδ T cell activation can be detrimental to the host (106).

1-1.3c CD1-restricted T cells in SA infections

The role of CD1-restricted T cells has not been well studied in SA infection. CD1 molecules can be divided into 2 groups, group 1 CD1 and group 2 CD1, based on lipid antigen reactivity and expression pattern. Group 1 CD1 is composed of 3 isoforms, CD1a, CD1b, and CD1c, while group 2 CD1 contains CD1d. Group 1 CD1 is found in humans and higher mammals, while group 2 CD1d is present in all mammals, including mice. NKT cells are restricted by CD1d and can be divided into 2 types: type I or invariant NKT (iNKT) cells utilize an Invariant TCRα chain paired with limited Vβ chains while type II NKT cells utilize diverse Vα/Vβ chains (108). Pretreating mice with the self-lipid sulfatide stimulated type II NKT cells and

protected mice from SA induced sepsis in a CD1d-restricted manner (109). Additionally, iNKT cells that express a conserved Vβ8 chain were activated by SA SEB, independent of CD1d and dependent on MHC-II (110). Depletion of iNKT cells in HLA-DR4-Tg humanized mice treated with SEB substantially reduced SEB-driven toxic shock syndrome, indicating that activation of iNKT cells by SEB was detrimental to host outcomes (111). Another murine study demonstrated that LN NK1.1$^-$ iNKT cells produced IL-17A in response to heat-killed SA stimulation *ex vivo* and *in vivo* (112). As will be discussed in the results section, our studies showed a beneficial role for NKT cells in protection against the USA300 strain of SA, the dominant methicillin-resistant community acquired SA strain in the United States (113). Importantly, the USA300 strain does not encode the SEB superantigen, which may explain the discrepancy between our studies and the above mentioned studies (113).

While CD1d-restricted NKT cells are found in mice and humans, group 1 CD1-restricted T cells are only found in humans and primates (108), making their study in the context of SA infection limited. One study generated SA specific human CD1b-restricted T cell clones by stimulating T cells with CD1b-dextramers loaded with SA lipid extract and enriching over multiple sort rounds. These CD1b-restricted T cell clones produced either autoreactive or CD1b-restricted IFN-γ after stimulation with CD1b transfected K562 cells loaded with SA total lipid extract and specifically recognized SA-derived PG loaded dextramers (114). Recent work by our lab, using a humanized group 1 CD1 transgenic mouse (hCD1Tg), demonstrated that group 1 CD1-restricted T cells recognized cardiolipin and PG lipid species derived from the SA cell membrane. Group 1 CD1-rectricted T cell clones, generated by pulsing hCD1Tg infected mouse splenocytes with SA derived lipids, produced a host of cytokines, including IL-17A, TNF-α, granzyme B, and IFN-γ. These group 1 CD1-restricted T cell clones controlled SA in infected DCs *in vitro* and in SA challenged mice *in vivo* by adoptive transfer (115). In summary, group 1

CD1-restricted T cells recognized SA lipid antigens and protected mice from SA systemic infection in a humanized mouse model.

1-1.3d Evidence for T cell protection against SA in humans

In addition to murine studies, there is evidence for T cell protection against SA infection in humans. As previously mentioned, patients with genetic deficiencies in the development of Th17 cells or patients depleted of $CD4^+$ T cells by HIV infection have increased susceptibility to developing SA infections (80, 82, 81). Additionally, SA colonized individuals develop antigen-specific high affinity class switched antibodies, which require T cell help (96, 116). T cells isolated from healthy donor PBMC were reactive to heat-killed SA and SA secreted extracellular proteins. T cell clones derived from these patients displayed a memory phenotype and produced a host of cytokines upon stimulation with SA antigens (117). The diverse number of SA strains capably of colonizing humans without resulting in clinical disease may explain the discrepancy of high numbers of memory SA antigen-specific T cells in otherwise healthy donors. IFN-γ producing memory $CD4^+$ T cells recognizing heat-killed SA and ClfA were also identified in patients with active SA blood stream infections (88). However, the only SA vaccine in clinical trials targeting the T cell response (SA4Ag targeting ClfA) as well as B cell response was recently discontinued due to lack of protective efficacy (75), suggesting that additional parameters of protection are needed to develop more effective vaccines.

1-2 NKT cells

1-2.1 Overview of NKT cells

NKT cells are innate resident T lymphocytes that are activated early in response to infection, and rapidly secrete a wide range of cytokines, depending on the nature of the stimuli (118). Unlike conventional T cells, which recognize peptides presented by MHC molecules, NKT cells recognize a wide range of both self and foreign lipid antigens presented by the MHC class-

I-like molecule CD1d (119). NKT cells can be divided into two groups, invariant NKT (iNKT) cells and type II NKT cells, based on TCR usage and lipid antigen recognition (119). Below I will discuss the development, subtypes and contribution of NKT cells towards SA and other infectious pathogens.

1-2.1a NKT cell development and subsets

NKT were only discovered approximately 30 years ago. Observational studies of T cells in the thymus identified a unique population of TCRβ^+ cells that was $CD4^-CD8^-$ and utilized the Vβ8 TCR (120). These cells also expressed the NK cell marker NK1.1 and produced IFN-γ, IL-4, and TNF-α after stimulation with anti-CD3 (121-123). Simultaneous studies identified a T cell population in the thymus and spleen utilizing Vβ2, Vβ7, and Vβ8 paired with a restricted Vα14-Jα281 rearrangement in mice and Vα24-Jα281 rearrangement in humans; these T cells required a self-ligand and a nonpolymorphic MHC class Ib molecule presented on hematopoietic cells for development in the mouse thymus (124, 125). V$\alpha14^+$ T cells required a MHC-I molecule on bone marrow derived hematopoietic cells for positive selection but did not require TAP1, suggesting that these cells were selected by a non-peptide self-antigen (126). Using a derived T cell hybridoma with Vα14-J$\alpha281^+$V$\beta8^+$ expression (DN32.D3), these T cells were determined to be restricted by the MHC class-I like molecule CD1.1 (127). CD1.1 is expressed on the surface of DCs, macrophages, and B cells and is one of two isoforms expressed in mice, which are homologs of human CD1d (128). CD1.1 will hence forth be referred to as CD1d. These compiled works identified a new class of T cells termed NKT cells that did not respond to peptide antigens.

A seminal study identified glycolipid antigens as ligands for V$\alpha14^+$ T cells, by this time termed iNKT cells, due their restricted TCR usage and NK cell characteristics (129). This study identified α-galactosylceramide (α-GalCer) and α-glucosylceramide (α-GlcCer), which share

common structural motif of an α-anomeric confirmation of a sugar moiety, as lipid antigens recognized by iNKT cells via CD1d presentation. Two independent groups developed CD1d tetramers loaded with α-GalCer to track iNKT cells *in vivo* and found iNKT cells to be most enriched in the mouse liver (20-30%), with smaller percentages found in the spleen (1%), gut (1%), thymus (0.7%), bone marrow (0.4%), and LN (0.4%) (130, 131). Additionally, α-GalCer loaded human CD1d tetramers identified iNKT cells in human PBMC (130). For both of these studies, it was discovered that α-GalCer CD1d tetramer positive iNKT cells contained both $NK1.1^+$ and $NK1.1^-$ populations, the latter of which were previously excluded due to the original identification of NKT cells by FACS staining using $NK1.1^+TCR\beta^+$ markers.

iNKT cells diverge from conventional T cell development at the $CD4^+CD8^+$ double positive (DP) stage (132). CD1d expressing a self-lipid on cortical DP thymocytes selects for iNKT cells at this stage and requires signaling through the Src kinase Fyn and SLAM-associated protein SAP (133). Co-stimulation of DP cells through the TCR and SLAM receptors upregulates Egr2 in iNKT precursors, which is essential for the upregulation of PLZF (134). Initial studies of α-GalCer CD1d $tetramer^+$ iNKT cell development in the mouse thymus identified a population of $CD24^{lo}D44^{lo}NK1.1^-$ (stage 0) precursor cells downstream of DP thymocytes which followed a developmental sequence to $CD44^{hi}NK1.1^-$ and finally $CD44^{hi}NK1.1^+$ terminally differentiated iNKT cells (135). iNKT cells from these three developmental stages had differential cytokine production to α-GalCer stimulation, with high IL-4 production in $CD44^{lo}NK1.1^-$ iNKT cells and high IFN-γ production in $CD44^{hi}NK1.1^+$ iNKT cells. While the majority of iNKT cells in the periphery were $CD44^{hi}NK1.1^+$, $CD44^{hi}NK1.1^+$ iNKT cells were also found in the thymus, and $NK1.1^-$ populations were exported to the periphery, which contradicted the initial conclusions in the field that the $NK1.1^-$ population in the thymus gives rise to the $NK1.1^+$ population in the periphery (136).

Because iNKT cell development, but not conventional T cell development, was perturbed in PLZF$^{-/-}$ mice, PLZF was identified as a key regulator of iNKT development (137). Following work showing that conventional CD4^{+} T cells can be divided into Th1, Th2, and Th17 cells subsets based on differential transcription factor expression of T-bet, GATA-3, and RORγt (138), Hogquist and colleagues demonstrated that iNKT cells can be divided into 3 distinct groups, NKT1, NKT2, and NKT17, based on differential expression of these transcription factors plus PLZF (139). Based on these studies, NKT cell subsets are defined as NKT1 (PLZF^{lo}T-bet^{+}), NKT2 (PLZF^{hi}GATA-3^{hi}), and NKT17 cells (PLZF^{int}RORγt^{+}). Moreover, it was identified that NKT1 cells predominantly express NK1.1, while NKT2 and NKT17 cells are NK1.1^{-}. Different strains of mice are predisposed to development of NKT1 cells (C57B/L6) or NKT2/NKT17 cells (BALB/c) in the periphery. The 3 NKT cell subtypes also produced different cytokines in response to α-GalCer stimulation: NKT1 produced IFN-γ, NKT2 produced IL-4, and NKT17 produced IL-17A. In addition to this seminal study, recent work has identified PLZF^{-}E4BP4^{+} NKT10 cells producing IL-2 and IL-10 in adipose tissue (140) and IL-21 producing Bcl-6^{+} NKT follicular helper (NKT_{FH}) cells in spleen germinal centers (141). Single cell RNAseq of NKT1, NKT2, NKT17, and a precursor population NKT0 from mouse thymus identified heterogeneity in gene expression within each subset population but failed to identify additional subsets of NKT cells such as NKT10 and NKT_{FH} cells, suggesting that these populations may arise in the periphery (142). These data demonstrated that iNKT cells follow a lineage diversification model rather than a sequential lineage development model, however the factors driving NKT cells into different subset development in the thymus are unknown.

While iNKT cells have received a majority of the attention due to availability of the α-GalCer CD1d tetramer, type II NKT cells represent a second subset of NKT cells that have been much less studied. Observations in MHC-II$^{-/-}$ mice identified a significant population of CD4^{+} T cells that were not MHC-II restricted (143). CD4^{+} T cell hybridomas derived from MHC-II$^{-/-}$ mice

were reactivate to CD1d and expressed diverse Vα and Vβ chains. Using transgenic mice (24αβ Tg) derived from one of these hybridomas, a CD1d autoreactive T cell clone utilizing Vα3.2 and Vβ9 TCR rearrangement (VIII24), it was shown that these CD1d-restricted T cells displayed a similar phenotype to iNKT cells (144). The majority of 24αβ Tg T cells were NK1.1^{+}CD122^{+} and displayed an effector memory phenotype (CD44^{hi}CD62L^{lo}). They also produced IL-4 and IFN-γ upon TCR stimulation and required CD1d for development. Together these results classified a new subset of NKT cells, termed type II or variant NKT cells, that do not express the invariant Vα14-Jα18 rearrangement utilized by iNKT cells.

iNKT cells were demonstrated to constitutively express IL-4 mRNA, measured by GFP^{+} expression, in IL-4 gene knockin bicistronic reporter mice (4get) (145). Utilizing 4get mice lacking iNKT cells, our lab demonstrated that the majority of 4get polyclonal type II NKT cells were NK1.1^{+}CD122^{+}CD44^{hi}CD62L^{lo} expressing cells, similar to 24αβ T cells (146). Polyclonal type II NKT cells also utilized diverse Vα/Vβ chains, similar to what was demonstrated with NKT hybridomas, with the majority utilizing Vβ8.1/8.2 TCRs in the mouse. Similar to iNKT cells, type II NKT cells expressed high levels of PLZF in the thymus and required PLZF and SAP for development. It is unclear at this time whether type II NKT cells have a similar development pathway to iNKT cells and whether subsets of type II NKT cells with similar characteristics to iNKT1, iNKT2, and iNKT17 cells, are present in mice and humans. However, given the similar surface expression profile of these two groups and developmental requirement for SAP and PLZF, it is likely that type II NKT cells develop from DP thymocytes, like iNKT cells, and have a similar development pathway to iNKT cells in the thymus.

1-2.1b Lipid antigen loading and presentation by CD1

Unlike MHC molecules, CD1 molecules are non-polymorphic and have deeper antigen-binding grooves that can present a variety of hydrophobic lipid antigens (147). CD1 molecules

are composed of non-covalently linked heterodimers, formed from isotype specific heavy chains, linked to β2-microglobulin, and undergo assembly and loading of self-lipids in the endoplasmic reticulum. After assembly, Group 1 CD1 (CD1a, b, and c) and group 2 CD1d traffic to the surface of the cell, where they present lipid antigens (148), while group 1 CD1e is expressed intracellularly and helps with processing of lipid antigens loaded onto CD1b (149). In the majority of cases, lipid antigen uptake by CD1 molecules from sources outside the cell require recycling of CD1 into endosomal compartments, where lipid loading occurs, before trafficking back to the cell surface. Differences in the size of the lipid antigen binding groove and endosomal trafficking patterns within the cell allow for different CD1 isoforms to present a wide variety of lipids. CD1a has the smallest binding groove of the CD1 molecules and recycles through early endosomes, CD1b has the largest binding groove and recycles through late endosomes, and CD1c has an intermediate binding groove and traffics through early and late endosomes (147). CD1d, which presents lipid antigens to NKT cells, also has an intermediate binding groove and recycles through early and late endosomes. In the following section, I will focus on the types of lipid antigens loaded onto CD1d, how loading occurs, and the cell types involved in lipid antigen presentation.

Once CD1d is assembled in the endoplasmic reticulum, it initially binds to polar and non-polar self-lipids, including sphingomyelins and phospholipids, to stabilize the CD1 complex (150-152). CD1d then shuttles to the cell surface and is internalized into early and late endosomal compartments regulated by expression of tyrosine sorting motifs bound to AP-2, where it samples both self and foreign lipid antigens, before trafficking back to the cell surface (153). In mice, CD1d associates with AP-3, allowing CD1d to traffic to late endosomes and lysosomes (154). Lipids can be taken up from the periphery through endocytosis, pinocytosis, or phagocytosis of lipids bound to scavenger proteins like low-density lipoprotein where they can be loaded onto CD1d in endosomes (155). Alternatively, lipid transfer proteins such as saposins can facilitate loading of foreign lipid antigens onto CD1d (156). However, since most of studies

identifying lipid antigens recognized by NKT cells have used NKT cell hybridomas and purified lipids, the mechanisms governing the breakdown and loading of microbial lipid antigens onto CD1d remain elusive.

CD1d is constitutively expressed by many hematopoietic and non-hematopoietic cells, including thymocytes, B cells, T cells, macrophages, dendritic cells, and epithelial cells (148). The CD1d binding groove contains 2 pockets, an A' and an F' pocket, which can bind lipids up to C42 in length (153). In the classical model of CD1d lipid antigen presentation, the alkyl chains of the lipid are inserted into the CD1d binding cleft, while the head group is exposed for recognition by the TCR of the NKT cell (157). While the head group is necessary for lipid antigen recognition, alterations in alkyl chain length and saturation affect lipid loading onto CD1d and subsequent NKT cell TCR recognition (158). Multiple self and foreign lipid antigens have been identified that can bind to CD1d and be recognized by NKT cells. Below we will describe these lipids and their role in the context of an infection setting.

1-2.1c NKT cell activation kinetics and effector function

Both iNKT cells and type II NKT cells are considered innate-like T cells, due to their ability to rapidly produce cytokines after activation and exert effector function prior to conventional T cell activation. iNKT cells can be activated by self and microbial products through two mechanisms (159). The first is direct lipid antigen presentation on CD1d to the TCR of iNKT cells along with CD40-CD40L co-stimulation with APCs. In addition to α-GalCer, iNKT cells recognized glycosphingolipids from *Sphingomonas* species (160) and glycoglycerol lipids from *Streptococcus pneumoniae* and *Borrelia burgdorferi (161)* presented by CD1d. iNKT cells also recognized CD1d presented phosphatidylinositol mannoside from *Mycobacterium tuberculosis* (162), a cholesterol ester with an α-linked glucoside from *Helicobacter pylori* (163),

α-GalCer derived from *Bacteroides fragilis* (164), and lipophosphoglycan from *Leishmania donovani* (165).

The second mechanism of iNKT cell activation occurs through cytokine driven signals with or without self-lipid antigen presented by CD1d. iNKT cells constitutively express receptors for IL-12 and IL-18 cytokines; stimulation of iNKT cells with these cytokines upregulated IFN-γ production by iNKT cells (166, 167). DC derived IL-12, driven by TLR activation, along with CD1d presentation of self-lipids was demonstrated to activate iNKT cells in models of *Aspergillus fumigatus* infection and *Salmonella enterica* Serovar Typhimurium (*S.* Typhimurium) infection (168, 169). TLR9 stimulating CpG oligodeoxynucleotide also induced CD1d-restricted IL-12-dependent IFN-γ production by iNKT cells (170). In some cases, foreign lipids antigen alone is too weak to stimulation iNKT cells. Phosphoinositol derived from *Entamoeba histolytica* required both IL-12 and CD1d-presentation to activate iNKT cells (171). In contrast, *E. coli* derived LPS stimulated iNKT cells to produce IFN-γ by IL-12 and IL-18 signaling alone independent of CD1d presentation of self-lipid (172). These studies suggest a conserved model of TLR recognition by DCs leading to activation of iNKT cells in microorganisms either lacking cognate lipid antigens or containing weak lipid antigens recognized by iNKT cells. It has also been demonstrated that cytokine driven signals rather than antigen-specific signals dominate to activate iNKT cells in various infection models (173).

Similar to iNKT cells, type II NKT cells can be activated by self-lipid antigens presented by CD1d. Sulfatide, a self-lipid antigen derived from myelin, was the first lipid antigen demonstrated to be recognized by type II NKT cells *in vivo* using sulfatide loaded CD1d tetramers (174). The type II NKT hybridoma XV19 ($V\alpha1^+V\beta16^+$), derived from $CD4^+$ T cells from $MHCII^{-/-}$ mice (143), recognized multiple isoforms of sulfatide presented by CD1d (175). Mouse sulfatide CD1d $tetramer^+$ T cells utilized diverse Vα/Vβ chains, demonstrating the polyclonal nature of type II NKT cells (176). Type II NKT cells also recognized CD1d loaded β-

glucosylceramides and glucosylsphingosine, sphingolipids that accumulate in Gaucher's disease (177), as well as lysophosphatidylcholine, a self-lipid which is upregulated in inflammatory conditions (178).

Like iNKT cells, type II NKT cells can recognize foreign lipid antigens presented by CD1d. Type II NKT cell hybridomas recognized phosphatidylglycerol, cardiolipin, and phosphatidylinositol from *Corynebacterium glutamicum* and *Mycobacterium tuberculosis* (179), as well as phosphatidylglycerol from *Listeria monocytogenes* (180). It is unclear whether type II NKT cells can be activated by cytokine driven signals in the absence of cognate lipid antigens, similar to iNKT cells. CpG induced partially CD1d-restricted IFN-γ production by hepatic Vα3.2$^+$Vβ9$^+$ type II NKT cells from transgenic mice (24$\alpha\beta$ Tg) (146). A recent study showed that sorted type II NKT cells from spleens of 24$\alpha\beta$ Tg mice stimulated with TLR agonists in the presence of DCs produced IFN-γ independent of CD1d-TCR receptor signaling and dependent on IL-12, with variable dependence on IL-15 and IL-18 (181). The discrepancy in these two studies could be due to the source of type II NKT cells (liver vs. spleen) or different requirements of various TLR agonists for TCR mediated signaling.

The iNKT cell agonist α-GalCer and its synthetic glycolipid PBS57 have been used to determine the downstream effects of iNKT cell activation. Stimulation of iNKT cells with α-GalCer presented by CD8α^+ DCs caused upregulation of activation markers, including CD69, CD25, and ICOS (182), as well as rapid production of large amounts of IL-4 and IFN-γ, due to constitutive cytokine mRNA expression which upon activation can be quickly made into protein (145). Activated iNKT cells cross-talk with other cell types, causing differentiation of DCs and macrophages, neutrophil modulation, induction of IFN-γ by NK cells, B cell help, and modulating CD4 and CD8 conventional T cell responses (159). iNKT cells also downregulate TCR and NK1.1 and undergo proliferation in spleen and liver (183). This expansion and cytokine production is short-lived, lasting 2-3 days, followed by upregulation of PD-1, apoptosis, and

contraction to homeostatic levels (184). α-GalCer treated iNKT cells also exhibit a hyporesponsive phenotype after secondary treatment, with reduced activation, blunted cytokine production (skewed towards loss of IFN-γ production, not IL-4), and inability to trans activate NK cells and DCs (185, 184). This hyporesponsive phenotype lasted for at least 1 month and could be overcome by administering α-GalCer loaded DCs or treatment with IL-2 (185). Mice infected with *Listeria monocytogenes* and *Mycobacterium bovis* also displayed a hyporesponsive phenotype to restimulation with α-GalCer *ex vivo* (186, 187). Additionally, iNKT cells from mice injected with heat-killed SA, *Escherichia coli*, or *S.* Typhimurium had a reduced capacity to produce cytokines to α-GalCer *ex vivo* stimulation, even up to 3 weeks post injection of heat killed-bacteria (188). iNKT cell activation can also lead to detrimental immune pathology in atherosclerosis and alcoholic liver disease (189, 190). Therefore, induction of a hyporesponsive phenotype in iNKT cells may be a protective mechanism induced by the host to reduce overactivation of expanded iNKT cells to prevent overt inflammation and pathology.

Due to the lack of unique tetramer or marker for type II NKT cells, their function and cytokine producing capacity after activation is not well studied. Polyclonal IL-4 mRNA expressing type II NKT cells produced IFN-γ, IL-4, IL-13, and GM-CSF after anti-CD3 stimulation and had an IL-4/ GM-CSF skewed response to CD1d overexpressing DCs (146). In contrast, monoclonal $V\alpha3.2^{+}V\beta9^{+}$ type II NKT cells from 24αβ Tg mice produced a cytokine profile skewed towards IFN-γ rather than IL-4 production after PMA/Ionomycin stimulation (191). These studies suggest some heterogeneity in cytokine response of type II NKT cells.

Information on the functional consequences of type II NKT cell activation has mainly been gleaned from studies of inflammatory conditions and infections using 24αβ Tg mice. Adoptively transferred 24αβ Tg T cells prevented type 1 diabetes onset in NOD mice by upregulation of ICOS and PD-1/PDL-1 signaling (192). Activation of type II NKT cells with sulfatide also protected mice from alcoholic liver disease (193) and hepatic ischemic reperfusion

injury (194) through inhibition of proinflammatory cytokine production by pathogenic iNKT cells. However, overexpression of CD1d in 24αβ Tg mice led to spontaneous development of colitis in these mice and production of IL-17A and IFN-γ by dysregulated 24αβ Tg T cells (195). These results demonstrated that type II NKT cells can have a regulatory or pathogenic role during autoimmune and inflammatory conditions dependent on the cytokines they produce.

1-2.2 NKT cell contribution to infection

Both iNKT cells and type II NKT cells have been demonstrated to protect mice from various pathogen infections (159, 196). iNKT cells and type II NKT cells can act independently or synergistically to contribute to infection control. As has been mentioned previously, iNKT cells and type II NKT cells recognize lipid antigens from diverse microbial sources, but presence of cognate lipid antigens is not required for NKT cells to become activated and perform effector functions during an infection. Below I will discuss the contribution of iNKT cells and type II NKT cells to various infections.

1-2.2a NKT cell contribution to bacterial and fungal infections

Many studies have used Jα18$^{-/-}$ mice (lacking iNKT cells) and CD1d$^{-/-}$ mice (lacking both iNKT cells and type II NKT cells) to assess the contribution of iNKT cells and type II NKT cells in infection control. Particular focus has been given to pneumonia and systemic infection models due to the enrichment of NKT cells in lung and liver. CD1d$^{-/-}$ mice had increased bacterial burden (CFU) following intravenous and oral infection of *Listeria monocytogenes*, however increased CFU was only detected at 2 dpi and returned to wild-type levels by 6 dpi (197). This reduction in CFU in wild-type mice was associated with an increase in IFN-γ production in liver and spleen and IL-12 production in liver of wild-type but not CD1d$^{-/-}$ mice. In an intragastric model of *Listeria monocytogenes* infection, Jα18$^{-/-}$ mice had decreased survival compared to

wild-type mice (198). Adoptive transfer of iNKT cells from Vα14 Tg mice protected mice from infection, which was mediated by IFN-γ production. iNKT cells were increased in the liver and spleen of mice infected intravenously with *Mycobacterium bovis* (199). Jα18$^{-/-}$ mice had no difference in CFU compared to wild-type mice after infection, however Jα18$^{-/-}$ mice had increased granuloma size and number driven by TNF-α production, suggesting that iNKT cells limit inflammation and granuloma growth during *Mycobacterium bovis* infection. iNKT cells were activated (upregulated CD69 and CD25) and produced IFN-γ after *Borrelia burgdorferi* infection (200). Jα18$^{-/-}$ mice also had increased joint (200) and cardiac inflammation and increased heart CFU after infection with *Borrelia burgdorferi* (201). iNKT cells produced IFN-γ to enhance the effector function of macrophages, which controlled inflammation and limited *Borrelia burgdorferi* CFU in the heart. Combined, these studies suggest that iNKT cells provide protection in many systemic infections.

In addition to systemic infection, iNKT cells have been studied in pneumonia infection. iNKT cells showed MCP-1 dependent expansion and recruitment during yeast *Cryptococcus neoformans* lung infection and were required for control of fungal growth (202). iNKT cells were activated and secreted IFN-γ in response *Aspergillus fumigatus* pulmonary infection and were required for early CFU and inflammation control (169). Jα18$^{-/-}$ mice had decreased survival and increased lung CFU after intratracheal *Streptococcus pneumonia* infection (203); protection was mediated by recruitment of lung iNKT cells from the vasculature to the interstitium via CCL17 (204) and mediated by iNKT cell production of IFN-γ (205). CD1d$^{-/-}$ mice also had reduced clearance of *Pseudomonas aeruginosa* from lungs; administration of α-GalCer improved bacterial clearance, mediated by IFN-γ (206). These studies demonstrated that iNKT cells protected mice from lung infection.

While the majority of studies have demonstrated a protective role for iNKT cells in infection, two studies demonstrated a pathogenic role for iNKT cells during infection. CD1d$^{-/-}$

mice had increased survival and decreased CFU and inflammation following pulmonary *Francisella tularensis* infection, which correlated with iNKT cell production of IFN-γ (207). Similarly, a second study determined that iNKT cells could be divided into NK1.1^{+} iNKT cells, which were depleted, and NK1.1^{-} iNKT cells, which were expanded and produced IFN-γ, following intravenous *Listeria monocytogenes* infection (208). However, in this model Jα18$^{-/-}$ mice had reduced CFU compared to wild-type mice, suggesting that iNKT cells are pathogenic during *Listeria monocytogenes* infection.

Like iNKT cells, several cognate lipid antigens from bacterial species have been identified that are recognized by type II NKT cells. However, the direct contribution of type II NKT cells to bacterial and fungal infection is very limited. In a mouse model of SA sepsis, administration of sulfatide, the self-lipid antigen recognized by a subset of type II NKT cells, protected mice from lethal SA systemic challenge (109). Further study is needed to determine the role of type II NKT cells *in vivo* in other bacterial and fungal infections.

1-2.2b NKT cell contribution to viral and parasitic infections

iNKT cells protect against a number of viral and parasitic infections. iNKT cells were depleted in livers of patients with chronic hepatitis C virus (HCV) infection and HCV cirrhosis (209), as well as in PBMC of PCR seropositive HCV patients versus PCR seronegative HCV patients and healthy controls (210), which suggested that iNKT cells played a role in HCV immunity. Adoptive transfer of human PBMC plus IFN-α treatment lowered viral RNA in HCV infected humanized hepatic chimeric mice (211). Protection was mediated by human iNKT cells producing IFN-γ, as depletion of either iNKT cells or administration of IFN-γ blocking antibody abolished reduction in viral RNA. iNKT cells were also decreased in PBMC of chronic hepatitis B virus (HBV) patients compared to inactive HBV carriers and healthy controls; antiviral therapy restored iNKT cell levels in chronic HBV patient PBMC (212). Using 4get and 4get Jα18$^{-/-}$ mice

to track iNKT cells and type II NKT cells, both iNKT cells and type II NKT cells were activated, noted by the upregulation of CD25 and CD69, produced IFN-γ after HBV infection, and were required for activation of other liver mononuclear cells, NK cells, T cells, and B cells, and reduction of HBV viral DNA (213). Hepatocytes presented endogenous lysophosphatidylethanolamine (lysoPE) lipid antigens that were altered after HBV infection on CD1d to type II NKT cells. Activated type II NKT cells in turn induced IL-12 production by APCs to activate iNKT cells. This study demonstrated that both iNKT cells and type II NKT cells acted synergistically to control HBV infection.

A number of studies have explored the protective effect of iNKT cells in influenza infection. Adoptive transfer of iNKT cells reduced mortality and viral titer in Jα18$^{-/-}$, but not CD1d$^{-/-}$ mice, after intranasal influenza A virus (IAV) H1N1 infection, by reducing myeloid-derived suppressor cell (MDSC) expansion and suppressive function (214). Using a higher dose of H1N1, another study demonstrated that increased mortality in Jα18$^{-/-}$ mice was due to increased inflammation by infiltrating MCP-1^{+} monocytes (215). iNKT cells directly targeted and lysed IAV infected MCP-1^{+} monocytes, contributing to lower lung pathology. iNKT cells also expanded and upregulated CD69 in the lungs in response to IAV H3N2 infection (216). Jα18$^{-/-}$ mice had increased mortality after H3N2 infection which was rescued by adoptive transfer of iNKT cells. However, unlike H1N1 infection, H3N2 infected Jα18$^{-/-}$ mice showed no difference in viral titer compared to wild-type infected mice but did have increased lung pathology and reduced IAV-specific CD8^{+} T cell expansion, which suggested that iNKT cells were important in limiting inflammation and activating CD8^{+} T cells but were dispensable for controlling viral titer during H3N2 infection. iNKT cells produced IL-22 in response to H3N2 IAV pulmonary infection, which required DC help via TLR7 and RIG-I sensing of viral RNA and was critical for limiting inflammation (217). These studies demonstrated that iNKT cells were critical for controlling

inflammation and lung pathology, and in some cases viral titer, in different strains of IAV infection.

NKT cells can be protective or pathogenic during parasitic infections. Jα18$^{-/-}$ mice were protected from *Toxoplasma gondii* gastric infection by loss of pathogenic lamina propria IFN-γ producing iNKT cells (218). Treatment of mice with α-GalCer skewed iNKT cell cytokine production to IL-4 and IL-10 and increased survival. In contrast, iNKT cells producing IFN-γ to lipopeptidoglycans were required for protection against *Entamoeba histolytica* infection (171). NK1.1^{+}TCR$\beta^{+}\alpha$-GalCer CD1d TET^{-} NKT cells (type II NKT) were activated in systemic *Plasmodium yoelii* infection but were not required for protection *in vivo* (219). In the case of both *Trypanosome cruzi* and *Schistosoma mansoni* infection, Jα18$^{-/-}$ mice had increased mortality and inflammation and increase egg burden respectively relative to wild-type and CD1d$^{-/-}$ mice, suggesting that iNKT cells were protective and type II NKT cells were detrimental to parasite infection outcomes (220, 221). In summary, NKT cells can play protective or detrimental roles during pathogen infections, however the role of type II NKT cells is understudied compared to iNKT cells.

1-2.3 Contribution of NKT cells during SA infection: what is known and unknown

The known contributions of NKT cells during SA infection are limited. As previously mentioned, mice infected intravenously with a high dose of the methicillin-sensitive SA strain LS-1 were protected from sepsis-induced mortality in a CD1d-dependent manner by pretreatment with sulfatide, a self-lipid known to stimulate a subset of type II NKT cells (109). This study also demonstrated that iNKT cells were activated and expanded after SA infection by upregulation of CD69, but loss of NKT cells alone did not affect survival outcomes. A more recent study demonstrated that NKT cells were not required for survival to SA lethal infection with the USA300 strain (222). These studies demonstrated that NKT cells were not required for

survival to high-dose SA infection, but did not answer whether NKT cells mediated SA immunity during sublethal infection and whether type II NKT cells were activated and produce cytokines *in vivo*.

SA lipid antigens recognized by NKT cells have not been identified to date. The SA cell membrane is composed primarily of PG, lysyl-PG, and cardiolipin lipid species (223). A study using HPLC coupled with mass spectrometry (LC-Q-TOF-MS) to characterize the SA lipidome identified multiple species of PG and lysyl-PG of varying chain lengths eluting at different times during fractionation, with PG species being enriched in methicillin-resistant SA compared to methicillin-sensitive SA strains (224). PGs of different chain lengths have been identified from *Mycobacterium tuberculosis, Corynebacterium glutamicum*, and *Listeria monocytogenes* with the ability to stimulate type II NKT cell hybridomas; the efficiency of activation was dependent on the affinity of biding to CD1d (179, 180). Therefore, we hypothesized that SA may contain PG and lysyl-PG species recognized by type II NKT cells. The SA superantigen SEB targeting Vβ8 has been shown to activate iNKT cells independent of CD1d and dependent on MHC-II, however the USA300 SA strain used in our study does not contain dominant superantigens such as SEB (225, 110). We focused on this strain of SA for our study given that it is the dominant methicillin-resistant strain seen in community-acquired infections (226). In summary, there is some evidence that NKT cells protect mice from SA infection, but the mechanism of protection and SA lipid antigen recognition by NKT cells is unknown.

1-3 MAIT cells

1-3.1 Overview of MAIT cells

Like NKT cells, mucosal-associated invariant T (MAIT) cells are another class of unconventional innate-like T cells that are activated rapidly in response to infection and secrete a host of cytokines (227). MAIT cells recognize vitamin B metabolites presented by the MHC

class-I-like molecule MR1 (228, 229). Below I will discuss the development, subtypes and contribution of MAIT cells towards SA and other infectious pathogen immunity.

1-3.1a MAIT cell development and subsets

A study of double-negative TCRβ^+ T cells from healthy donors identified 2 populations of TCRα expressing T cells conserved across donors (230). One population was later identified as Vα24-Jα18 expressing CD1d-restricted iNKT cells and the other utilized Vα7.2-Jα33 TCRs. The mouse homolog of this population, which utilized Vα19Jα33 paired with Vβ2, Vβ6, Vβ8, or Vβ13, was identified in mouse LNs, and its development was independent of MHC-II, CD1, or TAP and dependent on β2m, suggesting that it was restricted by a non-CD1 MHC-I molecule presenting non-peptide antigens (231). A seminal study identified that mouse Vα19-Jα33 T cells and human Vα7.2-Jα33 T cells were restricted by the MHC-I molecule MR1 and present in the gut lamina propria, which coined the new terminology of these cells as mucosal-associated invariant T cells (228). This study also demonstrated that MR1 expression on hematopoietic cells was required for MAIT cell development and that B cells, but not DCs or macrophages, along with gut commensal flora were required for MAIT cell expansion.

For a number of years, it was not known what antigens MAIT cells recognized. Mouse and human MAIT cells became activated to BMDCs infected with a majority of bacterial species tested (232, 233), suggesting that the MAIT cell antigen was conserved across many, but not all bacterial species. A key study identified vitamin B metabolites that bind to MR1, including the non-activating ligand 6-formyl pterin (6-FP), a vitamin B9 metabolite, which is not recognized by MAIT cells, and activating vitamin B2 derivatives from *S.* Typhimurium, which are components of the riboflavin biosynthesis pathway and recognized by MAIT cells (229). Bacterial species previously shown to activate MAIT cells contained riboflavin biosynthesis genes, while bacteria that did not activate MAIT cells did not contain these genes, emphasizing the importance of

riboflavin in MAIT cell antigen recognition (232, 233). A seminal study using *Lactococcus lactis* mutants with alterations in the riboflavin synthesis pathway identified additional antigens recognized by MAIT cells, including the pyrimidine intermate ligands 5-(2-oxoethylideneamino)-6-D-ribitylaminouracil (5-OE-RU) and 5-(2-oxopropylideneamino)-6-D-ribitylaminouracil (5-OP-RU) (234). MR1 loaded 6-FP (control) and 5-OP-RU tetramers were used to identify MAIT cells in human PBMC and mice (234, 235). MAIT cells are much more enriched in human PBMC (6%) compared to mouse blood (0.1%). Tetramer staining of MAIT cells in wild-type C57BL/6 mice identified MAIT cells enriched in lung (3.4%) and lamina propria (1.5%), with lesser amounts in the liver (0.7%), spleen (0.06%), LN (0.3%), and thymus (0.04%) (235).

Similar to NKT cells, MAIT cells develop in the thymus; the TCR of MAIT cells interact with MR1 expressed on $CD4^+CD8^+$ DP thymocytes to positively select MAIT cells (236). While it is thought that an endogenous antigen is needed for MAIT cell development, this antigen has not been identified. After selection by DP thymocytes, immature MAIT cells undergo stepwise development (237). Stage 1 MAIT cells are defined as $CD3^+$ 5-OP-RU MR1 $tetramer^+CD24^+CD44^-$ cells and are found only in the thymus. Stage 2 MAIT cells downregulate CD24 to become $CD3^+$5-OP-RU MR1 $tetramer^+CD24^-CD44^-$ cells, requiring expression of the miRNA miR-181a/b1 (238). At stage 3 MAIT cells are $CD3^+$5-OP-RU MR1 $tetramer^+$ $CD24^-$ $CD44^+$ and resemble peripheral mature MAIT cells. Stage 3 MAIT cells upregulate PLZF and IL-18R, which along with MR1 and miR-181a/b1 are required for the stage 2 to 3 transition. At stage 3, MAIT cells differentiate into MAIT-1 (IFN-γ producing t-bet^+) or MAIT-17 (IL-17A producing RORγt^+) sub-lineages, but the factors regulating their differentiation is unknown (235).

The majority of MAIT cell studies have focused on cells expressing $NK1.1^+V\alpha19$ TCR (or $CD161^+V\alpha7.2$ TCR in humans). Generation of MAIT cell tetramers has allowed for characterization of additional MAIT cell subtypes. Classical MAIT cells express the TRAV1-2 (formerly called Vα7.2) rearrangement and NK1.1 (CD161 homolog in humans). In mice the

majority of MAIT cells are DN, with smaller subsets of $CD8^+$ and $CD4^+$ cells, while in humans the majority of MAIT cells are $CD8^+$, followed by DN, $CD4^+$, and DP subsets (234, 235). Smaller subsets of TRAV1-2^+ MR1 tetramer$^+$ MAIT cells (8-31% of total 5-OP-RU MR1 tetramer$^+$ cells) have been identified in human PBMC that utilize TRAJ20 and TRAJ12 rather than TRAJ33 (239). These MAIT cells have similar ligand specificity and functional properties as $TRAJ33^+$ MAIT cells and are classified under the umbrella of classical MAIT cells (227).

Additional MR1-restricted T cells that are TRAV1-2^- have been identified in humans. A TRAV1-2^- MR1-restricted clone was generated by pulsing PBMC with *Mycobacterium smegmatis* (240). This clone utilized TRAV12-2 and recognized riboflavin expressing bacterial species as well as the riboflavin biosynthesis negative bacteria *Streptococcus pyogenes*, suggesting that this clone recognized a distinct antigen different from antigens recognized by classical TRAV1-2^+ MAIT cells. 5-OP-RU MR1 tetramer staining of human PBMC identified that 1-5% of human MAIT cells did not express TRAV1-2. A more recent study using $TRAJ33^{-/-}$ mice identified additional $TRAV1^-$ MR1-restricted T cells with diverse TCRα repertoire usage (241). The study then categorized 5-OP-RU MR1 tetramer$^+$ MAIT cells in human PBMC into distinct groups based on CD161, IL-18R (CD218α), and CD26 expression. TRAV1-2^- MR1 tetramer$^+$ cells (0.8% of MR1 tetramer$^+$ cells) could be divided into 2 groups, MAIT-like cells ($CD218\alpha^{hi}CD161^{hi}CD26^{hi}PLZF^+$) (0.1%) and non-MAIT like cells ($CD218\alpha^{lo}CD161^{lo}CD26^{lo}PLZF^-$) (0.6%). Single cell TCR-sequencing of MAIT-like and non-MAIT like cells was performed, revealing that a subset of MAIT-like cells had conserved TRAV36 usage and were MR1 5-OP-RU restricted, while the remainder of cells from each subset had diverse TCR usage. Combined, these studies demonstrate that the majority of MAIT cells have invariant TCR usage and antigen recognition, however recent studies have highlighted the diversity of small subsets of MR1-restricted T cells with diverse TCR usage and antigen specificity. New terminology now

classifies MR1-restricted cells into classical MAIT, non-classical MAIT, and atypical MR1-restricted T cells (227).

1-3.1b MAIT cell activation kinetics and effector function

MAIT cells can be activated via vitamin B metabolites presented on MR1 to the MAIT cell TCR, leading to cytokine production and cytotoxic killing (227). In human PBMC, MAIT cells preferentially produced Th1 cytokines such as IFN-γ and TNF-α over IL-17A, although a small minority of $CD4^+$ MAIT cells preferentially produced the Th2 cytokines IL-4 and IL-13 after stimulation with PMA/Ionomycin (242). MAIT cells from human adipose tissue were also capable of producing IL-10 (243). Mouse and human MAIT cells became activated (upregulated CD69) and produced IFN-γ to *Escherichia coli*-infected monocytes, which required MR1-TCR engagement and uptake of bacterial antigens via phagosomes and endocytosis (233). MAIT cells also became activated to BMDCs infected with *Pseudomonas aeruginosa*, *Klebsiella pneumonia*, *Lactobacillus acidophilus*, *Listeria monocytogenes*, *Mycobacterium tuberculosis*, *S.* Typhimurium, *Staphylococcus aureus*, and *Staphylococcus epidermidis* containing riboflavin intermediates but not to BMDCs infected with *Enterococcus faecalis* or *Streptococcus A* lacking riboflavin intermediates (232, 233). *In vivo*, mouse MAIT cells preferentially produced IL-17A over IFN-γ in response to *S.* Typhimurium and *Legionella longbeachae* infection (244, 245). These studies demonstrated differences in cytokine production profiles between mouse and human MAIT cells.

MAIT cells can be activated through TCR-dependent MR1 presentation of riboflavin intermediates produced by bacteria with or without TLR activation or can be activated through TCR-independent cytokine-mediated signaling (227). While intranasal administration of 5-OP-RU alone upregulated CD69 on MAIT cells *in vivo*, administration of TLR ligands Pam2Cys, CpG, or polyI:C + 5-OP-RU or infection were needed to expand mouse MAIT cells (244). In

human PBMC, TCR signaling alone could not induce sustained MAIT cell cytokine production, whereas signaling via IL-12/IL-15/IL-18 induced robust sustained MAIT cell cytokine production (246). TCR signaling plus TLR cytokine signaling by APCs induced the greatest magnitude of cytokine production by MAIT cells from both PBMC and MAIT cells isolated from human rectal mucosal biopsies. These data demonstrated that like NKT cells, MAIT cells can be activated via TLR signaling by APCs alone, but a combination of TLR signaling and TCR stimulation induces the most robust MAIT cell response. Indeed, the activation of MAIT cells by viral infections that lack MAIT cell antigens supports the ability of MAIT cells to be activated by TLR mediated signaling (247).

Once MAIT cells become activated, they can secrete granzyme B and perforin to directly kill pathogens (248). In addition, MAIT cells induced MR1-depedent CD40L-dependent maturation and IL-12 production by monocytes and DCs as well as transactivation of NK cells (249). In theory, MAIT cells could also activate conventional T cells, but this has not been tested to our knowledge. In summary, MAIT cells are activated by vitamin B metabolites produced by bacteria as well as activated by TLR driven cytokine signals, demonstrating their ability to respond rapidly to various pathogens.

1-3.2 MAIT cell contribution to infection

Given the ability of MAIT cells to become activated to both viral and bacterial pathogens, it is no surprise that they can contribute to infection control for a number of pathogens. Below I will discuss the contribution of MAIT cells to various pathogen infections.

1-3.2a MAIT cell contribution to bacterial and fungal infections

MAIT cells contribute to protection against both systemic and pulmonary infections. The first study to show a protective effect of MAIT cells during infection was performed using mice with enriched MAIT cells. Mice with enhanced MAIT cell % (iVα19 Tg and iVα19-Vβ6 Tg) had

decreased spleen CFU compared to their TCR transgenic MR1$^{-/-}$ counterparts in response to *Mycobacterium abscessus* systemic infection or *E. coli* intraperitoneal infection (233). However wild-type C57BL/6 mice had no difference in CFU compared to MR1$^{-/-}$ mice in response to *Mycobacterium abscessus* infection, which the authors contributed to the decreased % of MAIT cells in spleens of wild-type mice. This study also found a decrease in MAIT cell % in blood of *Mycobacterium tuberculosis* and pneumonia infected individuals compared to healthy controls, as well as the presence of MAIT cells in lung biopsies of infected patients, suggesting that MAIT cells migrated from the blood to the lungs during pneumonia infection. MAIT cells played a protective role during *Klebsiella pneumonia* intraperitoneal infection; MR1$^{-/-}$ mice had higher bacterial replication and increased mortality compared to wild-type mice, though the mechanism of protection was not explored (250).

Because of the enrichment of MAIT cells in the lungs, much attention has been given to MAIT cell immunity during lung infection. MR1$^{-/-}$ mice had delayed clearance of *Francisella tularensis* intranasal infection, delayed IFN-γ, TNF, IL-17A, and iNOS production, and delayed activated CD4^{+} and CD8^{+} T cell lung recruitment in response to infection, which demonstrated that MAIT cells were critical for mediating early host immunity (251). This group later showed that MAIT cells induced lung GM-CSF production, which promoted monocyte-derived DC differentiation and led to a reduction in *Francisella tularensis* CFU (252). MR1$^{-/-}$ mice had delayed clearance and increased CFU after intranasal *Legionella longbeachae* infection (245). Immunizing wild-type mice with 5-OP-RU and Pam2Cys one month prior to infection or adoptively transferring activated MAIT cells to Rag$^{-/-}$ mice enhanced MR1-dependent protection, which was mediated by MAIT cell IFN-γ production. MR1$^{-/-}$ mice intranasally infected with *Mycobacterium bovis* BCG had increased CFU at 10 dpi, but not 30 dpi, demonstrating a protective effect of MAIT cells during the early but not late host immune response (253). A more recent study showed no difference in lung CFU between mice pretreated to activate and expand

MAIT cells (using Pam2Cys and 5-OP-RU) versus unprimed mice after *Mycobacterium tuberculosis* infection (254). MAIT cells were activated and expanded in response to *S.* Typhimurium intranasal infection, however MAIT cells were dispensable for control of lung CFU, demonstrating that MAIT cells were not necessary for protection against all bacterial species that activate MAIT cells (244).

Despite the ability of MAIT cells to contribute to protection in some models of infection, they can play a pathogenic role in other bacterial infections. MAIT cell % were increased in PBMC and gastric mucosa of patients with *Helicobacter pylori* gastric infection (255). Increased stomach immune cell infiltrate and gastritis was observed in TCR transgenic mice enriched for MAIT cells ($V\alpha19iC\alpha^{-/-}$) relative to TCR transgenic $MR1^{-/-}$ mice. Boosting MAIT cells in wild-type mice by pretreatment with *S.* Typhimurium infection or Pam2Cys treatment recapitulated the same MR1-dependent pathology after *Helicobacter pylori* infection seen in transgenic mice. This demonstrated that MAIT cells were pathogenic during *Helicobacter pylori* infection, which was linked to the ability of MAIT cells to produce IL-17A, IFN-γ, and TNF-α in response to infection, which led to associated inflammation.

The role of MAIT cells in fungal infections is not clear. One study demonstrated that human MAIT cells upregulated CD69 and released perforin in response to stimulation with three different *Aspergillus* species, mediated by APCs and TCR-MR1 interaction (256). However, the ability of MAIT cells to control fungal infection *in vivo* has not been explored.

In summary, much of the work exploring the role of MAIT cells in outcomes of infection have focused on bacterial infections, due to the ability of MAIT cells to recognize riboflavin intermediates produced by bacteria. In bacterial infections where MAIT cells were necessary for reducing bacterial burdens, protection was mediated by IFN-γ, TNF, or IL-17A producing MAIT cells, however pathogenic MAIT cells producing these cytokines have been described for some bacterial infections.

1-3.2b MAIT cell contribution to viral and parasitic infections

As previously described, MAIT cells can be activated during viral infection in response to cytokine driven signals. MAIT cells accumulated and were activated in PBMC of infected Dengue virus patients compared to convalescent patients (247). Similar to bacterial infections, the percentage of MAIT cells decreased in PBMC of patients with various viral infections compared to healthy controls (227). MAIT cells expanded and upregulated CD69 and CD25 after intranasal Influenza PR8 infection, with partial dependence on IL-12, IL-15, and IL-18 signaling (257). $MR1^{-/-}$ mice also had increased mortality to influenza infection, which was partially rescued by the adoptive transfer of IFN-γ competent MAIT cells.

Similar to viral infections, the information of MAIT cells during parasitic infection is limited. Healthy volunteers infected intradermally with 25 thousand *Plasmodium falciparum* sporozoites had increased % of MAIT cells (defined as $CD3^{+}V\alpha7.2^{+}CD161^{+}CD8^{+}$ cells) in PBMC up to 168 days post infection, but no changes in activation or cytokine production at the timepoints tested (258). Single cell sequencing of MAIT cells from one donor identified some transcripts of IFN-γ and granzyme B upregulated at 9 dpi in MAIT cells but this was not explored in other study participants.

In summary, there have been very limited studies exploring the role of MAIT cells in viral and parasitic infections, with the majority of studies focusing on the ability of MAIT cells to be activated in response to infection. Further mechanistic studies in mice and other animal models will need to be performed to determine the relevance of MAIT cells to viral and parasitic control.

1-3.3 Contribution of MAIT cells during SA infection: what is known and unknown

SA infected BMDCs were shown to activate MAIT cells from TCR transgenic mice (iVα19-Vβ6 Tg) by upregulation of CD69 *in vitro* (233). SA contains the machinery to produce vitamin B metabolites, which could explain its ability to activate MAIT cells. Indeed cell free

supernatant of the SA strain 161:2 induced IFN-γ production by human MAIT cells (259). Human MAIT cells from healthy donors were also highly responsive to the SA superantigen SEB, as shown by enhanced MAIT cell IFN-γ production to SEB relative to iNKT cells, γδ T cells, and conventional T cells (260). MAIT cell IFN-γ production to SEB was Vβ8-specific, MR1-independent, MHC-II-restricted, and present in both human PBMC MAIT cells and hepatic MAIT cells. The MAIT cell response to SEB also required IL-12 and IL-18 signaling through p38 and MEK1/2 and was specific to SA SEB, as SA TSST-1, which targets Vβ2, and SEA, which targets Vβ5, did not induce cytokine production. MAIT cells pretreated with SEB were hyporesponsive to stimulation with bacteria harboring known MAIT cell antigens, and expressed exhaustion markers, demonstrating that SEB induced MAIT cell anergy. This anergy was recapitulated in MHC-II humanized mice treated with SEB. Despite the ability of SEB to activate MAIT cells, the USA300 strain does not contain SEB, and I did not expect potential MAIT cell activation by USA300 to be mediated through superantigens.

Direct evidence for the ability of MAIT cells to contribute to SA protection has not been demonstrated to our knowledge. It is possible that MAIT cells may play a role in SA pneumonia considering that MAIT cells are enriched in the lung and SA harbors the necessary proteins to produce riboflavin metabolites recognized by MAIT cells, however this has yet to be studied. In summary, SA contains MAIT cell antigens and can activate MAIT cells in vitro through antigen-specific or superantigen mediated mechanisms, but the contribution of MAIT cells to SA protection *in vivo* has not been explored.

1-4 Rationale of study

Methicillin-resistant *Staphylococcus aureus* is a leading cause of antibiotic-resistant sepsis-induced mortality in the United States. Due to the complex nature of this microbe and its ability to evade the host immune response, a successful vaccine offering protection against SA

is not currently available. Previously, B cells and antibody production were thought to be the driving arm of the immune response against extracellular pathogens like SA, but in recent years T cells, and more recently unconventional T cells that respond to non-peptide antigens, have been identified as important players in SA immunity. This includes work by our lab, which showed that group 1 CD1-restricted T cells, a group of lipid reactive T cells found in humans, protected humanized mice from systemic SA infection through production of IFN-γ, as well as work on $\gamma\delta$ T cells, which have emerged as key players in protection and production of IL-17A in models of SA skin infection. I sought to determine the role of two major subsets of innate-like T cells, CD1d-restricted NKT cells and MR1-restricted MAIT cells in SA infection, using $CD1d^{-/-}$ and $MR1^{-/-}$ mice to determine the contribution of these cells to the control SA systemic infection. Given that both NKT cells and MAIT cells respond rapidly to pathogen infections and can secrete proinflammatory cytokines such as IFN-γ and IL-17A, I hypothesized that they would be activated and play a role in SA infection control in the early stage of host immunity.

Previous work by another lab demonstrated a role for type II NKT cells in SA infection control to sepsis induced mortality. To parse out the role of iNKT cells vs. type II NKT cells to SA infection control, I utilized $J\alpha18^{-/-}$ mice deficient for iNKT cells. As both type II NKT cells and MAIT cells are enriched in humans relative to iNKT cells, I was particularly interested in exploring these subsets in SA infection in both mice and human PBMC. Given that previous bacterial infections have led to a decrease in total % of MAIT cells and iNKT cells in PBMC, I hypothesized the same would be true in SA infected patients. I did not have tetramers to track type II NKT cells *in vivo* therefore I resorted to using surrogate markers to define this population in mice and humans.

While antigens for MAIT cells and iNKT cells have been well defined, lipid antigens recognized by type II NKT cells have relied on the use of type II NKT cell hybridomas. Type II NKT cells recognized PG from *Mycobacterium tuberculosis, Corynebacterium glutamicum*, and

Listeria monocytogenes species. Given that PG species make up the majority of the SA cell membrane, I hypothesized that type II NKT cells would be reactive to PG lipid antigens from SA, which could contribute to host immunity. I used fractionated total SA lipids from the cell membrane of SA to test type II NKT cell lipid antigen recognition in ELISPOT assays. Indeed, a recent study from our lab demonstrated that group 1 CD1-restricted T cells were reactive to SA PG. Other studies have demonstrated the ability of lipid antigens such as sulfatide to activate both type II NKT cells and group 1 CD1-restricted T cells. Therefore, I hypothesized that type II NKT cells would recognize SA PG species after SA infection.

Chapter 2

Materials and methods

2-1 Mouse strains

Wildtype C57BL/6 (B6) mice and MHC class II deficient (MHC-II$^{-/-}$) mice were obtained from The Jackson Laboratory (Bar Harbor, ME). MyD88$^{-/-}$ mice were obtained from the Mutant Mouse Resource and Research Centers. Jα18(-10)$^{-/-}$ mice (hereafter referred to as Jα18$^{-/-}$ mice) were generated on the B6 background in Dr. Laurent Gapin's lab (University of Colorado). Jα18$^{-/-}$ mice lacked iNKT cells due to interruption of the TRAJ18 gene required for Vα14-Jα18 iNKT cell development (261). These mice were an improvement over the original Jα18$^{-/-}$ strain, which had lower TCR diversity due to suppressed transcription of TRAJ gene segments downstream of TRAJ18 (262). I backcrossed these Jα18$^{-/-}$ mice to B6 mice in our mouse colony to generate wild-type littermate controls. CD1d$^{-/-}$ mice, lacking iNKT cells and type II NKT cells, were generated in house and have been backcrossed to the B6 background for at least 12 generations (263). MR1$^{-/-}$ mice were provided by Dr. Ted Hansen (Washington University) and backcrossed to B6 mice to generate MR1$^{+/+}$ littermate controls. Vα3.2^{+}Vβ9^{+} transgenic mice (24$\alpha\beta$ Tg) were provided by Dr. Suzanna Cardell (University of Gothenburg); these mice were generated using the TCR variable chain regions of the type II NKT cell hybridoma VIII24 (144). MHC-II$^{-/-}$CD1d$^{-/-}$ mice were generated by crossing CD1d$^{-/-}$ mice and MHC-II$^{-/-}$ mice. Naïve mice were housed in a specific pathogen-free facility.

2-2 Genotyping of mice

Mice were genotyped by PCR, sequencing, or by FACS surface staining of blood samples. For PCR, mouse tail samples were obtained by snipping the tail ends off of 21 day to 28 day old weanlings. Tail samples were boiled in 75 μL of tail solution I (25mM NaOH, 0.2 mM EDTA) for 1 hr at 100º C. After cooling tail samples to room temperature, 75 μL of tail solution II

(40mM Tris-HCl) was added and tubes were spun down at 4000 rpm for 3 min. Supernatants were used to perform PCR reactions to detect the presence or absence of the *CD1d* gene (using CD1d F, CD1d R, and Neo44 primers) or *MR1* gene (using MR1 F, MR1 R, and MR1 mid primers). Amplified gene segments were run on a gel (1% agarose + 3 μL of Ethidium Bromide in 1x TAE) and imaged using a gel imager (Bio-Rad Universal Hood II). For Jα18$^{-/-}$ mice, PCR was used to amplify the region of DNA containing the TRAJ18 gene segment (using Jα18$^{-/-}$ F and Jα18$^{-/-}$ R primers). The PCR product was run on a gel and the amplified gene segment was cut out and DNA extracted using gel DNA extraction kit (Qiagen). The purified PCR product was mixed with Jα18$^{-/-}$ sequencing forward primer (Jα18$^{-/-}$ seq F primer) and sent to the sequencing core for DNA sequencing. Jα18$^{-/-}$ mice were confirmed by 10 bp deletion (TAG GGA GGC T) in the TRAJ18 gene segment. All primers are listed in **Table 2**.

Mice genotyped by FACS surface staining were bled of 30-50 μL of blood via tail snip and blood was collected using capillary tubes. Blood samples were treated with 700 μL of Gey's solution for 3 min at RT then washed with 700 μL of Hank's buffer (10 % HBSS + 2 % FBS in dH2O) and spun down at 7000 rpm for 1 min to lyse and remove red blood cells. Surface staining was performed as described in **2-9.1**. FITC anti-Vβ9 and PE anti-Vα3.2 were used to genotype 24$\alpha\beta$ Tg mice. BV510 anti-MHC-II and PerCP anti-B220 were used to genotype MHC-II$^{-/-}$ mice.

2-3 *Staphylococcus aureus in vivo* infection model

2-3.1 Growth and preparation of bacteria

All data were obtained using the USA300 methicillin-resistant SA clinical isolate strain, generously provided by Dr. Nancy Freitag (University of Illinois at Chicago). SA bacterial stock was stored in tryptic soy broth (MP Biomedicals, Solon, OH) + 30% glycerol at -80º C. Prior to infection, bacteria were streaked out on tryptic soy agar plates containing 5 μg/mL erythromycin,

using quadrant streaking to generate single colonies, and grown up overnight in a 37º C incubator. SA streaked plates were kept at 4º C for up to 2 weeks for inoculation purposes. For infection experiments, a few SA colonies were picked from streaked plates and inoculated into 5 mL of tryptic soy broth containing 5 μg/mL erythromycin. Bacteria were grown at 37º C shaking at a slant at 220 rpm overnight. The next day, the overnight culture was diluted 1:100 in fresh 5 mL of tryptic soy broth containing 5 μg/mL erythromycin. Freshly diluted culture tubes were grown at 37º C shaking at a slant at 220 rpm until the culture reached mid-log phase (Optical density=0.4-0.7). Bacteria optical density (OD) was read using a UV/Vis spectrophotometer (Beckman Coulter DU 530).

2-3.2 Intravenous injection model

Using the OD reading of the mid-log phase SA culture, I calculated the concentration of bacteria needed to inject 200 μL of bacteria per mouse. For example, an OD of 0.5 was equal to $5x10^8$ CFU of bacteria. Mice were infected with $1x10^7$ CFU (primary infection) or $2x10^6$ CFU (adoptive transfer experiments), therefore I made a $5x10^7$ CFU/mL (primary infection) or $1x10^7$ CFU/mL (adoptive transfer experiments) stock in 10 mL of PBS. SA from the mid-log phase culture was diluted in PBS to the correct concentration and washed 2x by spinning down bacteria for 5 min at 1500 rpm. Once bacteria were ready for infection, a small aliquot was taken and diluted to $1x10^3$ CFU/mL and 100 μL was plated on a tryptic soy agar plate containing 5 μg/mL erythromycin and grown overnight in a 37º C incubator to confirm infectious dose.

All SA intravenous infections were performed in a biosafety level 2 facility (BSL-2). Mouse tails were held under a heat lamp for a few seconds to bring the vein to the surface of the skin then sterilized with gauze-soaked 70% ethanol. 1 mL syringes were loaded with prepared SA stock then fitted with a 30-gauge needle. 200 μL of SA were injected into the tail

vein of each mouse. After infection, mice were housed in the BSL-2 facility up to study timepoints.

2-3.3 CFU plating method

Organs were prepped for CFU quantification by one of two methods. If organs were not being used for other immune cell assays, organs were homogenized in PBS by sonication then raised to a volume of 10 mL with PBS for plating. If organs were being used for other downstream assays, organs were homogenized in PBS using the methods described in **2-6** and raised to a volume of 10 mL with PBS. A 200 μL aliquot was taken prior to first spin for plating. For CFU plating all serial dilutions were plated on tryptic soy agar plates containing 5 μg/mL erythromycin. With the infectious doses I used for experiments, I expected mouse kidneys to contain approximately 10^7-10^8 CFU of bacteria at study timepoints. Kidney homogenates were diluted 1:10 to 5 serial dilutions, and 10 μL of each serial dilution plus neat were plated in duplicate by spot plating. I expected liver and spleen to contain approximately 10^2-10^3 CFU of bacteria. Liver and spleen were plated neat by streaking 100 μL of organ homogenate per plate. If liver and spleen CFU were too many to count, organs were diluted 1:10 to 2 serial dilutions and 50 μL of 1:10 and 1:100 dilutions were streaked on each half of a new plate. All plates were grown overnight in a 37º C incubator. Serial dilutions were counted using an automatic cell counter and back-calculations were performed to determine the total CFU per organ.

2-4 Hematoxylin and Eosin (H&E) imaging

SA-infected kidneys were collected from infected mice for H&E staining. Both kidneys were collected and fixed in 4% paraformaldehyde buffer for at least 2 days prior to sectioning. Once tissue was fixed, excess fiber was cleaned from the surface of each kidney and a scalpel was used to cut each kidney into 2 halves longitudinally. The 4 pieces of kidneys per mouse

were loaded into one cassette and stored in 4% paraformaldehyde prior to sectioning. Kidneys were sent to the Northwestern mouse histology and phenotyping core and paraffin embedded into blocks. These blocks were sectioned to generate slides containing all 4 kidney sections per mouse and H&E staining was performed on the slides by the core facility.

H&E slides were imaged using the TissueGnostics Imaging System and inflammatory foci were quantified using Tissue/HistoQuest software (TissueGnostics). Inflammatory foci were manually gated from each half of each kidney and the areas were quantified as a % of the total kidney section area. The average inflammatory foci for each mouse was calculated by taking an average of the % inflammatory foci from each of the 4 sections and recorded as one data point.

2-5 Mouse organ processing

Mouse leukocyte single cell suspensions were isolated from LN, liver, spleen, and kidneys of naïve and infected mice. If liver or kidney aliquots were needed for CFU quantification, organs were isolated directly and placed in 5 mL of PBS. If livers were not needed for CFU quantification, livers were perfused through the portal vein with 10 mL of Hank's buffer + 50 μg/mL gentamycin using a 27-gauge needle then placed in 5 mL of Hank's buffer + 50 μg/mL gentamycin. Kidneys and liver were homogenized by manually pressing organs through a 70 μM sterile filter using a 5 mL syringe top. Organs were washed with an additional 5 mL of media (Hank's buffer + 50 μg/mL gentamycin or PBS for organs needed for CFU quantification). For CFU quantification, samples were brought to 10 mL with PBS and a 200 μL aliquot was taken for CFU. For all samples the total volume was brought to 50 mL at this step with Hank's buffer + 50 μg/mL gentamycin. Samples were spun down at 1500 rpm for 5 min at 4º C then washed 1x with 15 mL of Hank's buffer + 50 μg/mL gentamycin. After wash, pellets were resuspended in 7 mL of 37.5% Percoll then transferred to 15 mL tubes for gradient centrifugation. Samples were spun at 2000 rpm for 10 min at RT. Pellets were resuspend using

a 200 μL pipette and transferred to a new 15 mL tube. Samples were resuspended in 5 mL of Gey's solution and incubated for 5 min at RT to lyse red blood cells. The reaction was quenched using 5 mL of Hank's buffer + 50 μg/mL gentamycin, then samples were spun down at 1500 rpm for 5 min at 4º C then washed 1x with 5 mL of Hank's buffer + 50 μg/mL gentamycin. Pellets were resuspended in Hank's buffer + 50 μg/mL gentamycin for counting using a hemocytometer.

For spleen and LN isolation, organs were isolated and placed in 5 mL of media (Hank's buffer + 50 μg/mL gentamycin or PBS if performing CFU quantification) and homogenized by breaking up organs with 2 glass slides. Homogenates were transferred to a 15 mL tube and passed through nylon mesh to remove any residual large debris. For spleen CFU quantification, samples were brought to 10 mL with PBS and a 200 μL aliquot was taken for CFU. Samples were spun down at 1500 rpm for 5 min at 4º C. LN were resuspended in 5 mL of Hank's buffer + 50 μg/mL gentamycin for counting. Spleens were treated with Gey's solution to lyse red blood cells, as described above, then washed 2x before resuspension in 10 mL of Hank's buffer + 50 μg/mL gentamycin for counting.

2-6 Human sample acquisition and processing

Blood samples from SA infected patients were acquired through the Northwestern Memorial Hospital. Gram positive cocci (GPC) blood culture positive individuals were screened for inclusion in the study using EPIC. The inclusion criteria for infected patients was as follows: patients with confirmed SA bacteremia (by at least 1 blood culture where blood has been collected by use of aseptic technique), patients who were inpatients at NMH at the time of study collection, patients over the age of 18, and patients able to give consent for blood collection. The exclusion criteria were as follows: pregnant individuals, mixed bacteremic patients, patients with known active infections with blood-borne viruses (including human immunodeficiency virus

Ab/Ag positive, hepatitis C RNA positive, hepatitis B sAg positive, and SARS-CoV-2 RNA positive individuals), patients with active malignancies (including hematologic and solid organ malignancies), solid organ transplant recipients, patients with steroid treatment for at least 1 month (>30 mg/day), and patients on cytotoxic immunosuppressive therapy (including calcineurin inhibitors, e.g. cyclosporine, tacrolimus, antiproliferative agents, e.g. azathioprine, cyclophosphamide, methotrexate, chlorambucil, mycophenylate mofetil, and immune-active monoclonal antibodies, e.g. adalimumab, alemtuzumab, belimumab, golimumab, infliximab, muromonab-CD3, natalizumab, ofatumumab, rituximab, tocilizumab, tocitumomab). All SA bacteremic patients were receiving Vancomycin treatment alone or a combination of Vancomycin plus another antibiotic (Tazobactam, Piperacillin, Cefepime, Zosyn, or Ceftriaxone) at the time of blood collection, with the exception of one patient that was not yet on antibiotic therapy. Each SA patient sample collected was paired with healthy donor blood for side by side processing and downstream assays.

PBMC were isolated from whole blood within 48 hrs of original blood draw by layering 1:1 onto prewarmed Histopaque-1077 (Sigma-Aldrich) then spun down at 400 g for 30 min at RT. Leukocytes were collected at the serum-cell interface and washed 3x with Hank's buffer, spinning down at 250 g for 10 min at RT between each wash. Leukocytes were resuspended in 5 mL of Hanks before counting cells with a hemocytometer and performing surface staining.

2-7 Mouse T cell enrichment

T cells were enriched from mouse spleen and liver single cell suspensions using MACS negative selection (Miltenyi Biotec). Cells were blocked for 15 min with 2.4G2 then washed with MACS buffer (PBS + 1% BSA + 0.5 mM EDTA) and spun down at 1500 rpm for 5 min at 4º C. Cells were resuspended in 1 mL of MACS buffer and incubated with biotinylated antibodies to CD8α/β, B220, MHCII, ter119, and Ly6G for 30 min rotating at 4º C to enrich $CD8^-$ T cells. For type II NKT cell enrichment, additional biotinylated mAb specific to TCR $\gamma\delta$ and CD11b were

added to further enrich type II NKT cells. Cells were washed with MACS buffer then resuspended in 1 mL of MACS buffer and incubated with 25 μL streptavidin biotin beads per 10^6 leukocytes for 30 min rotating at 4º C. After incubation, 2 mL of MACS buffer were added to each tube and placed on a MACS magnetic bead separator for 5 min at RT. Cells that did not bind to the magnet were collected and washed before counting.

2-8 Reagents and antibodies

Mouse and human CD1d tetramer (TET^+) unloaded or loaded with α-GalCer analog PBS57 and MR1 tetramer loaded with 6-FP (control) or 5-OP-RU were provided by the NIH tetramer facility. Fluorochrome-conjugated antibodies against mouse CD3, CD4, CD8α, CD69, NK1.1, TCRβ, Ly6G, CD11b, B220, CD11c, Ly6C, F4-80, IFN-γ, IL-17A, Vβ2, Vβ7, and Vβ12 and human CD3, CD4, CD8α, Vα7.2, CD161, CD14, and CD19 were purchased from BioLegend. Fluorochrome-conjugated antibodies against mouse Vβ4, Vβ5.1/5.2, Vβ6, Vβ8.1/8.2, Vβ9, Vβ11, and Vβ13 were purchased from BD. Fluorochrome-conjugated antibody against mouse Vβ10b was purchased from eBioscience. Live dead eFlour506 was purchased from Thermo Fischer Scientific.

2-9 Staining for fluorescence-activated cell sorting (FACS)

2-9.1 Mouse leukocyte surface staining

Mouse leukocytes were resuspended at a concentration of $1x10^7$ cells/mL and 100 μL were transferred to 96 well plate for surface staining. Samples were incubated for 15 min on ice with 50 μL of purified 2.4G2 blocking mAb (generated in house). Plates were spun down at 1500 rpm for 5 min at 4º C, then resuspended in antibody cocktails and incubated on ice for 45 min. Cells were washed then resuspended in 100 μL of Hank's buffer + 50 μg/mL gentamycin + 0.05 % PFA to fix cells and kill any intracellular SA before running FACS.

2-9.2 Human leukocyte surface staining

For human leukocyte surface staining, cells were resuspended at a concentration of $1x10^7$ cells/mL and 100 μL were transferred to 96 well plates for staining. Plates were spun down at 1500 rpm for 5 min at 4º C, then resuspended. For cells that were stained with surface markers only, pellets were resuspended in 100 μL of 25 μg/mL human Fc block (BD) and incubated at RT for 10 min. Plates were spun down and resuspended in antibody cocktails and incubated on ice for 45 min. Cells were washed then resuspended in 100 μL of Hank's buffer + 50 μg/mL gentamycin + 0.05 % PFA to fix cells and kill any intracellular SA before running FACS.

For cells that were stained with human α-GalCer loaded CD1d (α-GalCer/CD1d) tetramer, cells were washed 2x with 100 μL of PBS, then resuspended in 100 μL of PBS containing fixable viability dye eFlour 506 (eBioscience) and incubated for 30 min at 4º C. Cells were spun down and washed 2x with Hank's buffer, then blocked with human Fc block as described above. Plates were spun down and resuspended in antibody cocktail containing titrated human α-GalCer/CD1d tetramer or unloaded tetramer plus surface staining antibodies and incubated on ice for 45 min. Cells were washed then resuspended in 100 μL of Hank's buffer + 50 μg/mL gentamycin + 0.05 % PFA for FACS.

For cells that were stained with 5-OP-RU loaded MR1 (5-OP-RU/MR1) tetramer, cells were incubated with human Fc block (BD) as described above. Plates were spun down and resuspended in Hanks buffer containing titrated human 5-OP-RU/MR1 tetramer or control 6-FP loaded MR1 tetramer. Cells were incubated at RT for 40 min in the dark. Cells were washed then stained with other surface antibodies for 20 min in the dark at RT. After wash, cells were resuspended in 100 μL of Hank's buffer + 50 μg/mL gentamycin + 0.05 % PFA for FACS.

2-9.3 Intracellular staining for cytokine production

For mouse intracellular cytokine staining, cells were first stained with surface antibodies as described above. After overnight fixation in Hank's buffer + 50 μg/mL gentamycin + 0.05 % PFA, cells were spun down at 1500 rpm for 5 min at 4º C then washed 1x with PBS. Cells were resuspended in PBS + 1% BSA containing 0.05% saponin and permeabilized at RT for 10 min. Cells were washed 1x with PBS-BSA, then resuspended in antibody cocktail containing intracellular staining antibodies in PBS-BSA + 0.05% saponin and incubated in the dark at RT for 30 min. Antibody stained cells were washed 2x then resuspended in 100 μL of PBS-BSA + 0.05% saponin for FACS.

2-9.4 Ki67 staining

For Ki67 staining, cells were first stained with surface antibodies as described above then pelleted. 200 μL of Foxp3 Fixation/Permeabilization (Invitrogen) working solution was added to each well (resuspended from stock bottles at a 1:3 ratio). Cells were incubated in the dark for 30 min at RT, then spun down and resuspended in 200 μL of 1x Permeabilization buffer (Invitrogen, diluted 1:10 in dH_2O from 10x stock solution). After second spin, cells were resuspended in 50 μL of 1x Permeabilization buffer containing FITC Ki67 Ab (1:200 ratio). Plates were incubated in the dark for 30 min at RT, washed 2x, then resuspended in 200 μL of 1x Permeabilization buffer for FACS analysis.

2-10 SA antigen isolation and preparation

2-10.1 SA lipid isolation and fractionation

Bulk SA was grown up by inoculating a large scraping of -80º C SA stock into 500 mL of tryptic soy agar containing 5 μg/mL erythromycin. Bacteria were grown up overnight shaking at 220 rpm at 37º C then collected the next day and spun down in a floor centrifuge (Beckman

Coulter Avanti J-E centrifuge) at 15000 rpm, 10 min. Pellet was washed with PBS, then resuspended in 50 nM KH_2PO_4 buffer containing 2 μg/mL lysostaphin to break open the SA peptidoglycan cell wall and release protoplasts. Bacterial pellet was washed with PBS then resuspended in 100% EtOH for transport to our collaborator for SA lipid extraction. Total SA lipids were isolated from protoplasts using a $CHCl_3$-MeOH Bligh-Dyer extraction method (264). Total SA lipids were fractionated by polarity into 11 fractions using silica gel column chromatography (0.5 x 20 cm) and stepwise elution with chloroform, acetone, and methanol in chloroform as solvents (15 mL per fraction). SA lipids were characterized using 1D- and 2D-TLC with hexane/diethyl ether/acetic acid (85:15:1, v/v) for 1-D TLC, solvent A (chloroform/methanol/28% ammonia/toluene (64:30:6:10, v/v)), and solvent B (chloroform/methanol/acetone/acetic acid/water/toluene (70:30:5:4:1:10, v/v)). Lipids were visualized with 10% sulfuric acid in methanol with heating or using phosphomolybdate reagent to detect phospholipids (265).

2-10.2 Heat-killed SA (HKSA) preparation

Bulk SA was grown up overnight as described in **2-3.1**. Bacteria concentration was calculated then resuspended at a concentration of 10^{10} CFU/mL. Bacteria were placed at 80º C in a water bath and treated for 3 hrs to kill SA.

2-11 Cytokine ELISA and cytometric bead array (CBA)

$5x10^5$ splenocytes or $2x10^5$ liver lymphocytes were co-cultured in 96 well plates unstimulated or stimulated with α-GalCer (200 ng/mL) or $1x10^6$ CFU of HKSA for 48 hrs at 37º C. After 48 hrs, plates were spun down at 1500 rpm for 5 min at 4º C then supernatants were collected for ELISA. 96 flat well plates were coated with 4 μg/mL IFN-γ or 2 μg/mL IL-17A primary antibody, in 50 μL PBS per well, overnight at 4º C. The next day, plates were washed

3x with PBS-T (1x PBS + 0.05% Tween 20), then blocked with 200 μL of PBS + 10% FBS (PBS-F) for 1-2 hrs at RT. Top standard was diluted 1:2 in media to 8 standards. Plates were washed 3x with PBS-T, then 40 μL of standard, samples, or blank (untreated media) were added to each well and incubated at RT for 3 hrs. Plates were washed 6x with PBS-T then 50 μL of biotin conjugated IFN-γ (1:2000) or IL-17A (1 μg/mL) in PBS-F was added and incubated for 1 hr and 10 min at RT. Plates were washed 6x with PBS-T then 50 μL avidin-Alkaline phosphatase (1:1000) in PBS-F was added and incubated for 30 min at RT. In the meantime, the substrate was prepared by dissolving 2 tablets in 10 mL of substrate buffer. Plates were washed 6x with PBS-T then 100 μL of substrate buffer was added to wells and plates were incubated at RT until a colometric change was observed. Developed plates were read at an OD of 405 nm using a spectrophotomer (Molecular Devices v max kinetic microplate reader).

Supernatants from 48 hr co-cultures were tested for additional cytokine production using CBA. CBA was performed to detect IL-4, IL-6, IL-10, IL-13, IL-23, TNF-α, and GM-CSF cytokine secretion using BD CBA mouse flex kits (BD Biosciences) and following the manufacturer's instructions. Samples were run on a BD FACS Canto II and standard curves were used to calculate cytokine concentrations in each sample.

2-12 ELISPOT assay

BMDCs were derived from mouse bone marrow progenitor cells over the course of 6-7 days in complete RPMI (cRPMI) supplemented with 10 ng/mL GM-CSF (PeproTech, 315–03), 2 ng/mL IL-4 (PeproTech, 214–14), and 2 mL of cRPMI every other day. Mature BMDCs were pulsed with 10 μg/mL of total SA lipids or lipid fractions overnight. Total SA lipids and lipid fractions were prepared by drying down eluent buffer and resuspending at the appropriate concentration in cRPMI directly before pulsing BMDCs. All lipids were sonicated for 15 min in a

water bath sonicator before pulsing. Pulsed BMDCs were washed 3x with PBS prior to ELISPOT plating.

For ELISPOT assay, Multiscreen-IP plates (Millipore) were coated with 10 μg/ml mouse anti-IFN-γ or anti-IL-17A overnight at 4º C in PBS, then blocked with cRPMI for at least 1 hr at 37º C. Total liver lymphocytes ($2.5x10^5$ cells) or T cell enriched liver lymphocytes ($1x10^5$ cells) were cultured with unpulsed, total SA lipid pulsed, or SA lipid fraction-pulsed BMDCs ($5x10^4$ BMDCs/well) for 18-20 hrs before assay development. Plates were washed 5x 5 min with PBS-T then incubated with 50 μL of biotinylated anti-IFN-γ (0.5 μg/mL) or anti-IL-17A (1 μg/mL) for 1 hr and 40 min at RT. Plates were washed 5x 5 min with PBS-T then incubated with alkaline phosphatase-conjugated streptavidin (1 μg/ml) for 40 min at RT. Plates were washed 5x 5 min with PBS-T then developed using Alkaline Phosphatase Conjugate Substrate Kit (Bio-Rad Laboratories). Developed ELISPOT plates were imaged using an ImmunoSpot reader (Cellular Technology Ltd.).

For ELISPOT blocking experiments, enriched T lymphocytes and SA lipid pulsed BMDCs were incubated with 10 μg/ml mouse IL-12 blocking antibody (eBioscience) or isotype control for 18-20 hrs before development, as described above.

2-13 Activation co-cultures

Total liver lymphocytes ($1x10^6$ cells) from naïve B6 mice were incubated for 24 hrs with BMDCs ($5x10^5$ cells) unpulsed or pulsed with SA lipids or HKSA (BMDC pulsing conditions described in **2-12**). Cells were collected and FACS surface staining was performed for detection of activation markers on NKT cells. Mean fluorescence intensity (MFI) of CD69 on NKT cells cultured alone were normalized to 1. Data was plotted as CD69 MFI change on NKT cells incubated with DC pulsed SA antigens relative to NKT cell alone culture.

2-14 Adoptive transfer of T cells

Recipient mice ($CD45.1^+$ mice) were irradiated with 900 rads of cesium 1 day prior to adoptive transfer. Splenocytes from $CD45.2^+24\alpha\beta$ Tg mice were enriched for T cells as described in **2-7**. $5x10^6$ $24\alpha\beta$ Tg T cells were transferred to recipient mice by retro-orbital injection. 1 day after adoptive transfer, recipient mice were infected via tail vein with $2x10^6$ CFU of SA. Mice were euthanized at 2 dpi and organs were isolated for CFU quantification and intracellular staining.

2-15 RNA isolation and real-time PCR

T cells were enriched from $J\alpha18^{-/-}$ mouse liver or spleen lymphocytes using MACS negative selection as described in **2-7**. Type II NKT cells ($CD4^+NK1.1^+TCR\beta^+$) and conventional $CD4^+$ T cells ($CD4^+NK1.1^-TCR\beta^+$) were sorted from pooled enriched liver T cells or enriched spleen T cells respectively using a FACS cell sorter (BD FacsAria). RNA was extracted from sorted cells using an RNA-easy kit (QIAGEN) and cDNA was generated using Superscript II reverse transcriptase (Invitrogen). RT-PCR was performed using SYBR Green PCR master mix with cytokine primers (listed in **Table 2**) and MyiQ real-time detection system (Biorad). RT-PCR reactions were run in duplicate and cytokine values were normalized to β-actin as the housekeeping gene.

2-16 Statistical analysis

All statistical analyses were performed using GraphPad Prism software. Unpaired Student's *t* test was used for comparison of 2 groups, one-way ANOVA was used for comparison of more that 2 groups, and 2-way ANOVA was used for comparison of more than 2 groups and 2 variables. For CFU quantification statistics, Mann-Whitney test was used. Values are

represented as mean + SEM. Statistical significance is denoted by the annotations: *p<0.05; **p<0.01; ***p<0.001; ****p<0.0001.

Primer name	Primer sequence (5'-3')	Product length
For genotyping		
CD1d F	ATG TTT GAT GGC TGC CTC TGC TCA CTG	WT= 400 bp KO= 200 bp
CD1d R	TGA GTA CAG AGA AGC CAG TGG CCT GGT	
Neo44	CCA AGT GCC CAG CGG GGC TGC TAA AG	
MR1 F	AGC TGA AGT CTT TCC AGA TCG	WT= 426 bp KO= empty
MR1 R	ACA GTC ACA CCT GAG TGG TTG	
MR1 Mid	GAT TCT GTG AAC CCT TGC TTC	
Jα18$^{-/-}$ F	ACT CTG GCG GTG GAA AGA CTA TTG	WT= 301 bp KO= 291 bp
Jα18$^{-/-}$ R	GAT TGT CAT ACC TGG TGA GTA GGT T	
For sequencing		
Jα18$^{-/-}$ F Seq	CCC AAG CCA GGG AGA G	WT= 181 bp KO= 171 bp
For real-time PCR		
IFN-γ F	TCA AGT GGC ATA GAT GTG GAA GAA	92 bp
IFN-γ R	TGG CTC TGC AGG ATT TTC ATG	
TNF-α F	CCA CCA CGC TCT TCT GTC T	211 bp
TNF-α R	GGC ACC ACT AGT TGG TTG T	
IL-2 F	CTT GGA CCT CTG CGG CAT GTT CT	134 bp
IL-2 R	TGG CAC TCA AAT GTG TTG TCA GAG C	
IL-4 F	AAC TCC ATG CTT GAA GAA GAA CTC	134 bp
IL-4 R	CCA GGA AGT CTT TCA GTG ATG TG	
IL-10 F	GGT TGC CAA GCC TTA TCG GA	191 bp
IL-10 R	ACC TGC TCC ACT GCC TTG CT	
IL-13 F	CTC ACT GGC TCT GGG CTT CAT	167 bp
IL-13 R	GGG GAG TCT GGT CTT GTG TGA	
IL-17A F	ACT TTC AGG GTC GAG AAG A	198 bp
IL-17A R	TTC TGA ATC TGC CTC TGA AT	

Table 2. Primers used in this study

Chapter 3

Type II NKT cells contribute to protection against systemic methicillin-resistant *Staphylococcus aureus* infection

3-1 Introduction

Staphylococcus aureus (SA) is a leading cause of healthcare-associated and community-acquired infection in the United States, causing a range of infections in humans. These include skin and soft tissue infection, pneumonia, endocarditis, and bacteremia, which if left untreated, can lead to sepsis and mortality (1). Because SA is an extracellular pathogen, B cells and humoral immunity were thought to be the main drivers of protection. However, in recent years T cells have emerged as key players in SA immunity, as demonstrated in both humans and pre-clinical animal models. HIV patients with decreased $CD4^+$ T cells counts have increased susceptibility to SA bacteremia (80, 81) while patients with a STAT3 mutation resulting in the inability to develop Th17 cells have increased susceptibility to skin and pulmonary SA infections (82). In murine infection models, both $CD4^+$ T cells and $\gamma\delta$ T cells produce IFN-γ and IL-17A that contribute to SA protection. $CD4^+$ T cells produced IL-17A which directed neutrophils to clear SA nasal carriage (85). Additionally, $CD4^+$ memory T cells produced IFN-γ upon secondary peritonitis challenge and promoted recruitment of macrophages and clearance of SA (88). $\gamma\delta$ T cell production of IL-17A was required for protection against SA skin infection by recruitment of neutrophils to the site of infection (99, 100). $\gamma\delta$ T cell IL-17A production was also protective in SA surgical wound infection and in secondary peritonitis infection (102, 103). These studies highlight the important role that T cells play in SA immunity.

While conventional $CD4^+$ T cells and $\gamma\delta$ T cells have been well studied in SA infection, the role of other non-conventional T cells in SA infection is not well understood. NKT cells are innate resident T lymphocytes that are activated rapidly in response to infection and secrete a wide range of cytokines (118). Unlike conventional T cells, NKT cells are restricted by the MHC

class I-like molecule CD1d, which present lipid antigens rather than peptide antigens and can be divided into two groups based on TCR usage and lipid antigen recognition (143, 119). Invariant (iNKT) cells recognize the lipid agonist α-GalCer; CD1d tetramers loaded with this lipid can be used to identify iNKT cells *in vivo* (129-131). iNKT cells recognize glycosphingolipids from *Sphingomonas* species (160) and glycoglycerol lipids from *Streptococcus pneumoniae* and *Borrelia burgdorferi* (161). In murine models of *Streptococcus pneumoniae* and *Borrelia burgdorferi* infection, iNKT cells rapidly produced cytokines which recruited innate immune cells to the site of infection and contributed to bacterial clearance (203, 201). While iNKT cells are enriched in mice, they make up a minority of the NKT cell pool in humans, with type II NKT cells being the dominant human NKT cell subset (266). Type II NKT cells express more diverse TCR than iNKT cells and recognize a wider range of self and microbial lipid antigens. Type II NKT cells have been understudied compared to iNKT cells due to lack of specific tools to identify this polyclonal population *in vivo*, though some studies have demonstrated an active role for type II NKT cells during infection (196). In a mouse model of SA sepsis, administration of sulfatide, a self-lipid known to stimulate a portion of type II NKT cells, protected mice from lethal SA systemic challenge (109). Type II NKT cells recognizes phosphatidylglycerol (PG), cardiolipin, and phosphatidylinositol from *Corynebacterium glutamicum* and *Mycobacterium tuberculosis*, and PG from *Listeria monocytogenes* (179, 180). Both subsets of NKT cells can work synergistically or in opposition during infection. In *Trypanosoma cruzi* infection, type II NKT cells were proinflammatory, increasing parasite-induced mortality and decreasing generation of pathogen-specific antibodies, whereas iNKT cells were anti-inflammatory, contributing to reduced mortality (220). In hepatitis B virus (HBV) infection, iNKT and type II NKT cells protected mice from infection; type II NKT cells were activated by CD1d-presented HBV modified lysophospholipids then activated APCs to produce IL-12 which activated iNKT cells (213). These studies highlight the differential roles of NKT cell subsets in response to infection.

However, the relative contribution of iNKT cells and type II NKT cells to protective immunity against SA infection has not been explored.

In this study, I determined whether these NKT cell subsets play dominant or synergistic roles during systemic infection with the methicillin-resistant USA300 SA strain. I also determined whether NKT cell subsets recognize lipid antigens derived from SA that could be used in the creation of a subunit vaccine design. Our data showed that both NKT cell subsets were activated and expanded after SA infection. However, only type II NKT cells were necessary for lowering bacterial burden in SA infected liver and kidneys in early-stage infection. Protection was mediated by type II NKT cell IFN-γ production to polar lipid species derived from the SA cell membrane. This protective effect was unique for type II NKT cells, as mice lacking mucosal associated invariant T (MAIT) cells, another innate-like T cell subset which recognizes microbially derived vitamin B-related metabolites (267, 227), had no significant increase in SA bacterial burden. I also demonstrate that a population of T cells enriched for type II NKT cells, but not MAIT cells or iNKT cells, were elevated in PBMC of patients with systemic SA infection, demonstrating the relevance of our findings to the human setting.

3-2 Results

3-2.1 Mice lacking NKT cells had increased bacterial burden and neutrophil infiltration in infected liver and kidneys following systemic SA infection

Given that NKT cells play a protective role in the early response to many bacterial infections, I determined whether NKT cells were important for controlling bacterial growth in infected organs after bloodstream challenge with the methicillin-resistant SA strain USA300 LAC, a clinical isolate responsible for many community-acquired skin and soft-tissue infections as well as systemic infections (268). To investigate this, I used C57BL/6 mice (B6) and $CD1d^{-/-}$ mice on the B6 background; $CD1d^{-/-}$ mice lack NKT cells due to the absence of CD1d expression on double-positive thymocytes, which is required for positive selection of NKT cells in the thymus (263). After intravenous injection, the characteristic route of SA progression through the body is to be phagocytosed by liver Kupffer cells within 24 hrs after infection. SA then lyses Kupffer cells over a period of 2-5 days and migrates to the kidneys, where the bacteria establish abscesses (11, 48). I therefore quantified bacteria in the liver and kidneys of SA-infected mice at various times post infection. $CD1d^{-/-}$ mice had increased bacterial burdens in liver and kidneys compared to B6 mice at 4 days post infection (dpi), though both genotypes had equivalent burdens by 8 dpi (**Fig. 3-1A, B**). I characterized immune cell infiltrates in infected kidneys and liver by flow cytometry and identified that neutrophils were increased in the kidneys and liver of $CD1d^{-/-}$ mice relative to B6 mice (**Fig. 3-1C, D**).

Figure 3-1. Mice lacking NKT cells have increased bacterial burdens and neutrophilic infiltrate in SA infected organs.

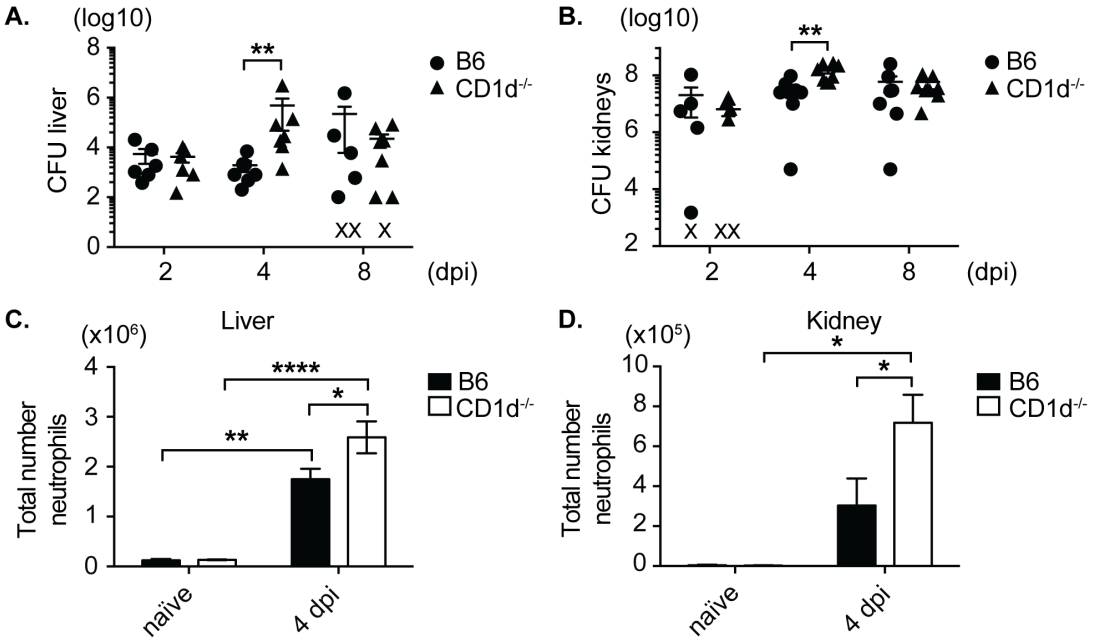

Figure 3-1: (A, B) Colony forming units (CFU) quantified in liver (A) and kidneys (B) of B6 and CD1d$^{-/-}$ mice at various times post infection (N=6-8 mice/genotype/timepoint). **(C, D)** Total number of neutrophils in the liver (C) and kidney (D) of infected mice (liver: N=3 naïve, N=14 4 dpi/genotype, kidney: N=4 naïve, N=11-12 4 dpi/genotype). Statistical analysis: (A-B) Mann-Whitney test; (C-D) 2-way ANOVA.

I also looked at expansion of other immune cell infiltrates, including APCs and conventional T cells, in the kidney and liver after SA infection. No significant difference in total number of B cells, macrophages, dendritic cells, and conventional T cells (CD4$^+$ and CD8$^+$) in infected liver and kidneys were detected between B6 and CD1d$^{-/-}$ mice (**Fig. 3-2, Fig. 3-3**). These data suggested that NKT cells were critical at early stages of infection to control SA growth and neutrophil infiltration in infected liver and kidneys.

Figure 3-2. Absence of NKT cells does not alter other antigen presenting cell expansion in infected organs.

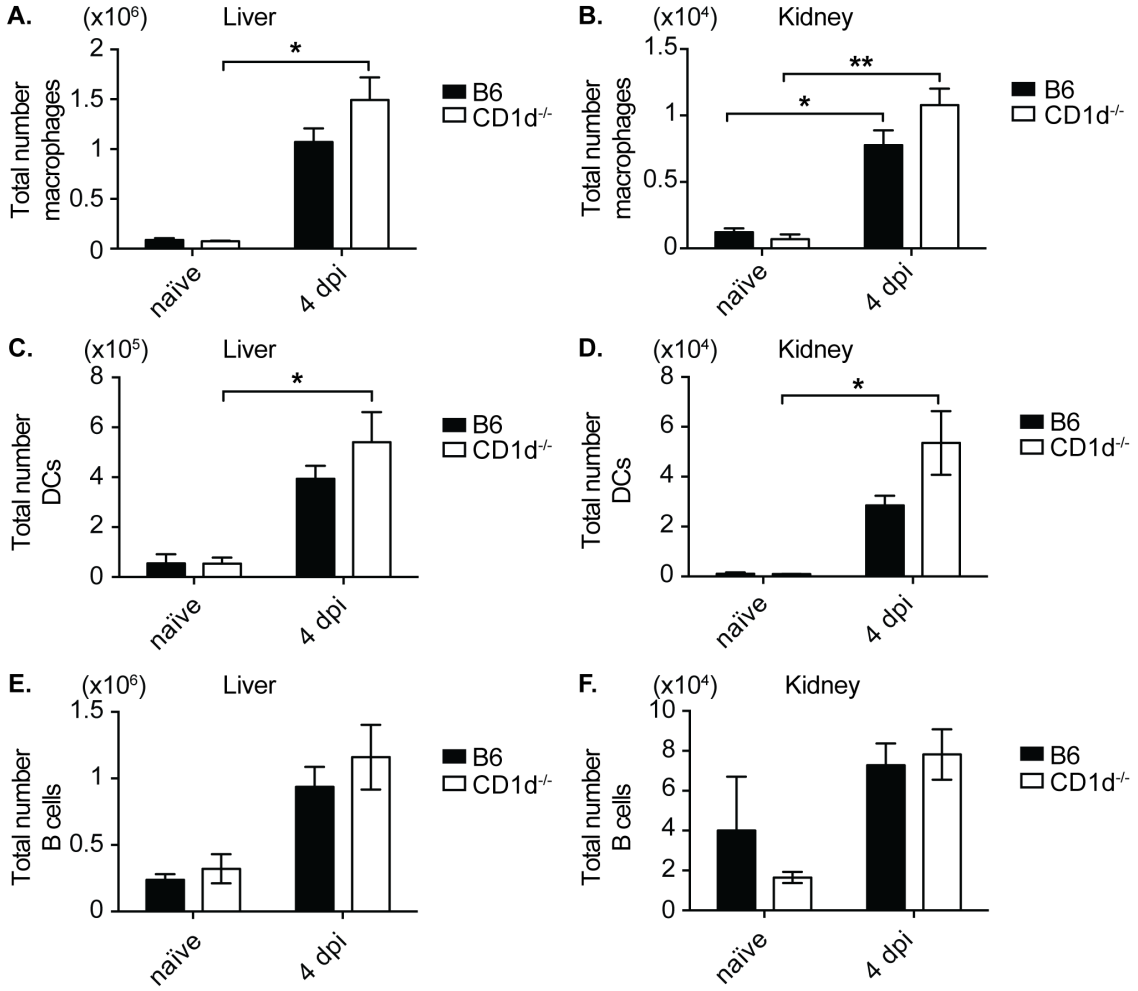

Figure 3-2: (A, B) Total number of macrophages in the liver (A) and kidney (B) at 4 dpi. (**C, D)** Total number of dendritic cells (DC) in the liver (C) and kidney (D) at 4 dpi. (**E, F)** Total number of B cells in the liver (E) and kidney (F) at 4 dpi. Kidney (N=2 naïve, N=7 4 dpi mice), liver (N=3 naïve, N=9-10 4 dpi mice). Statistical analysis: (A-F) 2-way ANOVA.

Figure 3-3. Absence of NKT cells does not alter conventional T cell expansion in infected organs.

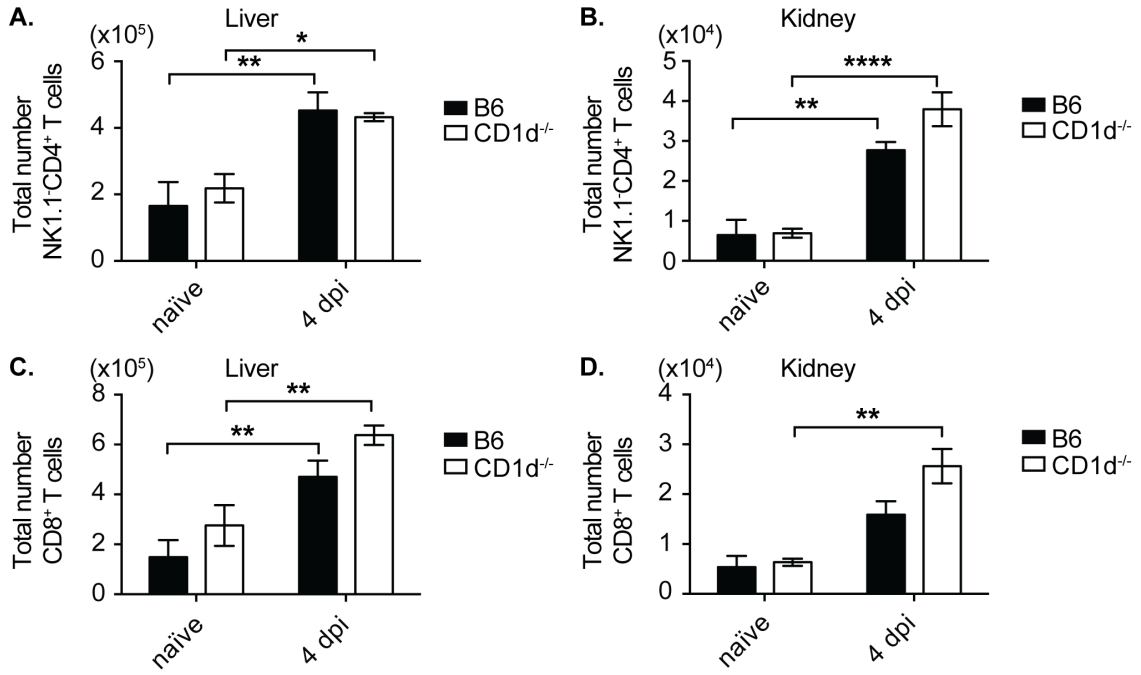

Figure 3-3: (A-D) Total number of conventional $CD4^+$ T cells and $CD8^+$ T cells from the liver (A, C) and kidney (B, D) at 4 dpi (N=3 naïve, N=7 4 dpi mice). Statistical analysis: 2-way ANOVA.

3-2.2 Type II NKT cells were sufficient to mediate cytokine production and SA control in infected organs

To determine whether type II NKT cells were sufficient to reduce SA bacterial burden, I infected Jα18$^{-/-}$ mice. These mice contain a 10-base-pair deletion in the *Traj18* gene and therefore do not develop Vα14-Jα18 expressing iNKT cells (261). These mice are a corrected version of the original Jα18$^{-/-}$ mouse strain, which had lower TCR diversity due to suppressed transcription of TRAJ gene segments downstream of TRAJ18 (262). A mouse model lacking type II NKT cells but retaining iNKT cells has not been developed, therefore I could not test the efficacy of iNKT cells alone in control of SA bacterial burdens. A summary of the three mouse strains used in this study are listed in **Table 3**.

Mouse strain	iNKT cell development	Type II NKT cell development
B6	Yes	Yes
Jα18$^{-/-}$	No	Yes
CD1d$^{-/-}$	No	No

Table 3: Summary of NKT cell development in mouse strains used in this study

B6 and Jα18$^{-/-}$ mice had similar bacterial burdens in the liver and kidney at all timepoints tested post infection, while CD1d$^{-/-}$ mice again had significantly increased bacterial burdens in the liver and kidney at 4 dpi (**Fig. 3-4A-C**), which suggested that type II NKT cells were sufficient to control SA growth in the absence of iNKT cells at this timepoint. I also assessed pathology of inflammatory foci and abscess formation in the kidney at 4 dpi by H&E staining (**Fig. 3-4D, E**). Compared to B6 and Jα18$^{-/-}$ mice, where inflammatory foci (marked with arrow heads) were predominantly found in the renal pelvis, CD1d$^{-/-}$ mice had significantly larger inflammatory foci found in all areas of the kidneys (additional histology images quantified in **Fig. 3-4E** shown in **Fig. 3-5**).

Figure 3-4. Type II NKT cells were sufficient to reduce bacterial burden and inflammatory foci in infected liver and kidneys of mice challenged with sublethal dose of SA.

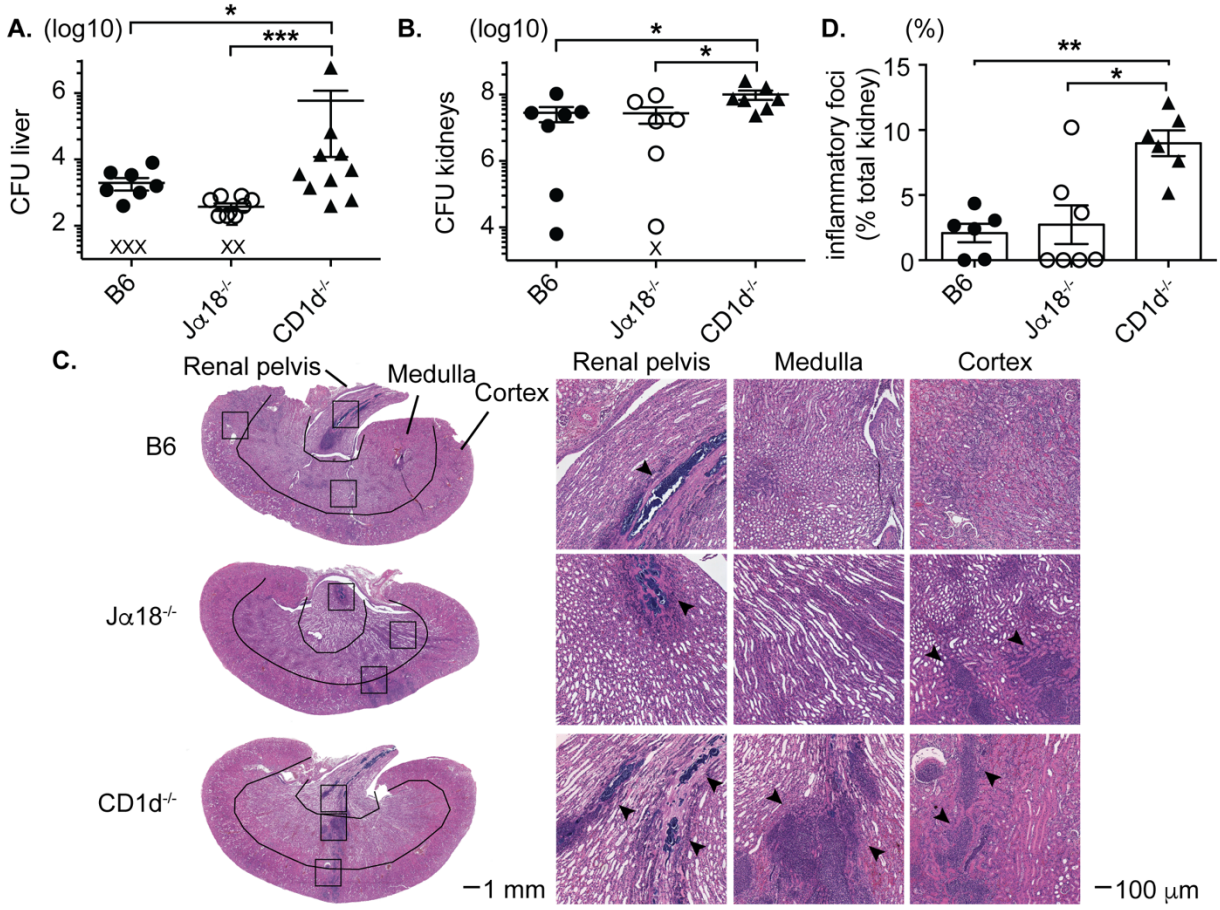

Figure 3-4: (A, B) CFU quantified in the liver (A) and kidney (B) of indicated mice at 4 dpi: liver (N=6-13 mice/genotype), kidney (N=6-8 mice/genotype) (X=below limit of detection). **(C, D)** H&E staining of kidney sections at 4 dpi, inflammatory foci area quantified in (D) (N=6-7 mice/genotype). Statistical analysis: (A, B, D) Mann-Whitney test.

Figure 3-5. H&E sections of quantified kidney inflammatory foci areas.

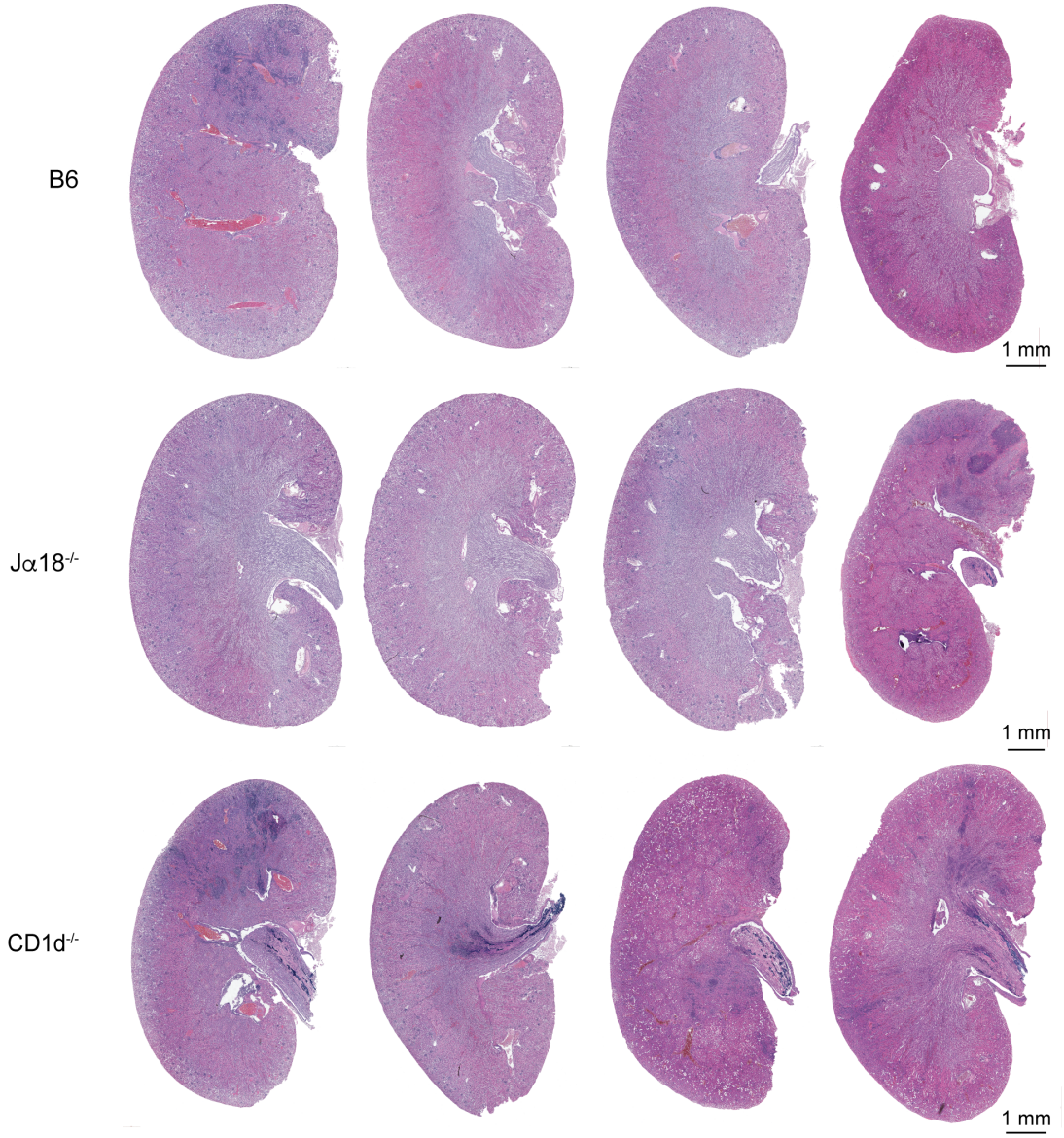

Figure 3-5: H&E sections of quantified kidney inflammatory foci areas.

I then tested which cytokines were induced after SA infection and whether cytokine production was altered in mice lacking NKT cells. I focused on the liver and spleen because these are the organs where NKT cells are enriched. I isolated liver and spleen lymphocytes from naïve and 4 dpi SA-infected mice, and restimulated them *in vitro* with heat-killed SA (HKSA) then tested cytokine production by ELISA. I focused on IFN-γ and IL-17A production because these cytokines have been demonstrated to play protective roles in models of SA infection. SA

infected mice produced IFN-γ in response to HKSA stimulation, whereas naïve mice did not, demonstrating that IFN-γ production was SA specific (**Fig. 3-6A, B**). In contrast to IFN-γ production, IL-17A production after HKSA stimulation was low and not increased after infection (**Fig. 3-6C, D**). CD1d$^{-/-}$ mice produced less IFN-γ in response to *in vitro* restimulation with HKSA compared to infected B6 and Jα18$^{-/-}$ mice at 4 dpi (**Fig. 3-6A, B**). In the liver, iNKT cells were partially responsible for the CD1d-restricted IFN-γ response to HKSA, as B6 liver lymphocytes produced more IFN-γ than Jα18$^{-/-}$ liver lymphocytes (**Fig. 3-6A**). However, type II NKT cells were sufficient for CD1d-restricted IFN-γ production in the absence of iNKT cells in the spleen (**Fig. 3-6B**). Together, these data suggested that type II NKT cells were sufficient to reduce bacterial burden and kidney inflammatory infiltrate while enhancing IFN-γ production in the early stages of SA infection.

Figure 3-6. Type II NKT cells were sufficient to mediate IFN-γ production in infected organs.

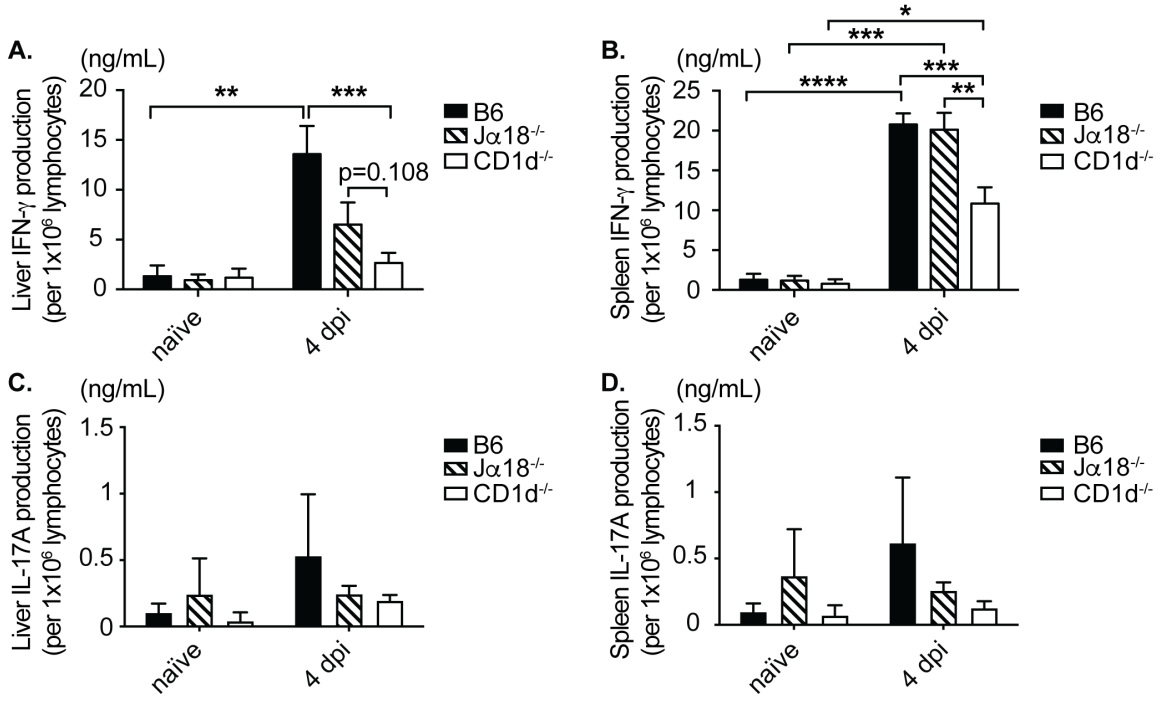

Figure 3-6: (A, B) IFN-γ ELISA of liver (A) and spleen (B) lymphocytes from 4 dpi mice pulsed with HKSA, unstimulated not graphed (undetectable) (N=2-4 naïve, N=7-10 infected mice/genotype). **(C, D)** IL-17A ELISA of liver (C) and spleen (D) lymphocytes from 4 dpi mice pulsed with HKSA, unstimulated not graphed (undetectable) (N=2 naïve, N=5-7 infected mice/genotype). Statistical analysis: (A-D) 2-way ANOVA.

3-2.3 NKT cells were activated and underwent expansion and proliferation after SA infection

Our data thus far demonstrated that NKT cells, and more specifically type II NKT cells, were crucial for limiting SA bacterial burden and neutrophil infiltrate to infected liver and kidneys. I then determined whether NKT cells became activated and expanded during SA infection. I identified iNKT cells *in vivo* using a CD1d tetramer loaded with PBS57, an α-GalCer analog (**Fig. 3-7A**). Since I did not have tetramers to specifically identify type II NKT cells *in vivo*, I used a negative gating strategy to remove iNKT cells and $CD8^+$ T cells, then gated on

$CD4^+NK1.1^+TCR\beta^+$ cells. This strategy allowed us to look at polyclonal type II NKT cells *in vivo* **(Fig. 3-7B**).

Figure 3-7. Time course of NKT cell kinetics during SA infection.

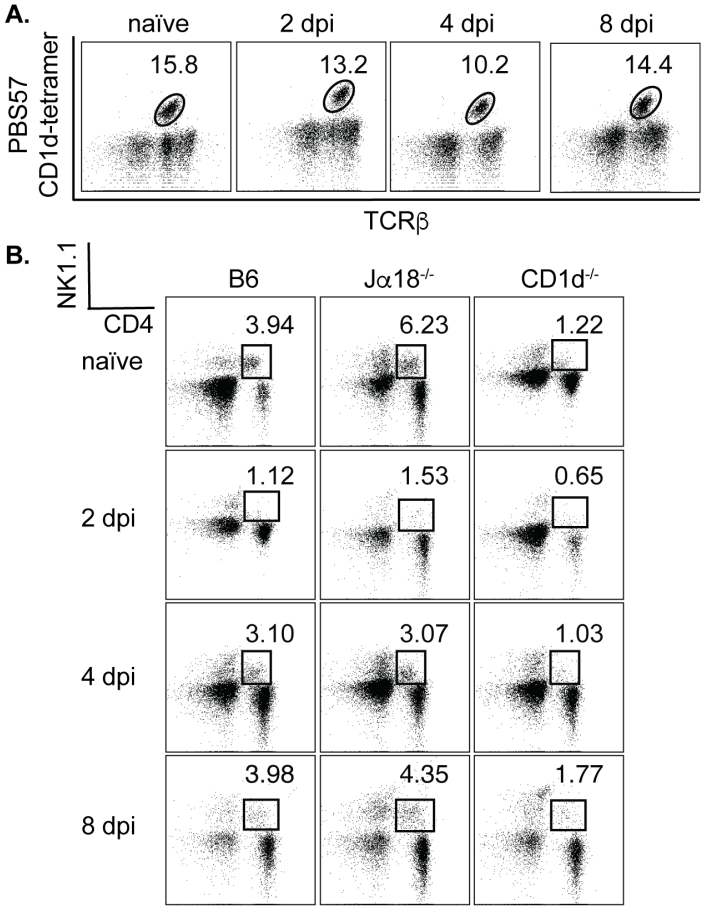

Fig. 3-7: (A) iNKT cells gated in B6 liver. (**B)** Type II NKT cells gated in B6, $J\alpha18^{-/-}$, and $CD1d^{-/-}$ liver.

Both iNKT cells and type II NKT cells expanded in the liver of SA-infected B6 and $J\alpha18^{-/-}$ mice (**Fig. 3-8A, B**) at 4 dpi, then contracted by 8 dpi. I confirmed that PBS57 CD1d $TET^-CD8\alpha^-$ $CD4^+NK1.1^+TCR\beta^+$ cells were CD1d-restricted type II NKT cells, as the percentage and total number of this population was reduced in $CD1d^{-/-}$ mice after infection (**Fig. 3-7B and Fig. 3-8B**). At 2 dpi, liver iNKT cells and type II NKT cells upregulated the activation marker CD69 (**Fig. 3-8C, D**). Both iNKT cells and type II NKT cells upregulated Ki67, a cell proliferation marker, at 2

and 4 dpi (**Fig. 3-8E-G**), demonstrating that NKT cells were proliferating in response to SA infection. By 8 dpi, Ki67 expression was reduced to naïve levels, suggesting that NKT cells underwent contraction or cell death after their function was performed. These data demonstrated that both iNKT and type II NKT cells were poised to respond quickly to SA infection as denoted by upregulation of activation markers and cell expansion at early times post-infection.

Figure 3-8. iNKT cells and type II NKT cells were expanded and activated in the liver after SA infection.

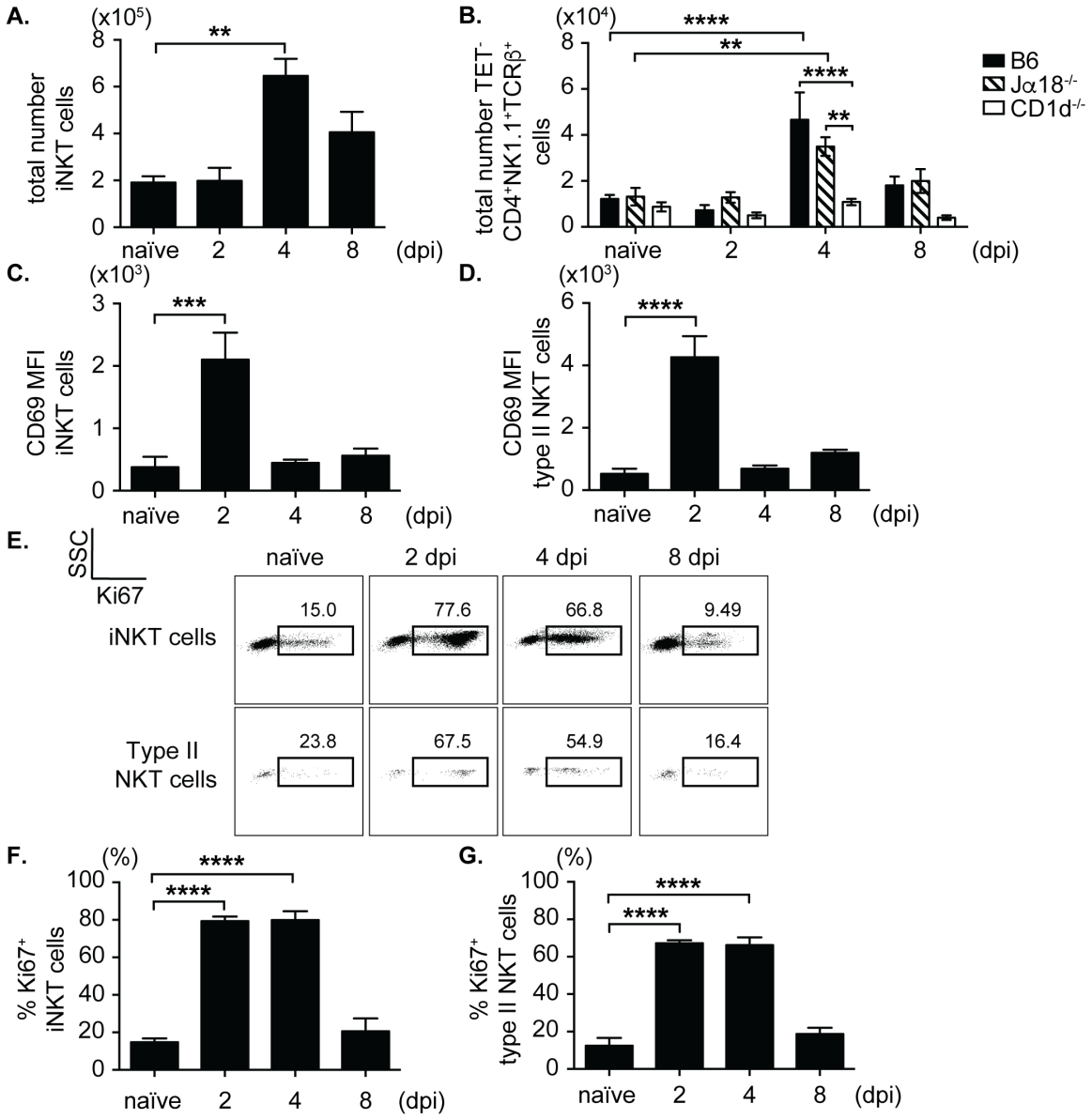

Figure 3-8: (A, B) Total number of iNKT cells (A) and type II NKT cells (B) in liver at various times post infection (N=4-5 naïve, N=4-8 infected mice/timepoint). **(C, D)** CD69 mean fluorescence intensity (MFI) of iNKT cells (C) and type II NKT cells (D) from the liver of SA-infected B6 mice or Jα18$^{-/-}$ mice respectively (N=4 naïve, N=4-6 infected mice/timepoint). **(E-G)** Ki67 expression in iNKT cells and type II NKT cells from SA-infected B6 livers. Representative Ki67 dot plot (E) quantified as % of iNKT cells (F) and type II NKT cells (G) (N=4 naïve, N=3-7 infected mice/timepoint). Statistical analysis: (A, C-G) one-way ANOVA, (B) 2-way ANOVA.

Type II NKT cells in the mouse can be $CD4^+CD8^-$ or $CD4^-CD8^-$ (196). To further confirm our gating strategy for type II NKT cells, I output PBS57 CD1d $TET^-CD4^-CD8^-$ $NK1.1^+TCR\beta^+$ cells and looked at the expansion of this population in the liver after SA infection (**Fig. 3-9**). $CD4^-NK1.1^+$ T cells were expanded at 4 dpi in the liver, but this expansion was not CD1d-restricted, demonstrating that these cells were not type II NKT cells (**Fig. 3-9A, B**). Additionally, this cell population was not activated until 8 dpi, behaving more similar to conventional T cells in terms of activation kinetics (**Fig. 3-9C**). This confirmed our gating strategy for type II NKT cells in the liver.

Figure 3-9. $CD4^-NK1.1^+$ T cells were expanded and activated independent of CD1d after SA infection.

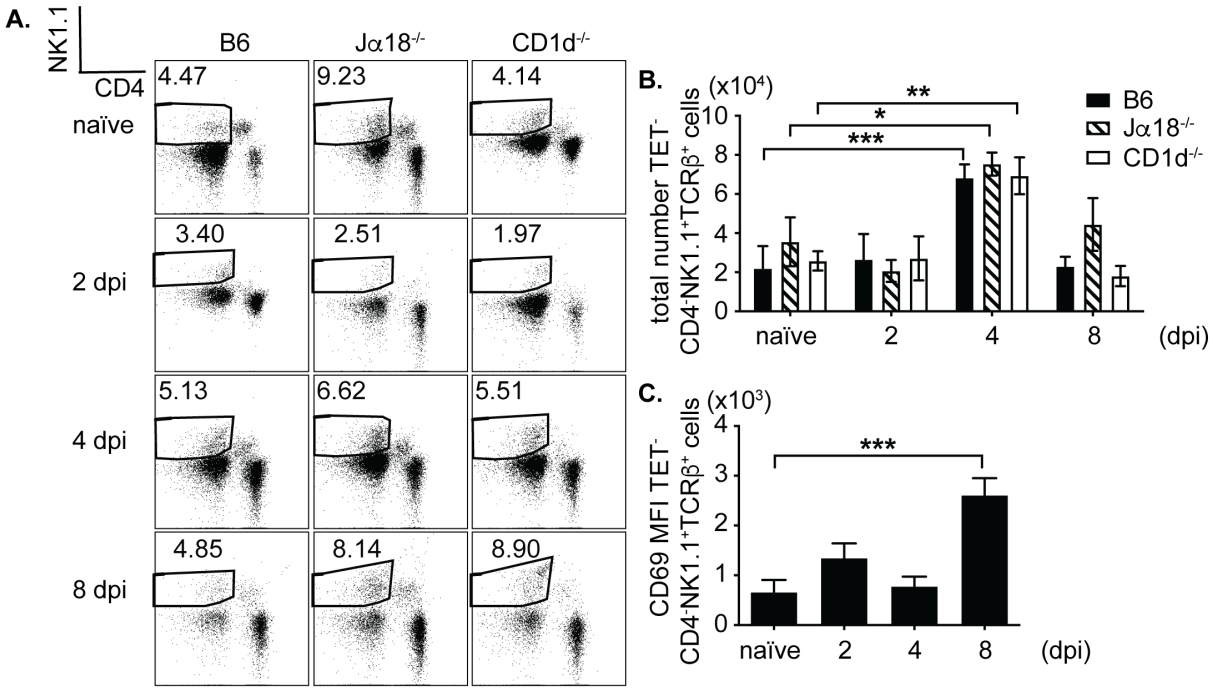

Figure 3-9: (A) $CD4^-NK1.1^+$ T cells gated in B6, $J\alpha18^{-/-}$, and $CD1d^{-/-}$ liver. **(B-C)** Total number (B), and CD69 MFI (C) of $CD4^-NK1.1^+$ T cells from the liver of SA-infected B6 mice (N=4-6 naïve, N=4-8 infected mice/timepoint). Statistical analysis: (B) two-way ANOVA, (C) one-way ANOVA.

I also looked at NKT cell activation and expansion in other organs after SA infection. In the spleen I saw activation, but not expansion of iNKT cells after SA infection (**Fig. 3-10A, B**). Using my gating strategy for type II NKT cells, I did not see an expansion of this population in B6 mice, however I did see a CD1d-restricted expansion of this population in Jα18$^{-/-}$ mice at 2 dpi (**Fig. 3-10C**). Because there are very few type II NKT cells in mouse B6 spleens, their lack of expansion could be due to the very small starting population in the spleen. iNKT cells and type II NKT cells fill a similar unconventional T cell niche, so it is possible that in the absence of iNKT cells, type II NKT cells could expand to a larger degree than in B6 mice. Like iNKT cells, type II NKT cells were activated in the spleen after infection (**Fig. 3-10D**). These data demonstrated that in addition to the liver, NKT cells were also activated in the spleen.

Figure 3-10. iNKT cells and type II NKT cells were activated but not expanded in spleen.

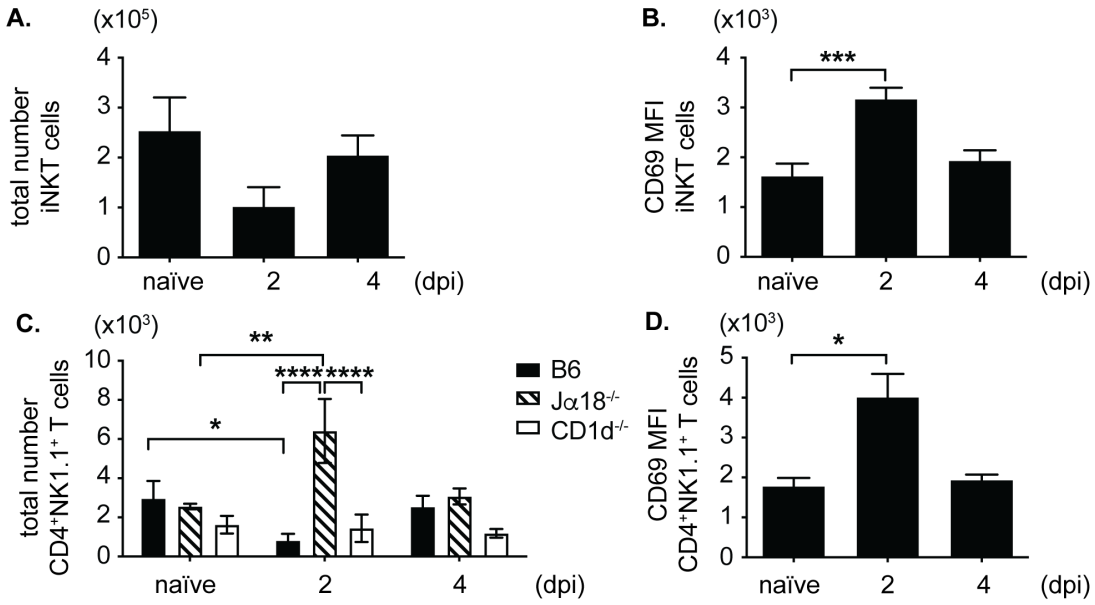

Figure 3-10: (A, B) Total number of iNKT cells (A) and type II NKT cells (C) in spleen at various times post infection (N=3-8 naïve, N=3-8 infected mice/timepoint). **(C, D)** CD69 mean fluorescence intensity (MFI) of iNKT cells (B) and type II NKT cells (D) from the liver of SA-infected B6 mice (N=4-5 naïve, N=4-7 infected mice/timepoint). Statistical analysis: (A-B, D) one-way ANOVA, (C) 2-way ANOVA.

In addition to spleen and liver where NKT cells are enriched, I also looked at NKT cell activation and expansion in the kidney and pooled peripheral and kidney draining LN after SA infection. Compared to the liver and spleen, iNKT cells made up a minor population of lymphocytes in the kidney and LN. iNKT cells were expanded in kidney, but not LN after SA infection (**Fig. 3-11B, E**). iNKT cells did not upregulate CD69 in kidney but did upregulate CD69 in the LN (**Fig. 3-11C, F**). I also attempted to quantify type II NKT cells in the kidney and LN, however I was not able to detect a significant CD1d-restricted T cell population using our gating strategy in these organs, due to the very small population of type II NKT cells in these organs.

Figure 3-11. iNKT cells were expanded in kidney but not lymph node after SA infection.

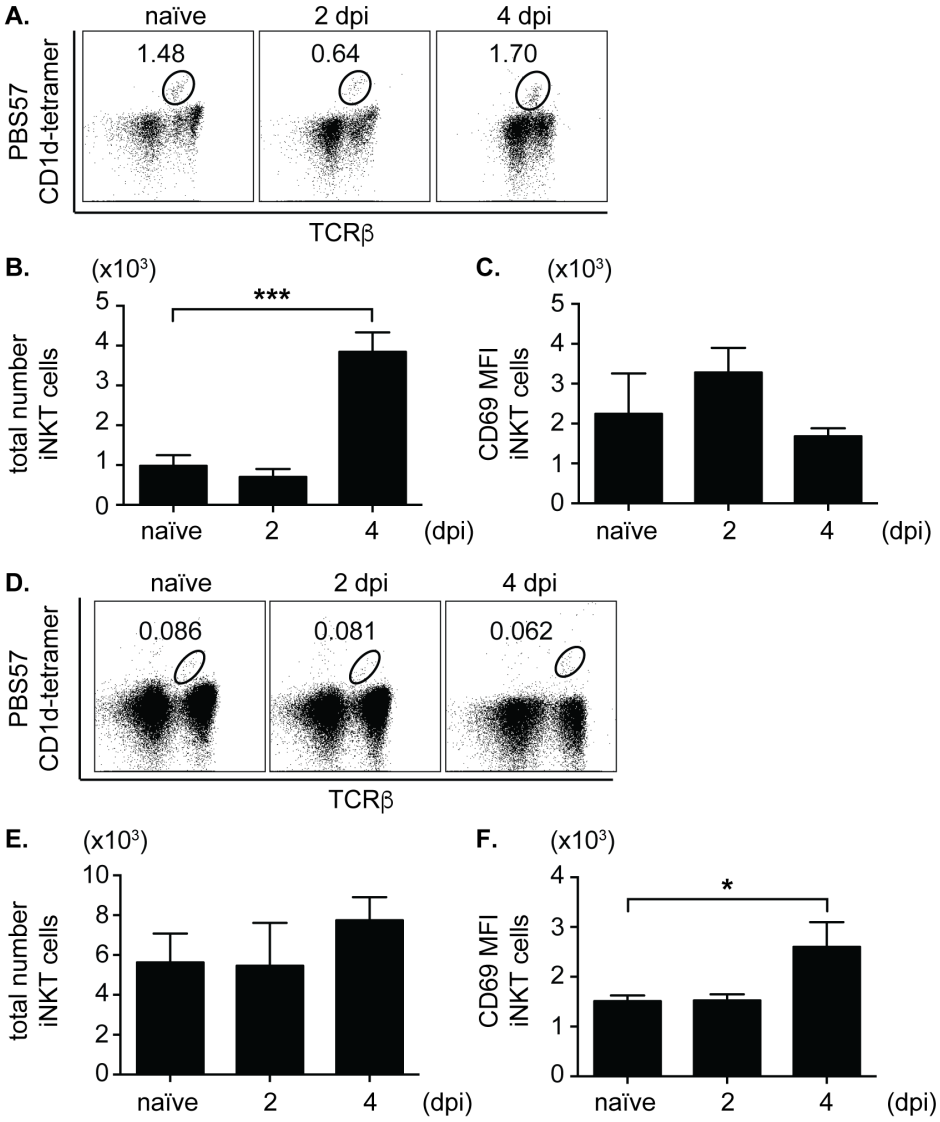

Figure 3-11: (A) Representative FACS plots of iNKT cells in the kidney of B6 mice at various times post infection. (**B, C)** Total cell number and CD69 MFI of iNKT cells in the kidney of B6 mice (N=3 naïve, N=4-6 infected mice/timepoint). (**D)** Representative FACS plots of iNKT cells in pooled peripheral and kidney draining lymph node (LN) of B6 mice at various times post infection. (**E, F)** Total cell number and CD69 MFI of iNKT cells in LN of B6 mice (N=5 naïve, N=5-10 infected mice/timepoint). Statistical analysis: (B-C, E-F) one-way ANOVA.

As previously described, type II NKT cells encompass polyclonal CD1d-restricted T cells recognizing lipid antigens from diverse bacterial species (179, 180). To determine whether specific type II NKT cell populations were expanded in the liver after SA infection, I probed type II NKT cell surface expression of different Vβ chains in naïve and infected Jα18$^{-/-}$ mice. Similar to previously published work (146), the majority of polyclonal type II NKT cells utilized the Vβ8.1/8.2 chain, with smaller populations expressing diverse Vβ chains (**Fig. 3-12A**). I saw no significant alteration of Vβ chain usage in naïve vs. infected mice, suggesting that type II NKT cells polyclonally expanded after infection. In contrast to type II NKT cells, conventional CD4^{+} cells had more diverse Vβ chain usage that was not altered after SA infection (**Fig. 3-12B**). In summary, I showed that NKT cells were activated and expanded in multiple organs after SA infection, demonstrating their potential relevance for contributing to anti-SA immunity.

Figure 3-12. Type II NKT cells polyclonally expanded after SA infection.

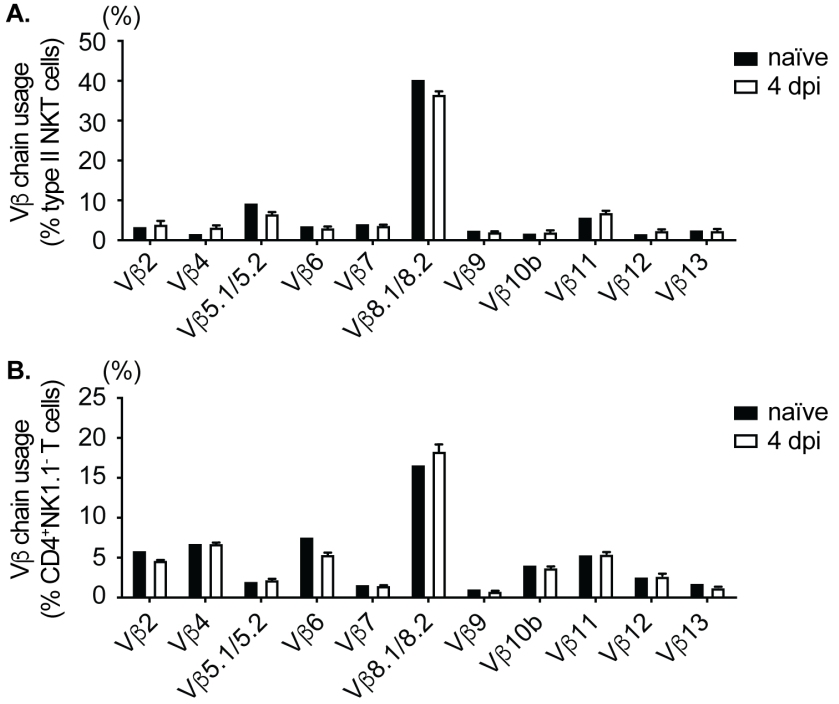

Figure 3-12: (A-B) Vβ chain usage of type II NKT cells (A) or conventional CD4^{+} T cells (B) in the liver of Jα18$^{-/-}$ mice at 4 dpi (N=3 pooled naïve, N=7 infected mice). Statistical analysis: (A-B) 2-way ANOVA.

3-2.4 NKT cells produced SA-specific IFN-γ after infection

After demonstrating that NKT cells were activated after SA infection, I then determined whether NKT cells produced cytokines directly in response to infection that could be driving the reduction in CFU I saw in CD1d expressing mice in the early phase of infection (**Fig. 3-1, 3-4**). To look at SA-mediated cytokine production, I isolated liver lymphocytes from SA-infected B6 mice at various timepoints and performed intracellular staining *ex vivo* without restimulation. I focused on IFN-γ production, as liver and spleen lymphocytes produced CD1d-restricted IFN-γ in response to HKSA stimulation (**Fig. 3-6**). Both iNKT cells and type II NKT cells produced IFN-γ at 1 dpi which was lost by 4 dpi (**Fig. 3-13**). This initial burst of cytokine production early in response to infection is in keeping with the kinetics of NKT cell cytokine production in other models of infection (198, 269, 270).

Figure 3-13. NKT cells produced IFN-γ early in response to SA infection.

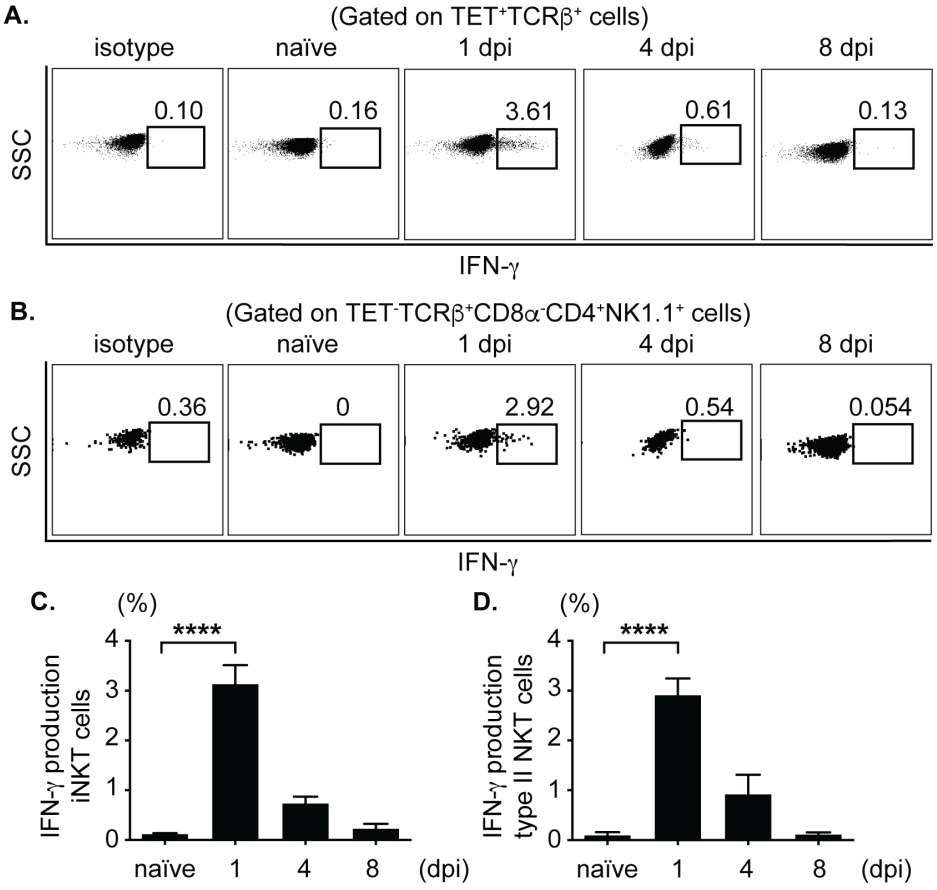

Figure 3-13: (A-B) Representative FACS plots of IFN-γ production, gated on iNKT cells (A) and type II NKT cells (B) in the liver of B6 mice at various times post infection. **(C-D)** % of IFN-γ producing iNKT cells (C) and type II NKT cells (D) in the liver of B6 mice at various times post infection (N=6 naïve, N=2-12 infected mice/timepoint). Statistical analysis: (C-D) one-way ANOVA.

In addition to quantifying IFN-γ by NKT cells after SA infection, I looked at a panel of cytokines known to be produced by NKT cells in other models of infection and disease states (196). The production of IL-2, IL-10, IL-17A and TNF-α by iNKT cells were either absent or remained unchanged between naïve and 1 dpi SA infected mice (**Fig. 3-14A**). iNKT cells produced some IL-4 in the naïve state that was decreased after SA infection, demonstrating a shift of cytokine production from IL-4 to IFN-γ. Type II NKT cell production of IL-2, IL-4, IL-10, IL-17A and TNF-α was either absent or remained unchanged between naïve and infected mice

(**Fig. 3-14B**). To determine whether type II NKT cells had upregulated cytokine mRNA relative to conventional T cells after infection, I isolated RNA from sorted type II NKT cells at 4 dpi from pooled liver lymphocytes of Jα18$^{-/-}$ mice for real-time PCR. I focused on this timepoint because this was when I saw the greatest expansion of type II NKT cells and was able to sort enough cells to obtain RNA (**Fig. 3-8**). RNA isolated from conventional CD4^{+}NK1.1^{-} T cells from the spleen of these mice were used for comparison purposes. At 4 dpi, type II NKT cells had upregulated Th1 and Th2 cytokine mRNA relative to conventional CD4^{+} T cells, with IFN-γ being the cytokine most upregulated (**Fig. 3-14C**). Interestingly, conventional CD4^{+} T cells had higher cytokine mRNA expression of IL-17A, demonstrating skewing towards a Th17 phenotype. In summary, these data suggest that NKT cells were poised to respond to SA at an earlier timepoint than conventional T cells by Th1 skewing and production of IFN-γ.

Figure 3-14. Type II NKT cells skewed towards a Th1 phenotype after SA infection.

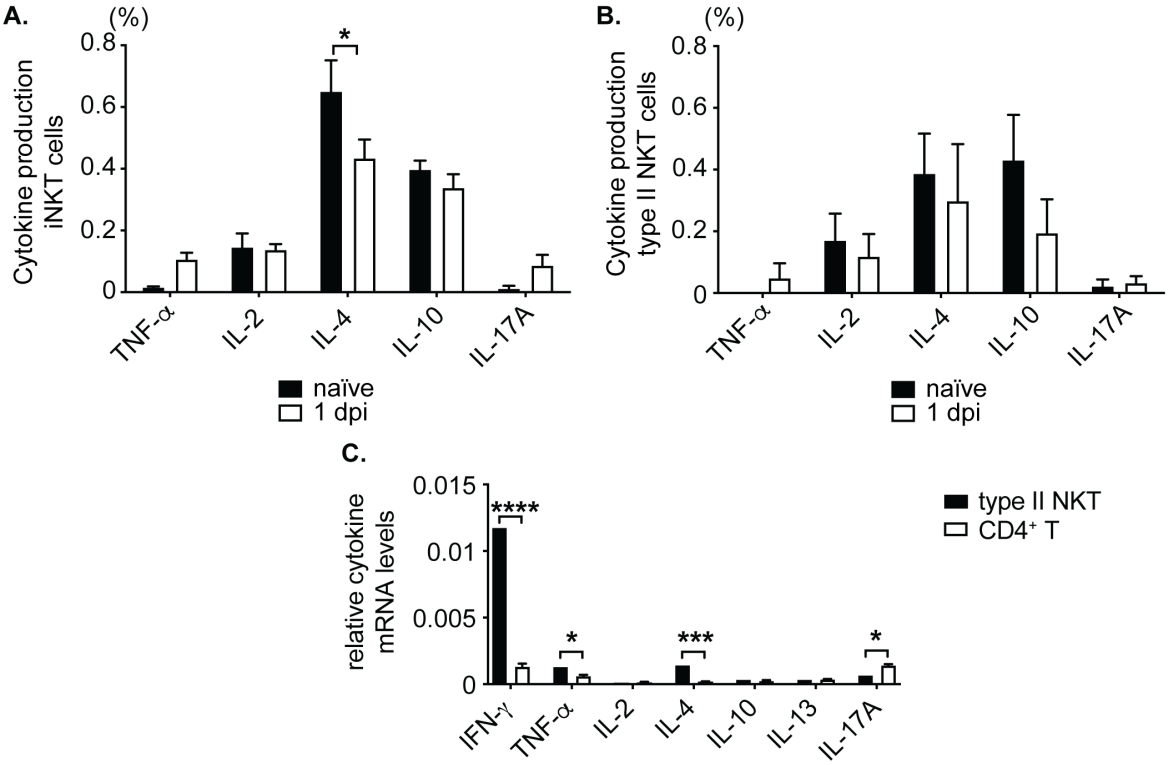

Figure 3-14: (A-B) % of cytokine producing iNKT cells (A) and type II NKT cells (B) in the liver of B6 mice at various times post infection (N=3-5 naïve, N=5-12 infected mice). **(C)** rt-PCR of cytokine mRNA of type II NKT cells sorted from 4 dpi Jα18$^{-/-}$ mouse pooled liver lymphocytes (N=10 mice) compared to sorted conventional CD4^{+}NK1.1^{-} T cells from Jα18$^{-/-}$ splenocytes (N=2 mice), data represented as cytokine mRNA levels relative to β-actin. Statistical analysis: (A-C) 2-way ANOVA.

Systemic exposure to a number of microorganisms was demonstrated to render iNKT cells hyporesponsive to antigen restimulation (186-188). To determine whether iNKT cells became hyporesponsive to restimulation after SA infection, I co-cultured B6 lymphocytes from naïve or 4 dpi mice with the iNKT cell agonist α-GalCer. While iNKT cells from naïve mice produced abundant IFN-γ after α-GalCer stimulation, iNKT cells from infected mice had severely reduced IFN-γ production (**Fig. 3-15A**). I took supernatants from these co-cultures and tested for additional cytokine production by CBA. Liver iNKT cells from SA-infected B6 mice produced less cytokines, including IL-4, IL-13, and GM-CSF, in response to *in vitro* α-GalCer stimulation compared to iNKT cells from naïve mice (**Fig. 3-15B**). In addition, iNKT cells from infected mice

produced less IFN-γ compared to their naïve counterparts in response to PMA/Ionomycin stimulation, demonstrating that iNKT cells became hyporesponsive to restimulation after SA infection (**Fig. 3-15C, E**). In contrast, type II NKT cells stimulated with PMA/Ionomycin did not have altered IFN-γ production after SA infection, and in fact had a slight increase in cytokine production after infection, demonstrating that type II NKT cells were able to respond to stimuli after SA infection (**Fig. 3-15D, F**). Given that type II NKT cells, and not iNKT cells were necessary for mediating CFU and inflammatory foci reduction in SA infected organs, I focused on type II NKT cells and their ability to help protect mice from SA infection.

Figure 3-15. iNKT cells were hyporesponsive to restimulation after SA infection.

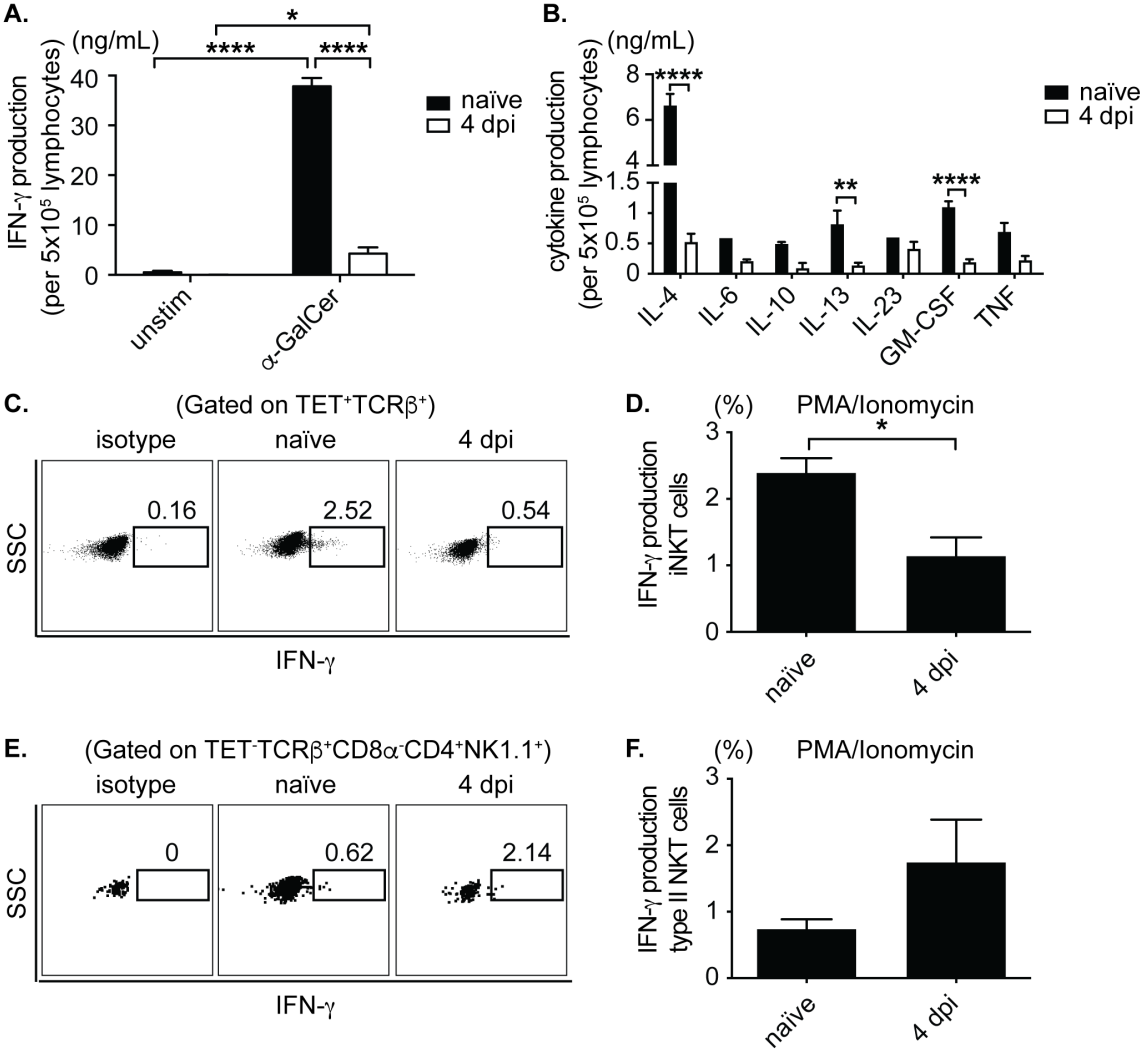

Figure 3-15: (A) IFN-γ ELISA of B6 liver lymphocytes co-cultured with α-GalCer (N=2-5 mice/timepoint, representative 1 of 5). **(B)** CBA of B6 liver lymphocytes cultured with α-GalCer (N=2-5 mice/timepoint, representative 1 of 2). **(C, E)** Representative IFN-γ FACS plots gated on iNKT cells (C) or type II NKT cells (E) in naïve and 4 dpi mouse liver lymphocytes stimulated with PMA/Ionomycin (2 hrs + 4 hrs BFA). **(D, F)** % IFN-γ production by iNKT cells (D) or type II NKT cells (F) in naïve and 4 dpi mouse liver lymphocytes stimulated with PMA/Ionomycin (N=3-5 naïve, N=5 infected mice). Statistical analysis: (A, B) 2-way ANOVA, (D, F) student's *t* test.

3-2.5 Type II NKT cell required both TCR-restricted and TCR-independent signals to become activated and produce IFN-γ in response to SA lipid antigens

Given that iNKT cells were dispensable for control of bacterial burden after systemic SA infection, I focused on how type II NKT cells were activated and contributed to protection. Work from our lab demonstrated that group 1 CD1-restricted T cells recognized polar lipids derived from the SA cell membrane (115), but SA lipid antigens recognized by type II NKT cells have not been described to date. I worked with a lipid biochemist to extract total SA lipids from the cell membrane of the USA300 SA strain (methods described in section **2-10.1**) To determine whether type II NKT cells recognized total SA lipids, total liver lymphocytes from infected Jα18$^{-/-}$ mice were co-cultured with BMDCs unpulsed or pulsed with total SA lipids. I utilized MHC class II knockout (MHC-II$^{-/-}$) DCs to remove any MHC-II conventional CD4 T cell-mediated response and compared MHC-II$^{-/-}$ to MHC-II$^{-/-}$CD1d$^{-/-}$ DC conditions to determine whether cytokine production to total SA lipids was CD1d-restricted. Total SA lipid pulsed MHCII$^{-/-}$ DCs induced CD1d-restricted IFN-γ and IL-17A production by liver lymphocytes isolated from Jα18$^{-/-}$ mice at 4 dpi (**Fig. 3-16**).

Figure 3-16. Type II NKT cells required CD1d to recognize total SA lipids.

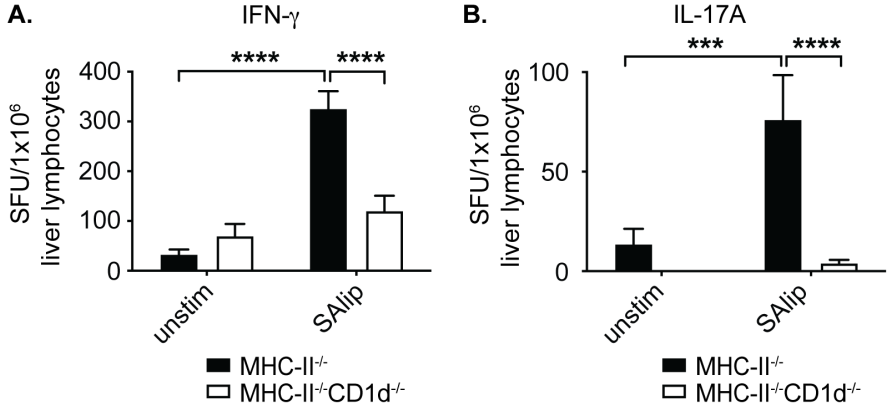

Figure 3-16: (A, B) IFN-γ (A) and IL-17A (B) ELISPOT of Jα18$^{-/-}$ total liver lymphocytes from 4 dpi livers and co-cultured with MHC-II$^{-/-}$ or MHC-II$^{-/-}$CD1d$^{-/-}$ DCs, unpulsed or pulsed overnight with 10 μg/mL total SA lipids (SAlip) (N=4 mice/experiment, representative 1 of 3). Statistical analysis: (A, B) 2-way ANOVA.

To determine whether specific lipids from SA induced IFN-γ production by type II NKT cells, our collaborator used a chloroform ($ChCl_3$)-methanol (MeOH) step gradient to fractionate total SA lipids into nine fractions based on polarity and identified dominant lipid species in each fraction by thin-layer chromatography (TLC) (methods described in **2-10.1**) (**Table 4**).

Fraction	Elution Method	Lipid Species
FR-1	$CHCl_3$/acetone	Neutral lipids/cardiolipin
FR-2	$CHCl_3$/MeOH 95:5	
FR-3	$CHCl_3$/MeOH 9:1	
FR-4	$CHCl_3$/MeOH 8:2	Neutral lipids/DPG/MGDG
FR-5		PG/MDGD mix
FR-6		Pure PG
FR-7	$CHCl_3$/MeOH 6:4	PG: lysyl-PG 95:5
FR-8	$CHCl_3$/MeOH 4:6	PG: lysyl-PG 60:40
FR-9	MeOH	Lysyl-PG: polar lipids 95:5

Table 4: List of SA lipid fractions. SA lipid fractions isolated from total SA lipids using silica gel column chromatography and chloroform-methanol gradient in order of increasing polarity. PG= phosphatidylglycerol, lysyl-PG= lysyl-phosphatidylglycerol, DPG= diacylphosphatidylglycerol, MGDG= monogalactosyldiacylglycerol

Type II NKT cells were enriched from livers of infected J$\alpha 18^{-/-}$ mice by depletion of $CD8^+$ T cells and various APCs, then co-cultured with MHC-$II^{-/-}$ and MHC-$II^{-/-}CD1d^{-/-}$ DCs pulsed with total SA lipids and SA lipid fractions. Again, total SA lipids induced antigen-specific CD1d-restricted IFN-γ production by type II NKT cells, however no IL-17A production was detected after enrichment, suggesting that CD1d-restricted IL-17A is not being produced by type II NKT cells, but that type II NKT cells drive the production of IL-17A by other cell types (**Fig. 3-17A**, IL-17A production undetectable, not plotted). Previous studies determined that PG and cardiolipin species from *Mycobacterium tuberculosis* and *Corynebacterium glutamicum* induced CD1d-restricted cytokine production by type II NKT cell hybridomas (179). Our screening identified that fractions FR-8 and FR-9, containing both PG and lysyl-PG species, induced IFN-γ production by enriched type II NKT cells (**Fig. 3-17A**). Only FR-8, containing a ratio of 60:40 PG: lysyl-PG,

showed a trend for CD1d-restriction, whereas FR-9 induced IFN-γ production completely independent of CD1d. To confirm whether FR-8 induced IFN-γ production was CD1d-restricted, I further enriched type II NKT cells from Jα18$^{-/-}$ liver lymphocytes, by additional depletion of γδ T cells and CD11b^{+} cells, and performed IFN-γ ELISPOT with MHC-II$^{-/-}$ and MHC-II$^{-/-}$CD1d$^{-/-}$ DCs pulsed with FR-8. I showed that FR-8 induced CD1d-restricted IFN-γ production by type II NKT cells (**Fig. 3-17B**).

In addition to TCR-CD1d-mediated antigen-specific activation, iNKT cells were shown to be activated by MyD88-dependent signals, which required IL-12 and IL-18 production by TLR activated APCs (159). To determine whether type II NKT cell IFN-γ production in response to total SA lipids was MyD88 and/or cytokine-dependent, I used B6 and MyD88$^{-/-}$ DCs pulsed with total SA lipids or FR-8 in the presence of IL-12 blocking antibody. Total SA lipid and FR-8 induced IFN-γ production was dependent on both MyD88 and IL-12 production, suggesting both CD1d-TCR engagement and IL-12 producing APCs were required for optimal IFN-γ production by type II NKT cells in response to phospholipids from SA (**Fig. 3-17C**). In summary, polyclonal type II NKT cells required CD1d, MyD88, and IL-12 for IFN-γ production to polar lipid species from the cell membrane of SA.

Figure 3-17. Type II NKT cells produced MyD88-dependent CD1d-restricted IFN-γ to polar SA lipids.

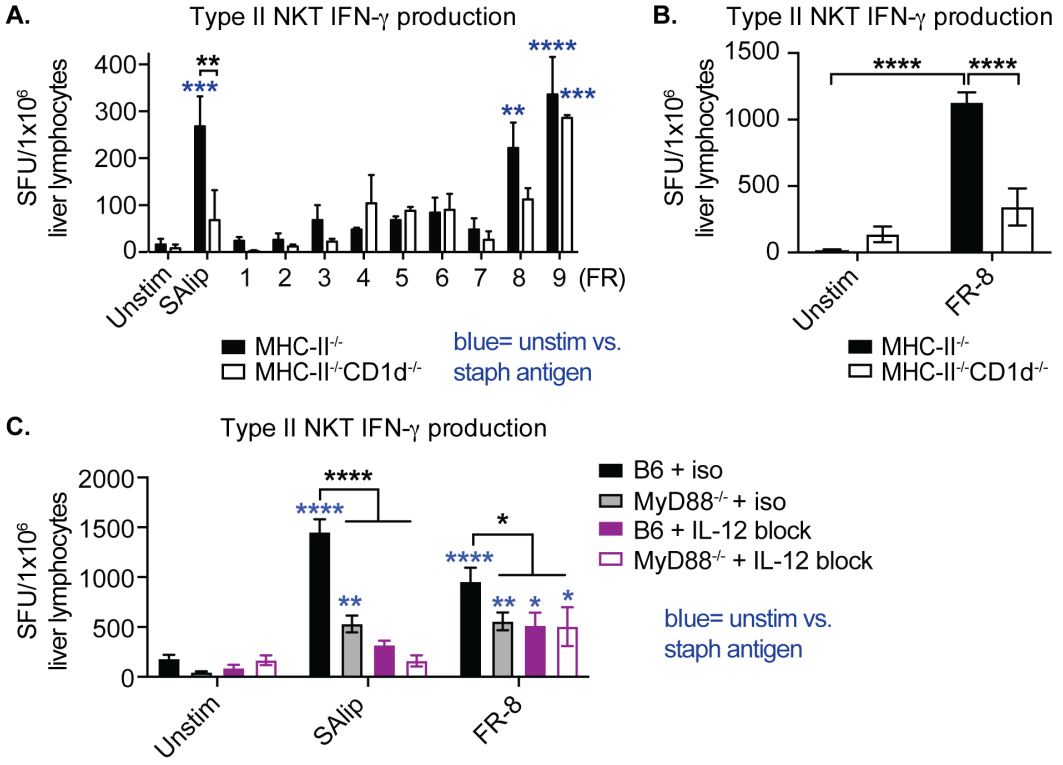

Figure 3-17: (A-C) ELISPOT of IFN-γ production by T cells enriched from 4 dpi Jα18$^{-/-}$ liver lymphocytes: (A, B) MHC-II$^{-/-}$ and MHC-II$^{-/-}$CD1d$^{-/-}$ DCs or (C) B6 and MyD88$^{-/-}$ DCs +/- IL-12 blocking antibody unpulsed (unstim) or pulsed with total SA lipids (Salip) and total SA lipid fractions (FR-1 to FR-9, 10 μg/mL pulsed overnight). (A-C) N=5-7 pooled mice, 2/3 replicates per condition, representative 1 of 2 experiments. Statistical analysis: (A-C) 2-way ANOVA.

Given that type II NKT cell IFN-γ production to total SA lipids and FR-8 was CD1d-restricted and MyD88-dependent, I determined whether type II NKT cells required CD1d and/or MyD88 for activation after SA infection, and compared their activation requirements to iNKT cells. I used total SA lipids and HKSA as SA antigens to measure activation status with TCR engagement. Naïve liver lymphocytes were co-cultured for 24 hrs with BMDCs pre-pulsed with total SA lipids or HKSA, then lymphocytes were collected for surface staining of NKT cells. I compared CD69 MFI fold change between lymphocytes cultured alone (normalized to 1) to lymphocytes co-cultured with BMDC pulsed SA antigens. iNKT cells and type II NKT cells from naïve B6 mice upregulated CD69 in response to HKSA and total SA lipids (**Fig. 3-18**). While

iNKT cells showed some CD1d-restricted activation, the majority of activation to both HKSA and total SA lipids was MyD88-dependent (**Fig. 3-18A, B**). Similarly, type II NKT cells required CD1d for activation, but the majority of activation was MyD88-dependent (**Fig. 3-18C, D**).

Figure 3-18. Type II NKT cells from B6 mice had dominant MyD88-dependent activation to SA antigens.

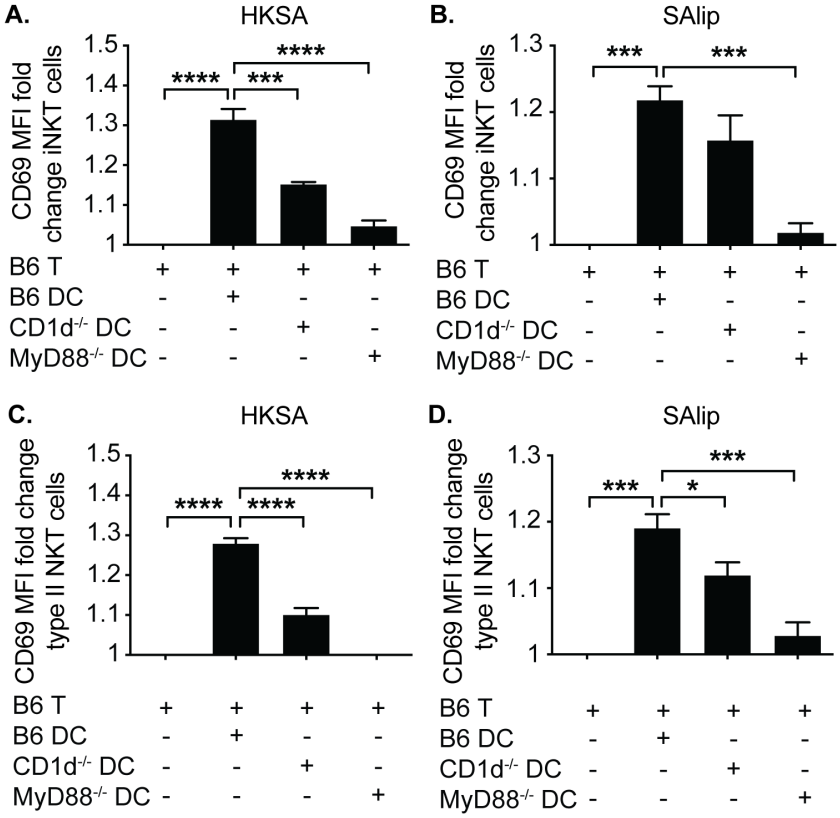

Figure 3-18: (A-B) CD69 MFI of iNKT cells from naïve B6 liver lymphocytes (B6 T) incubated for 24 hrs alone or with B6, CD1d$^{-/-}$, or MyD88$^{-/-}$ DCs pulsed with (A) HKSA or (B) total SA lipids (SAlip) (pooled N=4 mice, 3 replicates/condition). **(C-D)** CD69 MFI of type II NKT cells from naïve B6 liver lymphocytes incubated for 24 hrs alone or with B6, CD1d$^{-/-}$, or MyD88$^{-/-}$ DCs pulsed with (C) HKSA or (D) SAlip (pooled N=4 mice, 3 replicates/condition). Data represented as fold change relative to CD69 MFI of NKT cell culture alone (set to fold change of 1). Statistical analysis: (A-D) one-way ANOVA.

I performed the same activation experiments using naïve MHC-II$^{-/-}$ liver lymphocytes to determine whether NKT cell activation was altered in the absence of MHC-II and CD4^{+} T cells. iNKT cells were previously shown to be activated by the SA superantigen SEB via Vβ8-MHC-II engagement independent of CD1d (110), however the USA300 strain does not contain SEB. When I removed MHC-II expression, I saw that SA antigen-specific activation of both iNKT cells and type II NKT cells was completely CD1d-restricted, with partial MyD88 dependence (**Fig. 3-19**). This showed that NKT cells required both the CD1d-TCR complex and TLR expression on APCs to become activated to SA antigens, but activation was more skewed towards cytokine mediated activation in the presence of conventional CD4^{+} T cells and MHC-II expression. In summary, polyclonal type II NKT cells required both CD1d and MyD88 for activation and IFN-γ production to polar lipid species from the cell membrane of SA.

Figure 3-19. Type II NKT cells from MHC-II$^{-/-}$ mice had dominant CD1d-restricted activation to SA antigens.

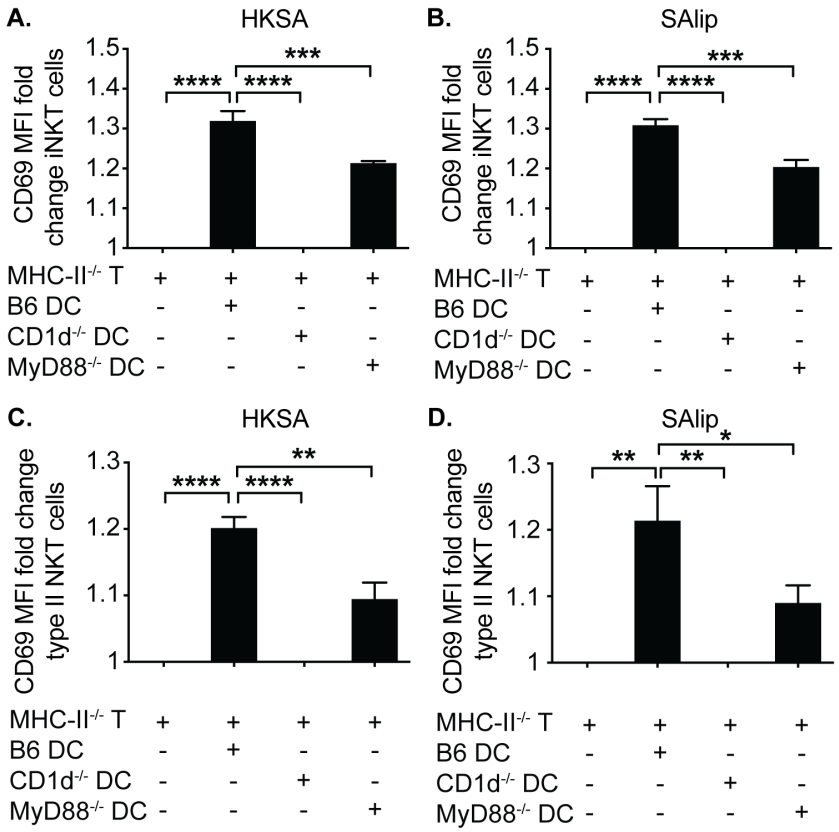

Figure 3-19: (A-B) CD69 MFI of iNKT cells from naïve MHC-II$^{-/-}$ liver lymphocytes (MHC-II$^{-/-}$ T) incubated for 24 hrs alone or with B6, CD1d$^{-/-}$, or MyD88$^{-/-}$ DCs pulsed with (A) HKSA or (B) total SA lipids (SAlip) (pooled N=4 mice, 3 replicates/condition). **(C-D)** CD69 MFI of type II NKT cells from naïve MHC-II$^{-/-}$ liver lymphocytes incubated for 24 hrs alone or with B6, CD1d$^{-/-}$, or MyD88$^{-/-}$ DCs pulsed with (C) HKSA or (D) SAlip (pooled N=4 mice, 3 replicates/condition). Data represented as fold change relative to CD69 MFI of NKT cell culture alone (set to fold change of 1). Statistical analysis: (A-D) one-way ANOVA.

3-2.6 Adoptive transfer of type II NKT cells protected mice from systemic SA infection.

Given the low prevalence of type II NKT cells in wild-type mice, I resorted to using T cells from a well-characterized 24$\alpha\beta$ TCR transgenic mouse model (24$\alpha\beta$ Tg) expressing the Vα3.2^{+}Vβ9^{+} TCR from a type II NKT cell hybridoma (143, 144) to test for the ability of type II NKT cells to protect against SA infection. I first tested the ability of 24$\alpha\beta$ Tg T cells to recognize lipids antigens from SA. Similar to polyclonal type II NKT cells, 24$\alpha\beta$ Tg T cells produced IFN-γ in response to total SA lipids (**Fig. 3-20A**). Unlike polyclonal type II NKT cells from SA infected

mice, antigen-specific IFN-γ production was independent of CD1d and MyD88, but dependent on IL-12 (**Fig. 3-20B**). This suggested that 24αβ Tg T cell IFN-γ production to total SA lipids occurred through the innate cytokine mediated pathway, whereas polyclonal type II NKT cells required both TCR engagement and TLR mediated cytokine production for activation and IFN-γ production.

Figure 3-20. 24αβ Tg T cells produced CD1d independent IL-12 dependent IFN-γ to total SA lipids.

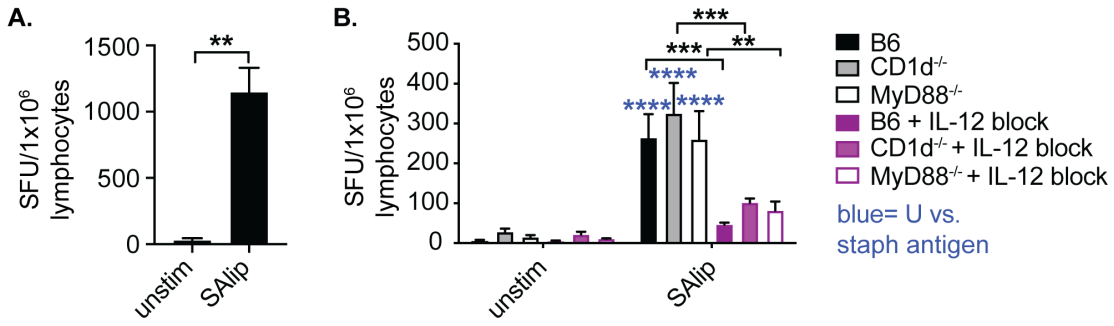

Figure 3-20: (A-B) IFN-γ ELISPOT of naïve lymphocytes from liver 24αβ Tg mice co-cultured with B6 BMDCs (A) or B6, CD1d$^{-/-}$, or MyD88$^{-/-}$ DCs (B) unpulsed or pulsed with total SA lipids (SAlip) (10 μg/mL) (B) +/- IL-12 blocking Ab. (N=1 mouse/experiment, 2/3 replicates per condition, representative 1 of 2). Statistical analysis: (A) one-way ANOVA, (B) two-way ANOVA.

To determine whether 24αβ Tg T cells protected mice from SA infection, I set up an adoptive transfer experiment using congenic markers to track 24αβ Tg T cells *in vivo* after infection (**Fig. 3-21**).

Figure 3-21. 24αβ Tg T cell adoptive transfer.

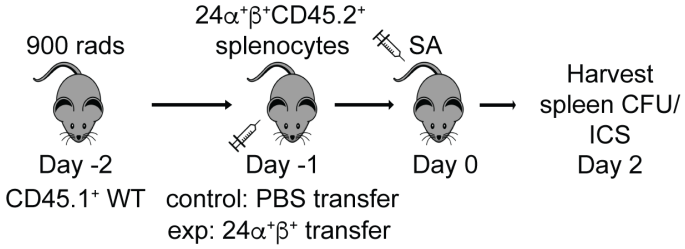

Figure 3-21: Schematic of 24αβ type II NKT cell adoptive transfer experiment.

A substantial number of 24αβTg T cells were detected in the spleen of recipient mice after adoptive transfer (**Fig. 3-22A**). As a result, I observed a significant reduction in CFU at 2 dpi in the spleen of mice receiving 24αβ Tg T cells compared to control (PBS injected) mice (**Fig. 3-22B**), demonstrating that type II NKT cells protected mice from SA infection by contributing to reduced CFU. The 24αβ Tg T cells isolated from SA-infected recipient mice produced significant amounts of IFN-γ after *ex vivo* stimulation with PMA/Ionomycin (**Fig. 3-22C**). These data demonstrated that type II NKT cells contributed to reduction in bacterial burden after SA infection and this effect was likely through enhanced IFN-γ production.

Figure 3-22. Type II NKT cells protected mice from systemic SA infection in spleen.

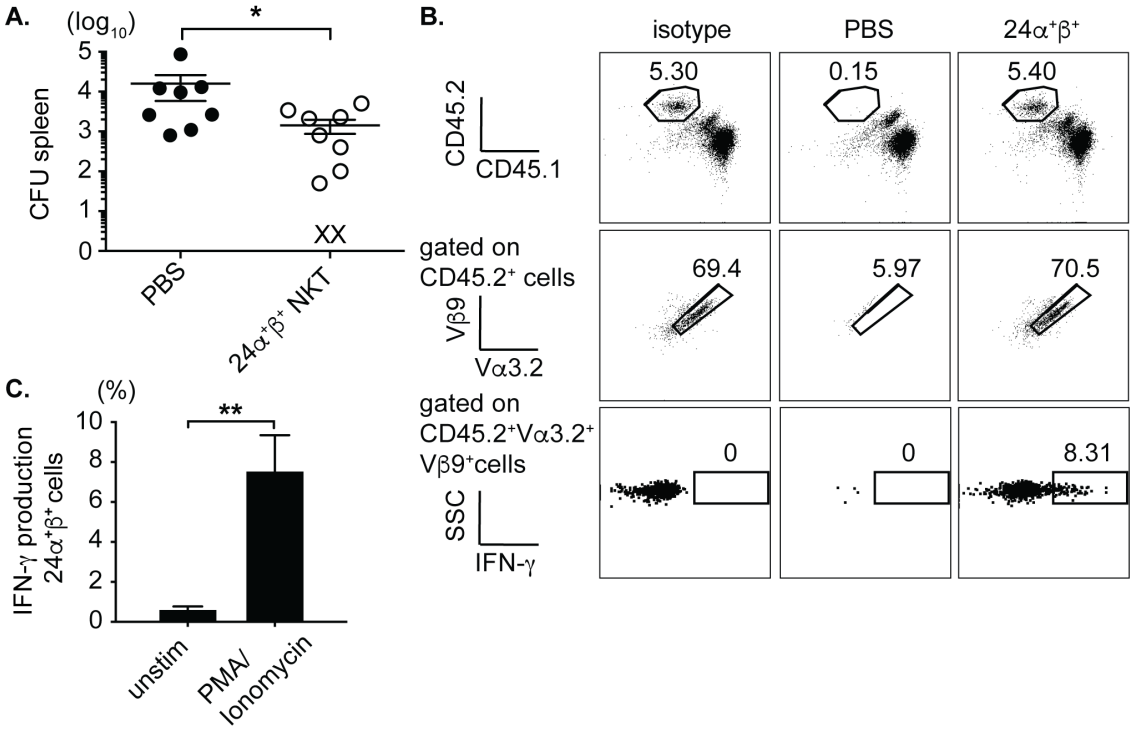

Figure 3-22: (A) Bacterial burdens in the spleen of recipient CD45.1$^+$ mice at 2 dpi that received that 24αβ Tg T cell adoptive transfer or PBS. **(B)** Representative FACS plots of adoptively transferred that 24αβ Tg T cell IFN-γ production from spleen of 2 dpi recipient mice, unstimulated or stimulated with PMA/Ionomycin (2 hrs + 4 hrs BFA) **(C)** % IFN-γ production from (B) quantified (N=8-10 mice/group). Statistical analysis: (A) Mann-Whitney test, (C) 2-way ANOVA.

I also quantified bacterial burdens in the liver and kidneys, where I saw higher CFU in mice lacking NKT cells after SA primary infection (**Fig. 3-1, 3-4**). However, I did not see any difference in CFU in the liver and kidneys of mice that received that 24αβ Tg T cell adoptive transfer vs. PBS (**Fig. 3-23A, B**). When I quantified 24αβ Tg T cells in these organs after adoptive transfer, I saw the majority of 24αβ Tg T cells migrated to the spleen, with a lower percentage in the liver and LN (no 24αβ Tg T cells were detected in the kidneys, not plotted) (**Fig. 3-23C, D**). While 24αβ Tg T cells in the liver produced higher amounts of IFN-γ than 24αβ Tg T cells in the spleen (**Fig. 3-23E, 3-22C**), the lack of CFU difference in the liver and kidneys may have been a result of fewer 24αβ Tg T cells migrating to these organs after adoptive transfer. In summary, adoptive transfer of type II NKT cells protected mice from SA infection in the spleen, likely through production of IFN-γ.

Figure 3-23. Type II NKT cells did not protect mice from systemic SA infection in liver or kidneys.

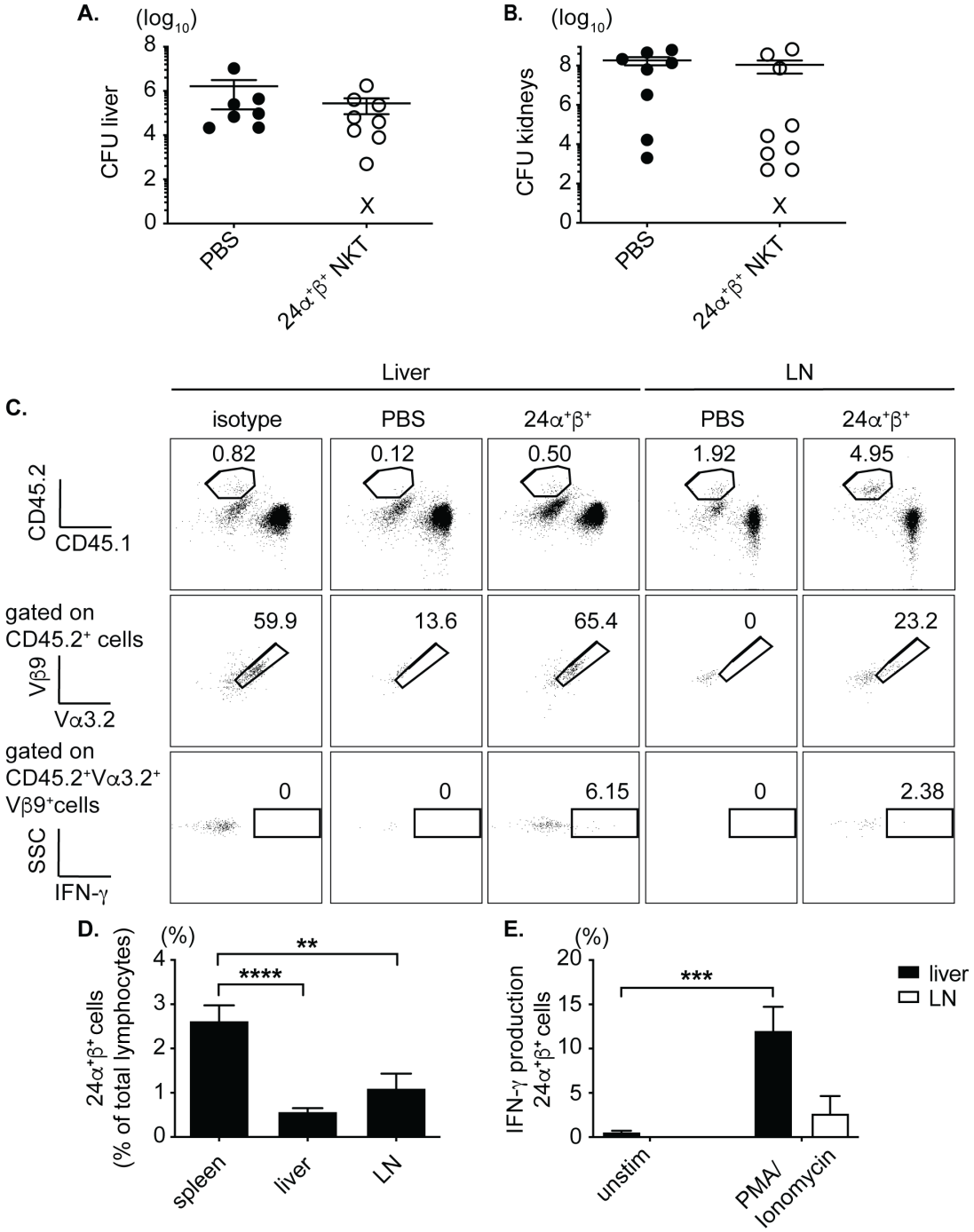

Figure 3-23: (A-B) Bacterial burdens in the liver (A) and kidneys (B) of recipient CD45.1$^+$ mice at 2 dpi that received that 24αβ Tg T cell adoptive transfer or PBS. **(C)** Representative FACS plots of adoptively transferred 24αβ Tg T cell IFN-γ production from liver and LN of 2 dpi recipient mice, unstimulated or stimulated with PMA/Ionomycin (2 hrs + 4 hrs BFA). **(D)** 24αβ Tg T cells represented as % of total lymphocytes in organs of mice that received 24αβ Tg T cell

adoptive transfer. **(E)** % IFN-γ production from (C) quantified (N=8-10 mice/group). Statistical analysis: (A-B) Mann-Whitney test, (D) one-way ANOVA, (E) 2-way ANOVA.

3-2.7 MAIT cells were dispensable for control of SA infection.

I also compared control of SA systemic infection by NKT cells to another subset of innate-like T cells, mucosal associated invariant T (MAIT) cells, which were activated by vitamin B metabolites present in various bacteria, including SA (233). This study demonstrated that MAIT cells protected mice from systemic *Mycobacterium abscessus* and *Escherichia coli* infection, both of which produce vitamin B metabolites. I used littermate $MR1^{+/+}$ and $MR1^{-/-}$ mice to quantify CFU in liver and kidney of SA infected mice at various times post infection. Mice lacking MAIT cells showed no difference in CFU in either liver or kidney at any timepoint tested (**Fig. 3-24**), demonstrating that MAIT cells were not required for protection against SA systemic infection.

Figure 3-24. MAIT cells did not protect mice from systemic SA infection.

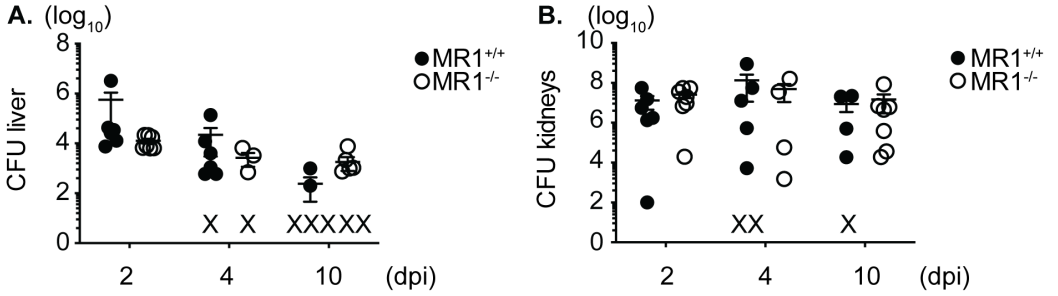

Figure 3-24: (A-B) Bacterial burdens in the liver (A) and kidneys (B) of wild-type ($MR1^{+/+}$) or $MR1^{-/-}$ mice at various times post systemic SA infection (N=5-7 mice/timepoint). Statistical analysis: (A-B) Mann-Whitney test.

I also looked at MAIT cell expansion and activation status after SA infection. MAIT cells were expanded and upregulated CD69 in the liver of infected mice at later timepoints (**Fig. 3-25**). There was some CD69 MFI upregulation at 2 dpi, but the greatest activation occurred at 8 dpi, demonstrating that MAIT cells kinetics behaved more similar to conventional T cell than NKT cell kinetics.

Figure 3-25. MAIT cells were activated and expanded at later times during SA infection.

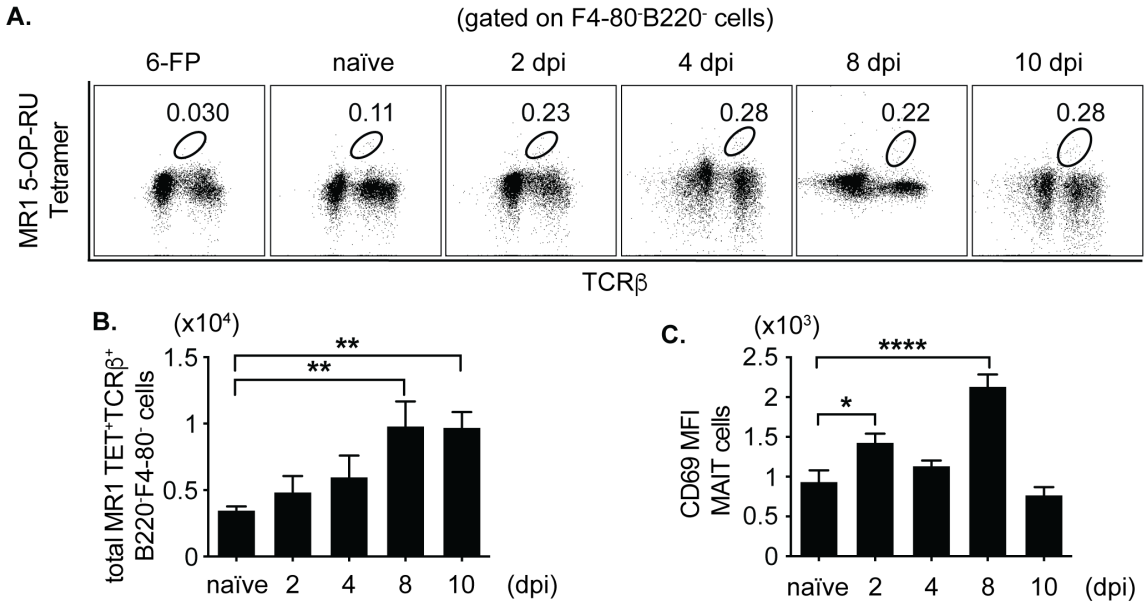

Figure 3-25: (A) Representative FACS plots of MAIT cells (gated on 5-OP-RU MR1 tetramer$^+$ TCRβ^+F4-80$^-$B220$^-$ cells) in liver of wild-type mice at various times post SA infection. **(B-C)** Total cell number (B) and CD69 MFI (C) of MAIT cells quantified from liver of infected mice (N=6 naïve, N=4-7 infected mice/timepoint). Statistical analysis: (B-C) one-way ANOVA.

MAIT cells are known to produce proinflammatory cytokines in response to bacterial infection, including IL-17A, IFN-γ, and TNF-α (227). To determine whether MAIT cells produced cytokines after systemic SA infection, I stimulated liver lymphocytes from wild-type mice at various times post-infection with PMA/Ionomycin. Naïve MAIT cells produced IFN-γ and IL-17A to PMA/Ionomycin stimulation that was not significantly altered after SA infection (**Fig. 3-26**). In summary, MAIT cells were activated after systemic SA infection, but were not required for enhanced cytokine production or protection from SA infection.

Figure 3-26. MAIT cells cytokine production was not altered after SA infection.

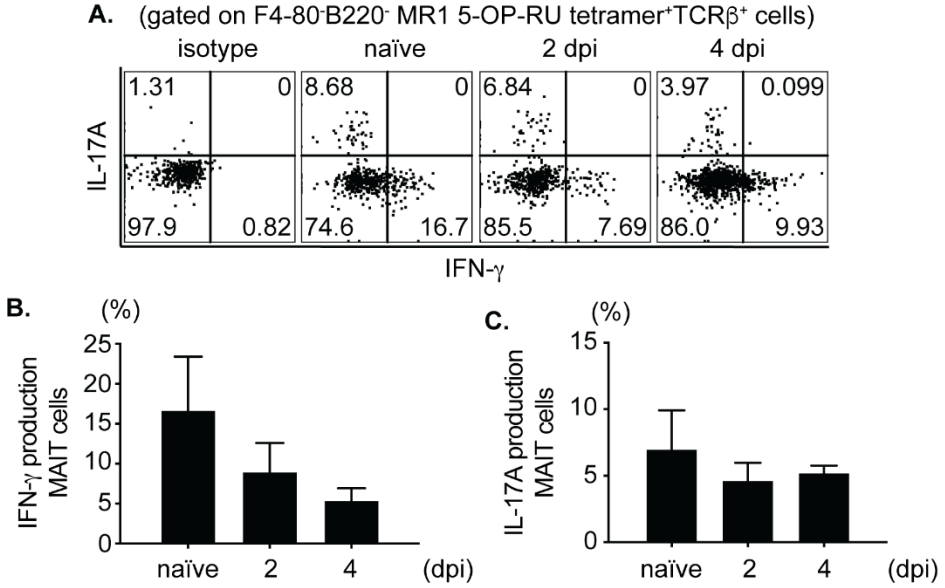

Figure 3-26: (A) Representative FACS plots of MAIT cells (gated on 5-OP-RU MR1 tetramer$^+$ TCRβ$^+$F4-80$^-$B220$^-$ cells) in liver of wild-type mice at various times post SA infection treated with PMA/Ionomycin (2 hrs + 4 hrs BFA). **(B-C)** % IFN-γ (B) and IL-17A (C) production by MAIT cells stimulated with PMA/Ionomycin (N=2 naïve, N=3-4 infected mice/timepoint). Statistical analysis: (B-C) one-way ANOVA.

3-2.8 Patients with SA bacteremia had increased NKT-like cells in PBMC

To determine whether unconventional T cells expanded in the blood of patients with SA bacteremia, I compared the frequency of NKT cells and MAIT cells in peripheral blood mononuclear cells (PBMC) isolated from patients at Northwestern Memorial Hospital with methicillin-sensitive (MSSA) or methicillin-resistant (MRSA) SA bacteremia to that from healthy donors (**Table 5**). The majority of our patient samples were MSSA positive and had type II diabetes co-morbidity.

	Healthy control (HC)	SA bacteremia (SA)
N (male/female)	9 (5/4)	7 (4/3)
Age (Mean ± SD)	31 ± 3.46	60 ± 16.21
MSSA/MRSA	-	6/1
Co-morbidities		
Type II diabetes	-	4
ESRD	-	2
COPD	-	1
Infection acquisition		
Skin break	-	2
Peripheral IV line	-	1
Arteriovenous graft	-	1
ICD implant	-	1
unknown	-	2
Complications		
SA endocarditis	-	2

Table 5: Summary of patient demographics from SA bacteremic patients and healthy controls. ESRD= end-stage renal disease, COPD= chronic obstructive pulmonary disease, ICD= implantable cardioverter defibrillator.

I used PBS57 loaded human CD1d tetramer and 5-OP-RU loaded human MR1 tetramer to identify iNKT cells and MAIT cells in PBMC (**Fig. 3-27A-B**). For type II NKT cell gating, tetramers are not available to define this cell population in human PBMC. The human homolog of NK1.1, CD161, is expressed by NK cells, MAIT cells, NKT cells, and a subset of $\gamma\delta$ T, $CD4^+$ T, and $CD8^+$ T cells. Gene-expression profiling of sorted $CD161^+$ T cells from human PBMC demonstrated that MAIT cells, $CD4^+$ T, $CD8^+$ T, and $\gamma\delta$ T cells expressing CD161 shared a similar genetic transcription profile of MRD1, RORγt, PLZF, IL-12R, and IL-18R expression and produced IFN-γ to IL-12/IL-18 stimulation, suggesting that a portion of these cells could be type II NKT cells (271). Therefore, I resorted to using a similar gating strategy to our mouse model, gating on $CD4^+CD161^+$hCD1d/PBS57 $tetramer^-$ T cells to define a population of T cells enriched for type II NKT cells (**Fig. 3-27C**).

Figure 3-27. Human PBMC donor-unrestricted T cell gating strategies.

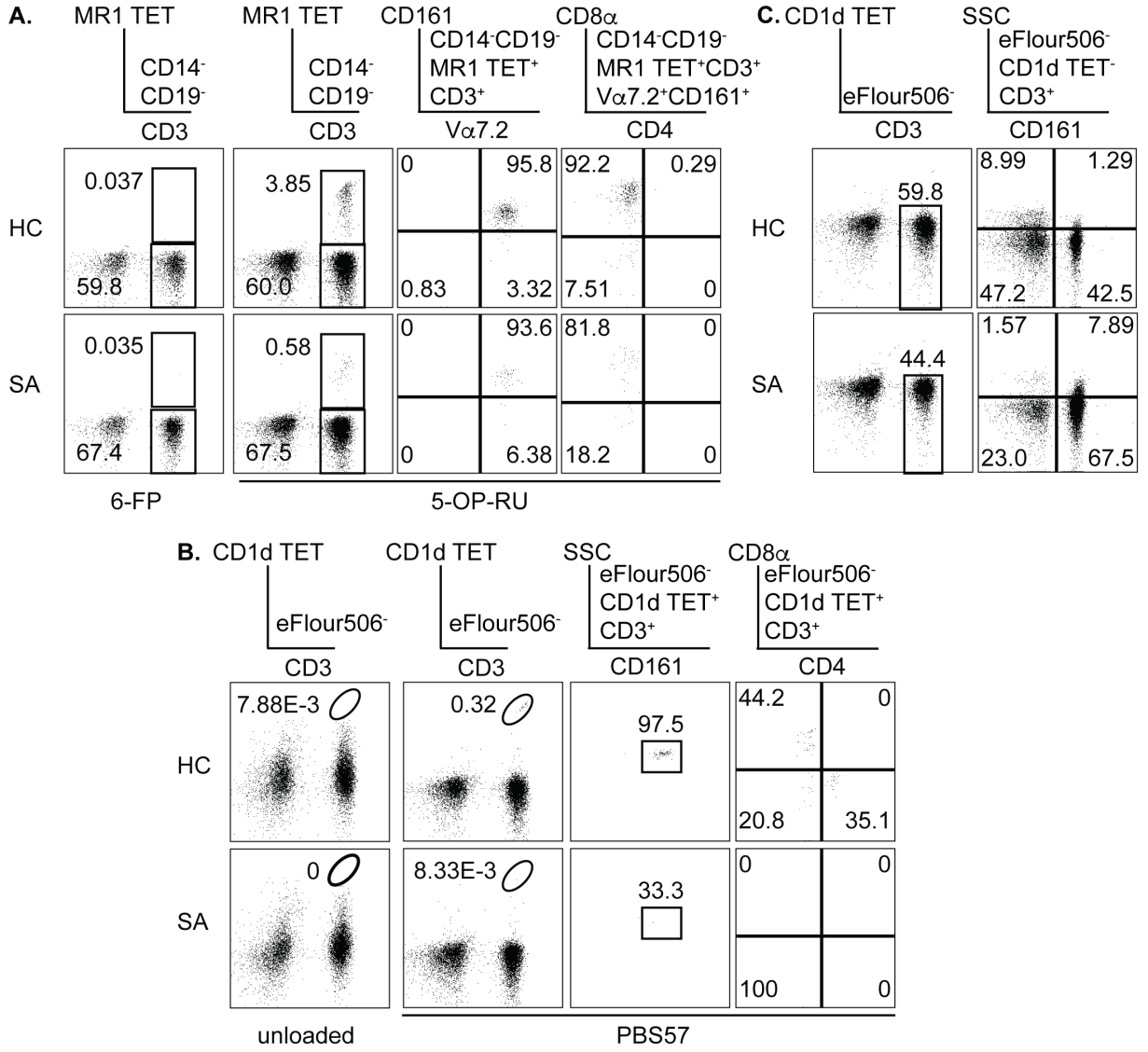

Figure 3-27: (A) Representative FACS plots of MAIT cells (gated on $CD14^{-}CD19^{-}CD3^{+}$hMR1 5-OP-RU tetramer^{+} cells) from healthy control (HC) and SA bacteremic (SA) patients, control staining with MR1 tetramer loaded with 6-FP. **(B)** Representative FACS plots of iNKT cells (gated on $eFlour506^{-}$PBS57 hCD1d-tetramer$^{+}CD3^{+}$ cells) from HC and SA patients, control staining with CD1d tetramer unloaded. **(C)** Representative FACS plots of $CD4^{+}CD161^{+}$ T cells (gated on $eFlour506^{-}$PBS57 hCD1d-tetramer$^{+}CD3^{+}CD4^{+}CD161^{+}$ cells) from HC and SA patients.

While iNKT cells were increased in the blood of mice infected with SA, iNKT cells were decreased in SA infected patients compared to healthy controls, although this was not statistically significant (**Fig. 3-28A, C**). Type II NKT cells were increased in the blood of mice

with SA bacteremia (**Fig. 3-28B**). Similarly, SA bacteremic patients had an increased percentage of $CD4^+CD161^+$ T cells, enriched for type II NKT cells, compared to healthy individuals (**Fig. 3-28D**). Since a substantial proportion of $CD161^+$ T cells in human PBMC are MAIT cells, I also determined the frequency of MAIT cells in SA bacteremic patients and healthy controls. In contrast to $CD4^+CD161^+$ T cells, the percentage of MAIT cells was decreased in SA bacteremic patients compared to healthy controls (**Fig. 3-28E**). In addition, most of the MAIT cells in SA-infected individuals were DN or $CD8^+$ cells (**Fig. 3-27A**). Thus, MAIT cells were unlikely to account for the increased $CD4^+CD161^+$ T cell population observed in SA-infected individuals. In conclusion, SA bacteremic patients had increased frequency of $CD4^+CD161^+$ T cells compared to healthy controls, suggesting that type II NKT cells could be relevant in the human setting for combatting SA bacteremia.

Figure 3-28. Type II NKT cells expanded in SA bacteremic mice and human patients.

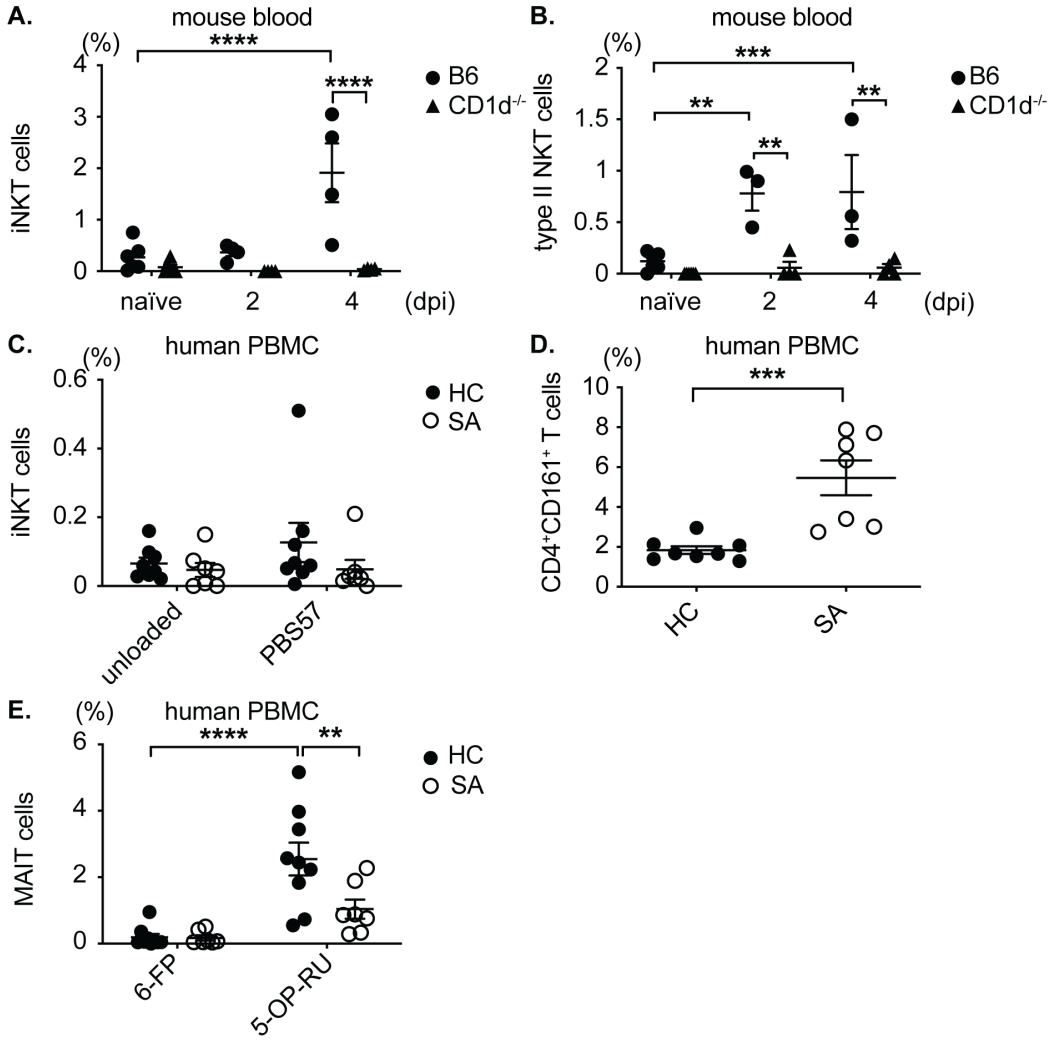

Figure 3-28: (A-B) Percentage of iNKT cells (A) and type II NKT cells (B) in blood of B6 and $CD1d^{-/-}$ mice (N=7 naïve, 3-4 infected mice/genotype). **(C-E)** Percentage of iNKT cells (C), $CD4^{+}CD161^{+}$ T cells (D) and MAIT cells (E) in SA and HC PBMC (N=8-10 HC, 7 SA patients). Statistical analysis: (A-C, E) 2-way ANOVA, (D) student's t-test.

3-3 Conclusion

In conclusion, I showed that type II NKT cells and not iNKT cells, were important for reducing bacterial burden and inflammatory foci, and controlling neutrophil infiltrate to infected liver and kidneys after SA systemic infection (**Fig. 3-29**). Protection was specific for type II NKT cells, as loss of MAIT cells did not increase SA bacterial burdens. Protection was mediated by type II NKT cell activation and IFN-γ production, which required both CD1d-TCR engagement and IL-12 production/MyD88 engagement by APCs. I determined that PG and lysyl-PG species from the cell membrane of SA induced type II NKT cell cytokine production. Additionally, I detected a population of T cells enriched for type II NKT cells that was expanded in patient with SA bacteremia compared to healthy controls, demonstrating the potential relevance of our findings to the human setting. Because of the nonpolymorphic nature of CD1d molecules, targeting of type II NKT cells with a lipid antigen vaccine could be a novel method to induce protection against SA infections where previous vaccines have failed.

Figure 3-29. Type II NKT cells contributed to control of SA systemic infection.

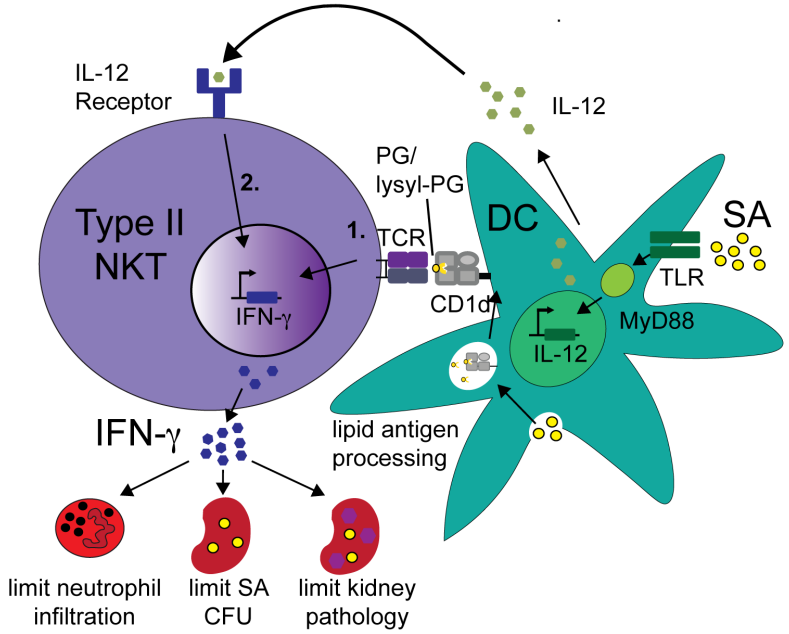

Figure 3-29: Schematic of type II NKT cell activation and cytokine production to SA infection. DCs recognized SA via two mechanisms. TLR recognition of PAMPs activated DCs via the MyD88 pathway to produce IL-12. Additionally, SA was taken up by endocytosis and PG/lysyl-PG lipids were processed and loaded onto CD1d then shuttled to the cell surface for presentation to type II NKT cells. Type II NKT cells were activated by two signals. **1.** Recognition of PG/lysyl-PG presented by CD1d to the TCR and **2**. Binding of DC-derived IL-12 to the NKT cell IL-12 receptor. These 2 signals activated type II NKT cells to produce IFN-γ, which contributed to limit neutrophil infiltrate, bacterial burden, and inflammation in SA infected organs.

Chapter 4

Discussion

In this study, I showed that type II NKT cells, a T cell population that is understudied relative to iNKT cells, played a protective role during SA systemic infection. Though iNKT cells, type II NKT cells, and MAIT cells were activated and expanded during SA infection, only type II NKT cells were necessary for reducing bacterial burden and neutrophilic infiltrate into liver and kidneys. A previous study demonstrated that vaccination of mice with the self-lipid antigen sulfatide, which is recognized by a subset of type II NKT cells, enhanced protection against SA induced sepsis in a CD1d-dependent manner (109), however this study did not track type II NKT cell expansion or cytokine production after infection. Due to the lack of specific markers to identify type II NKT cells *in vivo*, I resorted to the use of genetic knockout mice and surrogate markers to track their expansion and activation after SA infection. Previous studies have used CD1d tetramers loaded with lipid antigens such as sulfatide or IL-4 reporter mice to track subsets of type II NKT cells *in vivo* (174, 146), however I demonstrated that type II NKT cells skewed towards IFN-γ, not IL-4 cytokine production after SA infection. I identified a SA lipid fraction containing PG: lysyl-PG polar lipids that was recognized by polyclonal type II NKT cells in a CD1d-dependent manner, however further work needs to be done to identify the specific lipid within this fraction that is recognized by type II NKT cells. Once identified, this lipid can be loaded onto a CD1d tetramer to track type II NKT cells *in vivo*. Type II NKT cell recognition of this PG: lysyl-PG enriched lipid fraction was exciting, as our lab demonstrated that this same lipid fraction was recognized by group 1 CD1-restricted T cells (115), which could suggest a conserved mechanism of SA lipid antigen recognition between NKT cells and group 1 CD1-restricted T cells, simplifying targeting of these cell populations in new generation SA vaccine designs.

4-1 Status of the SA T cell field prior to our study

T cells have generated much interest in recent years in the SA field as key players in anti-SA immunity. In addition to evidence from humans with genetic or viral-mediated deficiency having increased SA infection risk, demonstrating the importance of $CD4^+$ T cells and their effector functions in SA immunity (80, 82, 81), many studies have explored the role of T cells in murine infection models. Studies of $CD4^+$ T cells in mice demonstrated that both IL-17A producing and IFN-γ producing $CD4^+$ T cells were beneficial for host protection against SA bacteremia and nasal carriage (86, 85, 88). In contrast to these studies, IFN-γ producing $CD4^+$ T cells played pathogenic roles in models of SA surgical wound infection and pneumonia (42, 90). Location of infection and superantigen expression by different SA strains may explain the different outcomes seen in these studies. To date, there is not a consensus on whether $CD4^+$ T cells are 'good' or 'bad' for SA outcomes, though the incidence of superantigen-mediated cytokine storm and sepsis is relatively rare in humans when compared to the total number of SA infections in the United States (95), suggesting that pathogenic $CD4^+$ T cells responses are rare in the human setting. IFN-γ producing memory $CD4^+$ T cells recognizing HKSA and ClfA were identified in patients with SA bacteremia, demonstrating the ability of humans to form antigen-specific memory T cell responses (88). It should also be noted that many murine SA infection models accessed T cell immune responses very early after inoculation (24-48 hrs) before activation of antigen-specific conventional T cell response, a caveat to be taken into consideration when accessing the role of $CD4^+$ T cells in SA immunity.

$\gamma\delta$ T cells have also received much attention in the SA field in recent years due to their ability to be rapidly activated to respond to infection. Many studies have demonstrated a protective role for $\gamma\delta$ T cells in SA skin infection by secretion of IL-17A (99, 100) or IFN-γ and TNF-α cytokines (101). $\gamma\delta$ T production of IL-17A was also beneficial for outcomes of SA surgical site infection (102) and SA peritonitis (103). Similar to $CD4^+$ T cells, $\gamma\delta$ T cells were

detrimental to outcomes of SA pneumonia; while γδ T cell IL-17A production decreased SA CFU, it also drove increased lung inflammation and pathology (104). γδ T cells were activated by intranasal inoculation of SA superantigen SEA to secrete IL-17A, which led to increased lung pathology (106). Collectively, these studies demonstrate the beneficial role of IL-17A producing γδ T cells in targeting SA infections, but activation of these cells in SA infected lung can be damaging to the host.

The role of CD1-restricted T cells in SA immunity was very limited prior to the present study. One murine study demonstrated that mice vaccinated with a self-lipid antigen, which is known to activate type II NKT cells, protected mice from SA sepsis in a CD1d-dependent manner (109). The protective effect of type II NKT cells in this study was measured indirectly through use of $CD1d^{-/-}$ mice, and type II NKT cell activation kinetics and mechanism of protection was not addressed. The only studies exploring iNKT cells in SA infection have focused on activation of iNKT cell by SA SEB *in vitro* and *in vivo* (110, 111); SEB treated humanized mice developed toxic shock syndrome, which was ameliorated by depletion of iNKT cells. No studies prior to the present study have characterized iNKT cell responses to SA primary infection. Knowledge of group 1 CD1-restricted T cell responses to SA infection are also very limited, however a recent study by our lab demonstrated that group 1 CD1-restricted T cells from SA infected hCD1Tg mice produced IL-17A and IFN-γ in response to PG and cardiolipin SA lipids, which peaked at 10 dpi (115). Group 1 CD1-restricted T cell clones derived from these mice produced IL-17A, TNF-α, granzyme B, and IFN-γ and killed SA *in vitro* and *in vivo*. In summary, $CD4^+$ T cells, γδ T cells, and group 1 CD1-restricted T cells have directly been shown to contribute to SA protection and shared the production of IFN-γ and IL-17A, which was beneficial to protection (**Fig. 4-1**).

Figure 4-1. T cells protect against SA infection.

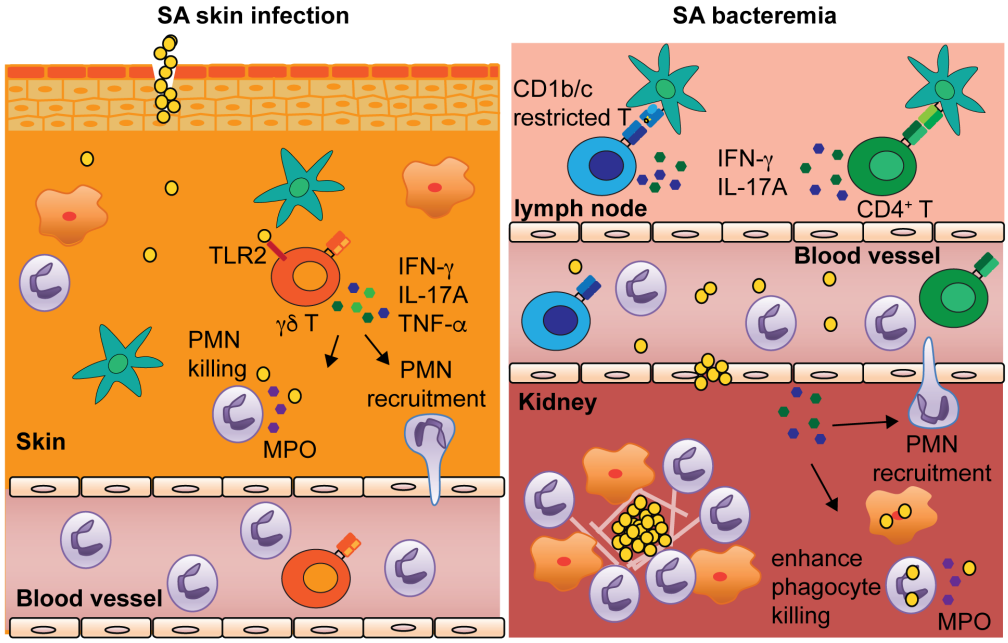

Figure 4-1: Schematic of known protective T cell responses to SA infections. **1.** SA enters the skin via a laceration. γδ T cells are recruited to skin and recognize SA PAMPs via TLR2, leading to activation via the MyD88 pathway and production of IFN-γ, IL-17A, and TNF-α at 1-7 dpi. These cytokines recruit and activate neutrophils to the skin to kill SA via MPO release. **2.** During SA bacteremia, SA enters kidneys via the bloodstream and begins to form abscesses, a colony of bacteria surrounded by a fibrinogen capsule and infiltrating neutrophils and macrophages. $CD4^+$ T cells are activated in the LN via TCR-MHC-II interaction to produce IFN-γ and IL-17A at 7-14 dpi. Group 1 CD1b/c restricted T cells are activated in the LN by PG presented on CD1b/c expressing DCs, leading to production of IFN-γ and IL-17A which peaks at 10 dpi. IFN-γ and IL-17A enhance macrophage and neutrophil phagocytosis of SA and release of MPO to kill SA in the kidneys. LN=lymph node, MPO= myeloperoxidase, PMN= neutrophil.

4-2 Role of T cell-driven neutrophil infiltration and IFN-γ production in SA infection

I demonstrated in this study that type II NKT cells were necessary for protection against SA systemic infection, by reduction of CFU, kidney pathology, and neutrophil infiltrate (**Fig. 3-1, 3-4**). Increased infiltration to the kidneys and liver in $CD1d^{-/-}$ mice was specific for neutrophils, as I saw no difference in immune infiltrate of other APCs and T cells between B6 and $CD1d^{-/-}$ mice after infection (**Fig. 3-2, 3-3**).

Neutrophils are the first line of defense against SA infection, and migrate to infected tissues to opsonize and kill SA. Conversely, SA has evolved many mechanisms to circumvent

neutrophil killing, including inhibiting activation, chemotaxis, phagocytosis, and oxidative/non-oxidative killing of SA by neutrophils (15). While neutrophils are necessary for clearing SA, they can also be detrimental in outcomes of infection. This was demonstrated in mouse models of wound healing and systemic SA infection, where increased neutrophilic infiltrate was correlated with enhanced disease severity due to the ability of SA to grow and persist inside neutrophils (41, 42). In our study, $CD1d^{-/-}$ kidneys and liver had enhanced neutrophil infiltrate, but worsened CFU and kidney pathology after SA infection (**Fig. 3-1**). The study by McLoughlin et al. identified that a capsular polysaccharide expressed on the surface of SA induced MHCII-dependent IFN-γ production by $CD4^+$ T cells, which drove chemotaxis of neutrophils to the surgical wound infection site and worsened bacterial burden. These studies demonstrated that while neutrophils are important for SA clearance, too much neutrophil influx correlates with worsened infection. In our model of SA systemic infection, loss of type II NKT cells led to decreased IFN-γ production by total liver and spleen lymphocytes in response to HKSA after infection (**Fig. 3-6**), demonstrating a beneficial role for IFN-γ in outcomes of infection.

IFN-γ is known to modulate neutrophil trafficking and activation; a study that administered IFN-γ to SA infected mice showed that IFN-γ treatment resulted in reduced mortality to SA septicemia and increased neutrophil phagocytic capability in early stage infection (272). However, IFN-γ treated mice also experienced increased septic arthritis at later stages of infection. These studies suggested that the timing and localization of IFN-γ secretion was important for determining when IFN-γ was beneficial or detrimental to the outcome of SA infection. Indeed, in our system, both iNKT cells and type II NKT cells preferentially produced IFN-γ in direct response to SA infection at a very early timepoint, which was lost after 1 dpi (**Fig. 3-13, 3-14**). This initial burst of IFN-γ production may be sufficient to stimulate the immune response without causing overactivation and detrimental effects seen with longer-term secretion of proinflammatory cytokines.

4-3 Measuring the contribution of type II NKT cells in SA infection

The majority of studies exploring the role of type II NKT cells in infection and disease have relied on the use of genetic knockout mice to indirectly measure the contribution of type II NKT cells to a given disease state (196). In this study, I also relied on Jα18$^{-/-}$ mice (lacking iNKT cells) and CD1d$^{-/-}$ mice (lacking iNKT and type II NKT cells) to indirectly determine the effect that loss of type II NKT cells had on the outcomes of SA infection. CD1d$^{-/-}$ mice had increased CFU, neutrophil influx, and pathology in infected liver and kidneys compared to Jα18$^{-/-}$ and B6 mice, demonstrating a critical role for type II NKT cells in the absence of iNKT cells in controlling SA infection (**Fig. 3-1, 3-4**). Previous studies utilized a Jα18$^{-/-}$ mouse that had a critical design flaw in deletion of the TRAJ18 region, which disrupted transcription of all TCRα regions downstream of TRAJ18 (262). As a result, these mice had a more limited TCRα repertoire than wild-type mice, making it difficult to interpret the results of studies using this mouse model, as any phenotype seen could be the result of absence of conventional T cells utilizing these TCRα chains and not absence of type II NKT cells. I utilized a more recently developed Jα18$^{-/-}$ mouse model for this study, which had a 10 bp deletion in the TRAJ18 gene segment that successfully disrupted transcription of this gene without affecting TCRα regions downstream of TRAJ18 (261). Therefore, any differences in phenotype between Jα18$^{-/-}$ mice and CD1d$^{-/-}$ mice I observed could be directly attributed to the loss of type II NKT cells.

Since I did not have a tetramer to track type II NKT cells *in vivo*, I relied on the use of surrogate markers to define this cell population. Our lab had previously used IL-4 reporter mice to track polyclonal type II NKT cells in naive mice (146). In initial experiments, I had attempted to use IL-4 reporter mice on the Jα18$^{-/-}$ background to track type II NKT cells *in vivo*, however I did not see a significant expansion of this population after SA infection, despite the presence of low levels of IL-4 mRNA in sorted type II NKT cells (**Fig. 3-14C**). This could be due to the skewing of the NKT cell response after SA infection to IFN-γ production rather than IL-4

production (**Fig. 3-13, 3-14**). This Jα18$^{-/-}$ IL-4 reporter mouse was also developed using the original Jα18$^{-/-}$ background which had flaws in TCRα repertoire mentioned above, limiting its usefulness to this study.

Both iNKT cells and type II NKT cells express the NK cell marker NK1.1. I defined type II NKT cells as PBS57 CD1d tetramer^{-}TCRβ^{+}NK1.1^{+}CD4^{+}CD8^{-} T cells (**Fig. 3-7**) and confirmed that this population was CD1d-restricted as it did not expand in CD1d$^{-/-}$ mice after infection (**Fig. 3-8**). NKT cells can express CD4 or be CD4^{-}CD8^{-} (DN) in mice. To determine whether DN NK1.1^{+} T cells were type II NKT cells, I also analyzed PBS57 CD1d tetramer^{-}TCRβ^{+}NK1.1^{+}CD4^{-} CD8^{-} cells. While this population expanded at 4 dpi, it was not CD1d-restricted, expanding to the same degree in B6, Jα18$^{-/-}$, and CD1d$^{-/-}$ mice (**Fig. 3-9**). DN NK1.1^{+} T cells were also activated at 8 dpi, suggesting that this population was in fact a conventional T cell population upregulating NK1.1. Therefore, I focused on CD4^{+}NK1.1^{+} T cell gating to define type II NKT cells. Using this gating strategy, I determined that polyclonal type II NKT cells utilized diverse Vβ chains, with the largest population utilizing Vβ8.1/8.2 (40%) (**Fig. 3-12A**). This Vβ chain usage was similar to the Vβ chain usage of polyclonal type II NKT cells defined with naïve IL-4 reporter mice (146).Type II NKT cell Vβ chain usage was not altered after SA infection, suggesting that type II NKT cells expanded polyclonally after infection. In contrast to type II NKT cells, conventional CD4^{+} T cells (NK1.1^{-}CD4^{+}) had more diverse TCR usage (**Fig. 3-12B**).

4-4 NKT cell activation kinetics in SA versus other bacterial infections

I demonstrated that NKT cells were activated very early in response to SA systemic infection, measured by upregulation of CD69 in liver, spleen, and LN (**Fig. 3-8, 3-10, 3-11**), and underwent expansion and proliferation in the liver and kidney (**Fig. 3-8, 3-11**). A previous study demonstrated that iNKT cells expanded and unregulated CD69 expression in the spleen following systemic infection with the SA strain LS-1 (109). It is important to note the methicillin-

sensitive strain LS-1 SA contains superantigens different from methicillin-resistant USA300 SA strain used in this study. iNKT cells were activated by the SA superantigen SEB independent of CD1d (225, 110), however the USA300 strain does not encode dominant superantigens such as SEB (113). Indeed, CD1d-restricted activation of iNKT cells by HKSA and total SA lipids in the absence of MHC-II suggested that iNKT cells could be activated independent of SA superantigens (**Fig. 3-19**).

Similar to SA infection, liver iNKT cells upregulated CD69 and CD25 and produced IFN-γ at 7 dpi following intradermal *Borrelia burgdorferi* infection (200). iNKT cells expansion was also detected in the liver and spleen after systemic *Mycobacterium bovis* infection at 8 dpi. However, this study did not look at activation of iNKT cells after infection. In our study, iNKT cells were activated at 2 dpi and expanded at 4 dpi in the liver following SA infection (**Fig. 3-8**). Dissemination route of bacteria and growth kinetics of different bacterial species may explain the difference in activation kinetics in these studies compared to SA infection.

In addition to activation and expansion, I showed that NKT cells produced IFN-γ in response to SA infection (**Fig. 3-13**). iNKT cells have been shown to increase IFN-γ production in response to other bacterial infections, including *S. pneumoniae*, *L. monocytogenes*, and *S.* Typhimurium (198, 269, 270), however this is the first study to our knowledge demonstrating that type II NKT cells produced IFN-γ in response to SA infection *in vivo*. The fast kinetics of NKT cell activation after SA infection is in keeping with the pre-activated state of NKT cells, which contain cytokine mRNA in their cytoplasm that can be quickly transcribed into cytokine proteins and secreted within minutes to hours after encounter of stimuli (145). Indeed, when I sorted type II NKT cells from SA infected mice at an early timepoint after infection and compared their cytokine mRNA levels to conventional $CD4^+$ T cells, type II NKT cells had upregulated IFN-γ and IL-4 mRNA compared to conventional $CD4^+$ T cells after infection (**Fig. 3-14C**).

Despite the similarity in activation kinetics between iNKT cells and type II NKT cells, it is interesting that iNKT cells, but not type II NKT cells, become hyporesponsive to restimulation after SA infection. It is possible that the restricted TCR usage of iNKT cells makes them more susceptible to superantigen-mediated cytokine production and subsequent anergy. Because the type II NKT cell population is polyclonal, utilizing more diverse Vα/Vβ usage, this could make them more resistant to superantigen-mediated activation and anergy as a whole. Another possibility is that type II NKT cells regulate iNKT cell anergy induction. In a model of concanavalin A-induced hepatitis, sulfatide-activated type II NKT cells activated liver DCs to produce IL-12, which induced anergy in iNKT cells and protected mice from liver hepatitis (273). Pretreatment of type II NKT cells with sulfatide also induced iNKT cell anergy and mediated protection in ischemic reperfusion injury (194) and alcoholic liver disease (193). Further work will need to be done to determine if a similar phenotype is occurring in bacterial infections, including SA. In summary, the loss of cytokine production by iNKT cells coupled with the increased kidney and liver CFU and kidney pathology seen in CD1d$^{-/-}$, but not Jα18$^{-/-}$ mice, demonstrated that type II NKT cells but not iNKT cells played the dominant role during SA infection.

4-5 SA lipids recognized by type II NKT cells

Given that type II NKT cells played the dominant role during SA infection, I focused on the ability of type II NKT cells to recognize lipid antigens derived from SA. In order to identify SA lipid antigens that could activate type II NKT cells, I isolated total SA lipids from the SA cell membrane (**2-10.1**). Total liver lymphocytes from infected Jα18$^{-/-}$ mice produced IFN-γ to total SA lipids that was CD1d-restricted (**Fig. 3-16A**). Interestingly, total SA lipids also induced IL-17A production that was CD1d-restricted (**Fig. 3-16B**). However, when I enriched for type II NKT cells by depleting endogenous APCs, γδ T cells and CD8^{+} T cells, I no longer saw any IL-

17A production to total SA lipids. This suggested that total SA lipid activated type II NKT cells stimulated the production of IL-17A by either γδ T cells or $CD8^+$ T cells. Another explanation for this observation was that γδ T cells could be producing CD1d-restricted IL-17A, as CD1d-restricted γδ T cell populations have been reported in humans and mice (274). I also performed pilot experiments with T cells enriched from Vα14 transgenic mice, which are enriched for iNKT cells, to determine whether iNKT cells produced cytokines to total SA lipids. However, I detected no cytokine production to total SA lipids by iNKT cells after infection (data not plotted), which suggested that (a) iNKT cells did not recognize SA lipids or (b) the hyporesponsive phenotype induced by SA infection made iNKT cells unable to respond to SA lipids. Given that the SA lipidome is enriched for lipids like PG and lysyl-PG, which contain long fatty acid tails and lack a ring structure connected to an α-linkage preferentially recognized by iNKT cells (275), it is more likely that SA does not contain lipids recognized by iNKT cells. The cytokine production by iNKT cells we saw in response to SA infection was likely mediated through innate cytokine-driven signals rather than antigen-specific activation.

I showed that naïve type II NKT cells required both CD1d and MyD88 expressing DCs to be activated by total SA lipids (**Fig. 3-18C, D**). iNKT cell activation occurs either through direct TCR-CD1d engagement with foreign lipid antigens, or through IL-12/IL-18, produced by APCs recognizing PAMPs on bacteria, binding the IL-12/IL-18 receptor on NKT cells with or without TCR-CD1d engagement with self-lipids, but the mechanism of type II NKT cell activation is less clear (159). Previous studies have reported that type II NKT cell hybridomas are activated by microbial lipids *in vitro* in a CD1d-restricted MyD88-independent manner (179, 180), but the activation requirements in primary cells during an infection response were less clear. Interestingly, I showed that for SA antigens, these pathways were not exclusive, as type II NKT cells required both CD1d presentation of foreign lipids plus MyD88-driven signals for activation to total SA lipids and HKSA (**Fig. 3-18C-D**). It has been suggested that during an infection,

CD1d-restricted and MyD88-dependent pathways could be acting simultaneously to activate type II NKT cells (196), and this is likely the case in SA infection.

The SA cell membrane is composed primarily of PG, lysyl-PG, and cardiolipin lipid species, with smaller percentages of diacylglycerols, diglycosyldiacylglycerols, and monoglycosyldiacylglycerols (223, 224). I showed here that a mixture of polar lipids containing PG: lysyl-PG species at a 60:40 ratio (FR-8) induced IFN-γ production by type II NKT cells that was both CD1d-restricted and IL-12-dependent (**Fig. 3-17**). In contrast, the fraction containing pure PG (FR-6) did not induce any IFN-γ production and the fraction containing 95% lysyl-PG + 5% unidentified polar lipids (FR-9) induced IFN-γ production that was not CD1d-restricted (**Table 4, Fig. 3-17A**). It is important to note that SA contains multiple PG and lysyl-PG species of varying chain lengths. A study using HPLC coupled with mass spectrometry (LC-Q-TOF-MS) to characterize the SA lipidome identified multiple PG and lysyl-PG lipid moieties of varying chain lengths eluting at different times during fractionation, with PG species being enriched in methicillin-resistant SA compared to methicillin-sensitive SA strains (224). Fatty acid chain length and confirmation of fatty acid chains in the cis or trans position affects lipid loading onto CD1d molecules and subsequent NKT cell TCR engagement (276). PGs of different chain lengths have been identified from *Mycobacterium tuberculosis, Corynebacterium glutamicum*, and *Listeria monocytogenes* with the ability to stimulate type II NKT cell hybridomas; the efficiency of activation was dependent on the affinity of binding to CD1d (179, 180). Therefore, it is possible that PG/lysyl-PG lipids from FR-8 contained unique fatty acid chain lengths that affected the binding affinity of these lipids to CD1d and the strength of type II NKT cell TCR engagement, relative to PG from FR-6 and lysyl-PG species from FR-9. Further work needs to be done to characterize the type II NKT cell response to SA lipids, including isolating individual SA lysyl-PG or PG lipid moieties from FR-8 for antigen screening using ELISPOT. Once these individual lipid species are identified, they can be loaded onto CD1d tetramers to track SA lipid

reactive type II NKT cells *in vivo*. In summary, type II NKT cells were activated and produced CD1d-restricted MyD88/IL-12-dependent IFN-γ to PG: lysyl-PG species derived from SA.

4-6 Protective capability of type II NKT cells during systemic SA infection

Given that type II NKT cells were necessary for reducing bacterial burden and neutrophil infiltrate early in response to SA infection, I determined mechanistically how type II NKT cells provided protection *in vivo*. Since there are too few type II NKT cells in B6 or Jα18$^{-/-}$ mice to isolate and adoptively transfer directly, I used a well characterized type II NKT cell transgenic mouse, 24αβ Tg, to perform adoptive transfer experiments (**Fig. 3-21**). 24αβ Tg T cells played both beneficial and detrimental roles during models of inflammation and autoimmunity. 24αβ Tg T cells suppressed type I diabetes onset in mice, but exacerbated colitis when CD1d was overexpressed in 24αβ Tg CD1dTg mice (192, 195). Additionally, the VIII24 hybridoma, the type II NKT cell clone used to make 24αβ Tg mice (144), recognized both polar *Mycobacterium tuberculosis* lipids and tumor-derived self-lipids (277, 179). I showed that liver lymphocytes from naïve 24αβ Tg mice produced IFN-γ in response to total SA lipids (**Fig. 3-20A**). Unlike polyclonal type II NKT cells, which produced CD1d-restricted MyD88/IL-12-dependent IFN-γ to total SA lipids following SA infection, 24αβ Tg T cell IFN-γ production to total SA lipids was not CD1d-restricted or MyD88-dependent, but dependent on IL-12 production (**Fig. 3-20B**). A recent study showed that 24αβ Tg T cells stimulated with TLR agonists in the presence of DCs produced IFN-γ independent of TCR receptor signaling and dependent on IL-12 (181). This suggested that 24αβ Tg T cells recognition of SA antigens was driven by innate cytokine signals rather than antigen-specific TCR stimulation.

Irradiated CD45.1^{+} mice that received splenic 24αβ Tg T cells showed enhanced recruitment of 24αβ Tg T cells to the spleen of recipient mice and reduced bacterial burden in the spleen after SA infection (**Fig. 3-22A, B**), demonstrating a direct role for type II NKT cells in

control of SA bacterial burden. 24αβ Tg T cells produced IFN-γ in the spleen after adoptive transfer (**Fig. 3-22C**), similar to polyclonal type II NKT cells after infection, suggesting that IFN-γ was important for mediating protection. I also determined CFU in the liver and kidneys after adoptive transfer, as these were the organs where I saw differences in CFU in mice lacking NKT cells after SA infection. However, I did not see a difference in CFU in liver or kidneys of mice that received 24αβ Tg T cells vs. control mice (**Fig. 3-23A, B**). 24αβ Tg T cells were recruited to liver and LN after adoptive transfer (**Fig. 3-23C**), however the percent of 24αβ Tg T cells in these organs was significantly lower than 24αβ Tg T cells in the spleen (**Figure 3-23D**). Despite the ability of 24αβ Tg T cells to produce IFN-γ in the liver after adoptive transfer (**Fig. 3-23E**), the absence of protection in the liver could be due to the lower number of 24αβ Tg T cells trafficking to the liver.

4-7 MAIT cells did not contribute to protection against systemic SA infection

In addition to characterizing NKT cell responses during SA infection, I determined the necessity of another donor-unrestricted T cell population, MAIT cells, in control of SA infection. MAIT cells were critical for clearance of systemic infections in mice, including *Escherichia coli*, *Klebsiella pneumoniae*, and *Mycobacterium abscessus* (233, 250). All of these bacteria express riboflavin proteins, which generate the riboflavin metabolites recognized by MAIT cells. Considering SA also expresses riboflavin proteins, I hypothesized that MAIT cells could be activated and contribute to protection against SA systemic infection. However, when I compared bacterial burdens in infected liver and kidneys of $MR1^{+/+}$ and $MR1^{-/-}$ mice after SA infection, I saw no difference in CFU between these groups at any timepoint tested (**Fig. 3-24**), demonstrating that MAIT cells were dispensable for control of SA systemic infection.

MAIT cells were expanded and activated in the liver after SA infection, however this occurred at later timepoints after infection (8-10 dpi) (**Fig. 3-25**). Similar activation kinetics for

MAIT cells were demonstrated after *Legionella longbeachae* and *S.* Typhimurium pulmonary infections (244, 245). A previous study showed that SA infected BMDCs activated MAIT cells from TCR transgenic mice (iVα19-Vβ6 Tg) by upregulation of CD69 *in vitro* (233). I also looked at MAIT cell cytokine production after SA infection. A recent study showed that MAIT cells from healthy human PBMC could be activated independent of MR1-TCR engagement to produce IFN-γ in response to the SA superantigen SEB (260). Using the SEB deficient USA300 SA strain, I saw a slight, but not significant, decrease in IFN-γ and IL-17A production by MAIT cells after infection (**Fig. 3-26**), demonstrating that MAIT cells were not required for cytokine production to SA infection. Evidence for a role of MAIT cells in SA infection is very limited, and this is the first study to our knowledge to show that MAIT cells are dispensable for control of systemic SA infection in mice.

Considering MAIT cells are most enriched in the mouse lung, a protective role for MAIT cells has been demonstrated in pulmonary *Francisella tularensis, Legionella longbeachae,* and *Mycobacterium bovis* BCG infection (253, 244, 245), however they were not necessary for clearance of *S.* Typhimurium pulmonary infection (251). It is possible that MAIT cells may play a role in SA pulmonary infection, however this has yet to be studied. SA that is administered intratracheally is eliminated from the lungs of mice very rapidly (within 48 hrs) (278). Increasing the inoculation of SA can improve CFU enumeration in lungs, however higher inoculums lead to increased SA sepsis and mortality (11). Therefore, mice may not be the best model organism to study the contribution of MAIT cells to SA pulmonary infection. Similar to type II NKT cells, characterization of MAIT cells during infection are limited, however the recent development of the 5-OP-RU MR1 tetramer should lead to better characterization of this T cell population and its contribution to infection (234, 235).

4-8 Unconventional T cell responses in SA bacteremic patients

To corroborate the roles that NKT cells and MAIT cells play in mouse systemic SA infection, I determined whether unconventional T cells were expanded in patients with SA bacteremia compared to healthy donors. Both MAIT cells and type II NKT cells are more enriched in human PBMC compared to iNKT cells (266, 228), therefore I expected these populations to make up a majority of the unconventional T cell pool in healthy control patients. Indeed, the iNKT cell population made up a very small fraction of total T cells in healthy donor PBMC, and there was high background staining in unloaded CD1d tetramer controls (**Fig. 3-28B**). I detected a slight, but not significant, decrease in iNKT cells in SA bacteremic patients (**Fig. 3-29C**), in contrast to mice, which had increased iNKT cell percentage in blood after SA infection (**Fig. 3-29A**). A decrease in iNKT cells has been reported for PBMC of active *Mycobacterium tuberculosis* patients vs. latent patients and healthy control PBMC, however this study used surrogate markers rather than CD1d tetramers to track iNKT cells, limiting the interpretation of this study (279). Further studies are needed to determine if iNKT cells are being recruited to infected tissue in humans during SA infection, and whether they have any benefit to the outcome of SA infection. Additionally, repeating characterization of iNKT cells using α-GalCer human CD1d tetramers to confirm the results of initial studies using surrogate markers will better illustrate the contribution iNKT cells make to various disease states in the human setting.

Using our defined gating strategy for type II NKT cells, I observed an increase in type II NKT cells in the blood of SA-infected B6 mice, but not $CD1d^{-/-}$ mice (**Fig. 3-29B**). I did not have a CD1d tetramer to specifically identify type II NKT cells in human PBMC. Therefore, I resorted to use of the surrogate markers CD161 and CD4 to gate on this population (**Fig. 3-28C**). PBS57 human CD1d $tetramer^{-}CD161^{+}CD4^{+}$ T cells were expanded in the blood of SA bacteremic patients compared to healthy controls (**Fig. 3-29D**). RNAseq of sorted $CD161^{+}$ T cells from human PBMC identified a heterogeneous population of $\gamma\delta$ T cells, MAIT cells, and conventional

Th17 producing $CD4^+$ T cells that shared a similar genetic transcription profile of MRD1, ROR$\gamma\tau$, PLZF, IL-12R, and IL-18R expression and produced IFN-γ to IL-12/IL-18 stimulation (271). While this study did not specifically identify type II NKT cells within this population, the shared genetic transcription profile of mouse type II NKT cells and human $CD161^+$ T cells suggested that this population could be enriched for human type II NKT cells. Since the majority of human $\gamma\delta$ T cells are $CD8^+$ or DN, with $CD4^+$ $\gamma\delta$ T cells being rare in human PBMC, it was unlikely that the $CD161^+CD4^+$ T cell population I identified in SA bacteremic patients contained $\gamma\delta$ T cells (280). I also confirmed that $CD161^+CD4^+$ T cells did not contain MAIT cells, as MAIT cell percentages were decreased in SA bacteremic patients (**Fig. 3-29E**), and the majority of MAIT cells from PBMC were $CD4^-$ (**Fig. 3-28A**). Due to the presence of Th17 cells within the $CD161^+$ T population, I cannot definitively say that human $CD161^+CD4^+$ T cells are type II NKT cells, but it is likely that this population is enriched for type II NKT cells. Functional assays with enriched T cells from SA patients will need to be performed to confirm that human $CD161^+CD4^+$ T cells are CD1d-restricted and whether they produce cytokines to SA lipid antigens in healthy vs. SA bacteremic patients.

Previous studies have used CD1d tetramers loaded with lipid antigens to identify type II NKT cells in human PBMC. Glucosphingolipids were shown to be dysregulated in patients with metabolic disorders, including obesity and Gaucher disease. Glucosphingolipid-loaded human CD1d tetramers identified polyclonal populations of type II NKT cells in healthy human PBMC that produced antigen-specific CD1d-restricted cytokines (177). This study also identified that human PBMC from patients with Gaucher disease had elevated levels of glucosylsphingosine CD1d $tetramer^+$ type II NKT cells compared to healthy donors. In another study, lysophosphatidylcholine (LPC) was enriched from multiple myeloma patient plasma. LPC loaded human CD1d dimers identified CD1d-restricted LPC reactive type II NKT cells in human PBMC that were expanded in multiple myeloma patients (281). A small population of sulfatide-loaded

human CD1d tetramer^{+}CD161^{+} type II NKT cells were also identified in human liver (282). I identified a SA lipid fraction containing PG: lysyl-PG polar lipids that were recognized by mouse type II NKT cells in a CD1d-dependent manner, however further work needs to be done to identify the specific lipid within this fraction that is recognized by type II NKT cells. Once identified, this lipid can be loaded onto human CD1d tetramers to track type II NKT cells in human PBMC.

4-9 Contribution of CD1-restricted T cells during SA infection

In addition to innate-like NKT cells that are activated early in response to infections, humans harbor group 1 CD1-restricted T cells (restricted by CD1a, CD1b, and CD1c). Like NKT cells, group 1 CD1-restricted T cells recognize lipid antigens, however they behave differently than NKT cells in terms of activation kinetics (283). Indeed, work by our lab using transgenic hCD1Tg mice (expressing CD1b and CD1c) identified the peak of group 1 CD1-restricted T cell cytokine production to total SA lipid antigens at 10 dpi (115), similar to conventional T cell kinetics. While NKT cells produced IFN-γ in the liver following SA infection (**Fig. 3-13, 3-14**), group 1 CD1-restricted T cells produced IFN-γ and IL-17A to SA lipid antigens in the LN. Both IFN-γ and IL-17A production by T cells are critical for protection during SA infection (**Fig. 4-1**), illustrating the importance of both NKT cells and group 1 CD1-restricted T cells in SA immunity.

While group 1 CD1-restricted T cells were not necessary for controlling kidney CFU during primary infection, hCD1Tg^{-} mice had increased kidney pathology compared to hCD1Tg^{+} mice at 10 dpi (115). This limiting of kidney pathology by group 1 CD1-restricted T cells was similar to the contribution of type II NKT cells to limit kidney pathology early in response to infection (**Fig. 3-4, 3-5**). Group 1 CD1-restricted T cells also recognized PG from the same fraction (FR-8) as type II NKT cells after SA infection (**Fig. 3-17**), suggesting that FR-8 contained lipid species recognized by both of these CD1-restricted T cell populations. Since this

lipid fraction contains a mixture of multiple PG and lysyl-PG isoforms, I do not know at this time whether group 1 CD1-restricted T cells and type II NKT cells recognize the exact same lipid moiety. Some lipid antigens, such as the self-lipid antigen sulfatide and phospholipids from bacteria, can be presented by multiple CD1 isoforms (284). Therefore, dual recognition of a polar SA lipid antigen by type II NKT cells and group 1 CD1-restricted T cells is possible. Further studies will need to be performed to synthesize individual lipid moieties from SA FR-8 and retest these lipid moieties in ELISPOT screening assays to determine the specific PG and lysyl-PG lipid antigens recognized by type II NKT cells and group 1 CD1-restricted T cells.

4-10 Future Directions in the SA field

4-10.1 Perspectives of T cell help during SA infection

The work described in this study adds to the knowledge of T cell responses during SA infection. I showed that type II NKT cells, but not iNKT cells or MAIT cells, were beneficial for protection against systemic SA infection through production of IFN-γ early in response to infection. I also identified a population of T cells enriched for type II NKT cells that was expanded in patients with SA bacteremia compared to healthy control patients, demonstrating the potential relevance of our study to the human setting. Given the failure of previous vaccines targeting B cell responses in SA infection (**1-1.2c**), identifying additional parameters of immune protection is critical to the success of next generation SA vaccine design. Murine studies demonstrating a protective role for T cells in SA infection have identified T cell production of IL-17A and/or IFN-γ as critical for protection (**4-1**).

Prior to this study, a large body of work in the SA T cell field has focused on 1) the detrimental effect of superantigen-mediated overactivation of T cells or 2) the effect of T cells in SA sepsis at very early timepoints after high-dose infection. While it is important to study SA superantigen-mediated T cell responses, different SA strains encode different SA superantigens

(84) and the total burden of SA-induced sepsis is low relative to total SA infections in humans (95). Therefore the focus of T cell studies to SA superantigens such as SEB is not directly translatable to most clinical cases of SA, considering endemic strains such as the USA300 strain used in our studies do not encode SEB (113). It is possible that SA vaccines targeting the T cell response may run into issues of T cell overactivation in vaccinated patients that later become infected with SA, inducing sepsis. Indeed, mice vaccinated with irradiated-killed SA developed a pathogenic IFN-γ producing $CD4^+$ T cell response to SA bacteremia challenge, leading to increased mortality compared to the unvaccinated group (89). However, identifying T cell-specific antigens to vaccinate patients with, rather than whole killed bacteria, should reduce the effect of deleterious T cell activation.

Identifying SA T cell-specific antigens will be critical for developing new SA vaccines. However, many studies have only focused on T cell responses at early times post-infection. Given that antigen-specific conventional T cell responses take time to develop (7-10 dpi), studying these T cell responses at early timepoints does not provide the full picture of the SA T cell response. By isolating lipid species from the cell membrane of SA and screening them in ELISPOT assays with lymphocytes from infected mice, I identified lipid antigens that were recognized by both type II NKT cells and group 1 CD1-restricted T cells (115). Given the large number of proteins encoded by SA and potential peptide antigens that could induce a conventional T cell response, unbiased identification of SA immunodominant peptides poses some challenges. One method to screen for potential candidates could involve use of the SA mutant transposon library generated by the Nebraska center for *Staphylococcal* research. This library consists of transposon insertions which disrupt approximately 2,000 non-essential genes in the SA genome. Screening this library with $CD4^+$ T cell clones generated from SA infected mice or even PBMC from SA infected patients to identify which genes are necessary for IFN-γ and IL-17A cytokine production could narrow the identification of new immunodominant

antigens. However, this approach would not identify peptides from essential genes that could induce a conventional T cell response.

4-10.2 Development of lipid antigen-based vaccines targeting CD1-restricted T cells

While the vaccine field has focused on conventional T cell responses to induce protective memory T cells, targeting CD1-restricted T cells has many advantages. CD1 molecules are nonpolymorphic, therefore vaccines targeting these T cells would be broadly acting across the human population. Additionally, NKT cells and group 1 CD1-restricted T cells have different activation kinetics, therefore vaccines targeting both these groups could protect against both early and late-stage infection. NKT cells are also enriched at mucosal surfaces where many pathogens invade the host, therefore they are ideal for responding quickly to an infection.

In the case of SA infection, our lab identified a lipid fraction enriched for PG and lysyl-PG species recognized by both type II NKT cells and group 1 CD1-restricted T cells. Further work will need to be done to identify the specific immunodominant lipid(s) within this fraction that activate these CD1-restricted T cell groups. Once done, these lipid(s) can be tested in a vaccine challenge with SA infected mice. Our lab has also found that immunizing hCD1Tg mice with bacteria-derived lipid antigen-pulsed group 1 CD1 expressing DCs induced robust lipid-antigen specific group 1 CD1-restricted T cell responses (285, 115). A more recent approach by our lab administered *Mycobacterium tuberculosis* lipid antigen-loaded nanoparticles to mice to induce a robust group 1 CD1-restricted T cell response in the lung (286).

It is not currently known whether NKT cells and group 1 CD1-restricted T cells develop into memory cells following an infection. NKT cells already express an activated memory phenotype ($CD44^{hi}CD62L^{lo}$) in the naïve state prior to antigen recognition. Mice immunized with DC pulsed α-GalCer develop long-lived $KLRG1^{+}$ iNKT cells persisting in lung and liver for at least 90 days after immunization that mount a more robust cytokine response after secondary

antigen challenge (287), suggesting that targeting NKT cell memory with lipid antigens is possible. Work is ongoing in our lab to characterize the memory response of group 1 CD1-restricted T cells using secondary challenge with *Mycobacterium tuberculosis* infection and using *Mycobacterium tuberculosis* lipid-loaded nanoparticles to vaccine mice then challenge with live bacteria (unpublished data). These proof-of-concept studies to define memory responses in CD1-restricted T cells are critical to determine the feasibility of designing CD1-restricted T cell vaccines.

4-10.3 Identifying correlates of SA protection in humans with a T cell focus

I demonstrated that a T cell population enriched for type II NKT cells is expanded in the blood of SA bacteremic patients compared to healthy control subjects, correlating with our findings in SA infected mice. Given the success of targeting B cells responses in murine SA infections and ultimate failures in clinical trials, it will be important in the future to identify correlates of SA T cell protection in human studies. While mice are the dominant preclinical animal model used in research laboratories, they have significant differences in their immune system makeup compared to humans that can skew the interpretation of findings and their relevance to the human setting. The most pressing example of this in SA infection is the differences in makeup of HLA molecules between mice and humans. Many SA superantigens act by crosslinking MHC-II and TCR and are specific for human HLA MHC-II molecules. Therefore, mice are innately resistant to the superantigen-mediated effects of SA infection (94). As a result, many murine studies exploring the contribution of SA superantigens in outcomes of infection have used much higher inoculums of bacteria than is physiologically relevant to the human setting. Use of HLA-humanized mice have alleviated some of these concerns, however interpretation of previous studies of conventional $CD4^+$ T cells in SA infection without humanized mice must be confirmed with human studies or humanized mice. While the CD1d protein is largely conserved between mice and humans, there are subtle differences in CD1d

lipid antigen affinity and intracellular trafficking between mice and humans (288). Therefore, confirming that the T cell population I identified in SA bacteremic patients is CD1d restricted and reactive to SA lipid antigens will be important to confirming the relevance of targeting type II NKT cells in SA infection in humans.

4-11 Future Directions in the innate-like T cell field and infection

Due to the difficulty of studying type II NKT cells *in vivo*, the knowledge of their relevance to infection is still very understudied. Lack of lipid-antigen specific tetramers and lack of unique surface markers have hampered the ability to study type II NKT cells. The advent of new technologies, such as single cell RNAseq, to identify rare populations of cells could serve as a great tool to define new markers of type II NKT cells and allow for more specific tracking of these cells in an infection setting. One limitation of using single cell RNAseq in an infection setting is the requirement to perform experiments in BSL-2 conditions, however, use of fixation protocols prior to single cell RNA seq could overcome this hurdle. A recent study performed single cell RNA seq on human iNKT cells sorted from patient PBMC and identified five iNKT subpopulations in peripheral blood (289). Using this approach with sorted $CD4^{+}NK1.1^{+}$ T cells from SA-infected $J\alpha18^{-/-}$ mice, I could identify additional markers expressed by type II NKT cells.

An additional 'omics' approach to further define the characteristics of rare populations of cells such as type II NKT cells is to perform TCR repertoire sequencing of sorted type II NKT cells. From our surface staining experiments, I determined that $CD4^{+}NK1.1^{+}$ type II NKT cells utilize diverse $V\alpha/V\beta$ chains (**Fig. 3-12**). TCR repertoire sequencing can tell us whether type II NKT cells utilize diverse or clonal complementarity determining regions (CDRs) and whether a specific CDR recognizing a SA lipid moiety is expanded after SA infection. Since this has not previously been done for type II NKT cells to our knowledge, I would have to sort type II NKT

cells from naïve and infected mice to make a comparison study in alteration of the TCR repertoire after infection.

A few lipid antigens have been identified that are recognized by type II NKT cells using T cell clones derived from human PBMC (179, 180), however further work needs to be done to identify additional lipid antigens from other bacterial infections that activate type II NKT cells. The CD1-restricted T cell field has lagged behind the conventional T cell field in part due to the lack of advances in the field of lipidomics. Lipid extraction and purification is largely limited to techniques developed in the late 1950s using organic solvents and phase extraction (264). One particular CD1-T cell lab with a focus in lipid purification has made use of a unique LC-MS system consisting of a UV detector, a single quadrupole mass spectrometer, an evaporative light scattering detector (ELSD) and a photodiode array detector to fractionate lipids based on ELSD and retention time (180). However, this system requires a dedicated machine since organic solvents must be used to separate out lipid species, and is not commercially available. More advanced techniques to characterize lipid polarity are available, such as electrospray ionization coupled with different mass analyzers like ion trap and time-of-flight (290), however these methods require fragmentation of lipids, therefore they cannot be used for purification purposes. Further advances in the field of lipidomics are needed to enhance isolation and identification of lipid antigens recognized by CD1-restricted T cells.

4-12 Concluding Remarks

The study of NKT cells and MAIT cells and their relevance to infection control is much understudied relative to the conventional T cell response. In this work, I demonstrated that type II NKT cells, not iNKT cells or MAIT cells, were important for reducing bacterial burden and controlling neutrophil infiltrate to infected liver and kidneys of mice with SA systemic infection (**Fig. 4-2**). This protection was mediated by type II NKT cell IFN-γ production, which required both CD1d-TCR engagement and IL-12 production/MyD88 engagement by APCs. I also

determined that PG and lysyl-PG species from the cell membrane of SA induced type II NKT cell cytokine production. I identified a population of T cells, enriched for type II NKT cells, that expanded in patients with SA bacteremia relative to healthy controls, suggesting the potential relevance of type II NKT cells in human SA infection. Due to lack of specific markers to track type II NKT cells *in vivo*, study of this unconventional T cell population has lagged far behind iNKT cells. However, given the higher prevalence of type II NKT cells in humans relative to iNKT cells, it will be important for future studies to characterize type II NKT cell responses in different disease states. Because of the nonpolymorphic nature of CD1 molecules, targeting of type II NKT cells with a lipid antigen vaccine could be a novel method to induce protection against SA infections where previous vaccines have failed.

Figure 4-2. Type II NKT cells protect against SA infection.

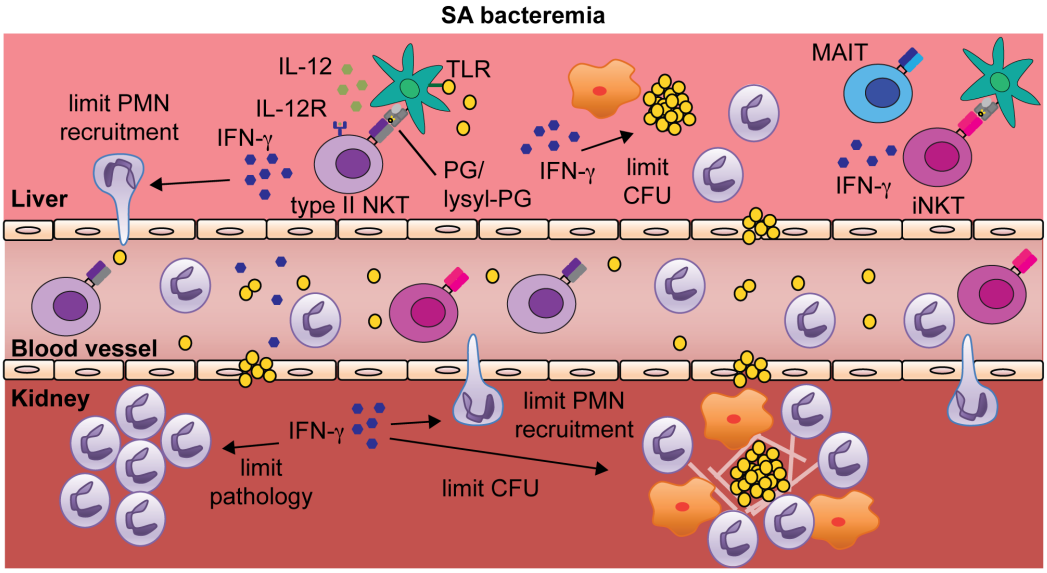

Figure 4-2: Schematic of known protective type II NKT cell responses to SA systemic infection. During SA bacteremia, SA enters liver and kidneys via the bloodstream and begins to form abscesses in the kidneys, a colony of bacteria surrounded by a fibrinogen capsule and infiltrating neutrophils and macrophages. TLR recognition of PAMPs on SA activates DCs via the MyD88 pathway to produce IL-12. Type II NKT cells were activated by recognition of PG/lysyl-PG presented by CD1d to the TCR and binding of DC-derived IL-12 to the type II NKT cell IL-12 receptor. These 2 signals activated type II NKT cells to produce IFN-γ, which contributed to limit neutrophil infiltrate and bacterial burden in the kidneys and liver, and inflammation in the kidneys. iNKT cells were also activated via CD1d and MyD88 to produce IFN-γ in response to SA infection, but were not required for protection. MAIT cells were dispensable for control of SA infection.

References

1. Thomer, L, Schneewind, O, and Missiakas, D (2016). Pathogenesis of Staphylococcus aureus Bloodstream Infections. *Annu Rev Pathol* 11**,** 343-364. doi: 10.1146/annurev-pathol-012615-044351.
2. Fridken, S (2016). "Antibiotic Resistance Patient Safety Atlas". Centers for Disease Control and Prevention).
3. McGuinness, WA, Malachowa, N, and DeLeo, FR (2017). Vancomycin Resistance in Staphylococcus aureus. *Yale J Biol Med* 90(2)**,** 269-281.
4. Licitra, G (2013). Etymologia: Staphylococcus. *Emerg Infect Dis.* 19(9)**,** 1553. doi: https://doi.org/10.3201/eid1909.ET1909.
5. Mendy, A, Vieira, ER, Albatineh, AN, and Gasana, J (2016). Staphylococcus aureus Colonization and Long-Term Risk for Death, United States. *Emerg Infect Dis.* 22(11)**,** 1966-1969. doi: https://dx.doi.org/10.3201/eid2211.160220.
6. Maayan-Metzger, A, Strauss, T, C., R, Jaber, H, Dulitzky, M, Reiss-Mandel, A, et al. (2017). Clinical evaluation of early acquisition of Staphylococcus aureus carriage by newborns. *Int J Infect Dis.* 64**,** 9-14. doi: 10.1016/j.ijid.2017.08.013.
7. Sakr, A, Brégeon, F, Mège, J, Rolain, J, and Blin, O (2018). Staphylococcus aureus Nasal Colonization: An Update on Mechanisms, Epidemiology, Risk Factors, and Subsequent Infections. *Front Microbiol.* 9**,** 2419. doi: 10.3389/fmicb.2018.02419.
8. Hanberger, H, Walther, S, Leone, M, Barie, PS, Rello, J, Lipman, J, et al. (2011). Increased mortality associated with methicillin-resistant Staphylococcus aureus (MRSA) infection in the intensive care unit: results from the EPIC II study. *Int J Antimicrob Agents* 38(4)**,** 331-335. doi: 10.1016/j.ijantimicag.2011.05.013.
9. Fournier, B, and Philpott, D (2005). Recognition of Staphylococcus aureus by the innate immune system. *Clin Microbiol Rev* 18(3)**,** 521-540. doi: 10.1128/CMR.18.3.521-540.2005.
10. Cheng, AG, McAdow, M, Kim, HK, Bae, T, Missiakas, DM, and Schneewind, O (2010). Contribution of coagulases towards Staphylococcus aureus disease and protective immunity. *PLoS Pathog* 6(8)**,** e1001036. doi: 10.1371/journal.ppat.1001036.
11. Kim, HK, Missiakas, D, and Schneewind, O (2014). Mouse models for infectious diseases caused by Staphylococcus aureus. *J Immunol Methods* 410**,** 88-99. doi: 10.1016/j.jim.2014.04.007.
12. Singer, M, Deutschman, CS, Seymour, CW, Shankar-Hari, M, Annane, D, Bauer, M, et al. (2016). The Third International Consensus Definitions for Sepsis and Septic Shock (Sepsis-3). *JAMA* 315(8)**,** 801-810. doi: 10.1001/jama.2016.0287.
13. McAdow, M, Kim, HK, Dedent, AC, Hendrickx, AP, Schneewind, O, and Missiakas, DM (2011). Preventing Staphylococcus aureus sepsis through the inhibition of its agglutination in blood. *PLoS Pathog* 7(10)**,** e1002307. doi: 10.1371/journal.ppat.1002307.
14. Xu, SX, and McCormick, JK (2012). Staphylococcal superantigens in colonization and disease. *Front Cell Infect Microbiol* 2**,** 52. doi: 10.3389/fcimb.2012.00052.
15. Guerra, FE, Borgogna, TR, Patel, DM, Sward, EW, and Voyich, JM (2017). Epic Immune Battles of History: Neutrophils vs. Staphylococcus aureus. *Front Cell Infect Microbiol* 7**,** 286. doi: 10.3389/fcimb.2017.00286.
16. Ley, K, Hoffman, HM, Kubes, P, Cassatella, MA, Zychlinsky, A, Hedrick, CC, et al. (2018). Neutrophils: New insights and open questions. *Sci Immunol* 3(30). doi: 10.1126/sciimmunol.aat4579.

17. Olaru, F, and Jensen, LE (2010). Staphylococcus aureus stimulates neutrophil targeting chemokine expression in keratinocytes through an autocrine IL-1alpha signaling loop. *J Invest Dermatol* 130(7)**,** 1866-1876. doi: 10.1038/jid.2010.37.
18. Laarman, AJ, Mijnheer, G, Mootz, JM, van Rooijen, WJ, Ruyken, M, Malone, CL, et al. (2012). Staphylococcus aureus Staphopain A inhibits CXCR2-dependent neutrophil activation and chemotaxis. *EMBO J* 31(17)**,** 3607-3619. doi: 10.1038/emboj.2012.212.
19. de Haas, CJ, Veldkamp, KE, Peschel, A, Weerkamp, F, Van Wamel, WJ, Heezius, EC, et al. (2004). Chemotaxis inhibitory protein of Staphylococcus aureus, a bacterial antiinflammatory agent. *J Exp Med* 199(5)**,** 687-695. doi: 10.1084/jem.20031636.
20. Prat, C, Bestebroer, J, de Haas, CJ, van Strijp, JA, and van Kessel, KP (2006). A new staphylococcal anti-inflammatory protein that antagonizes the formyl peptide receptor-like 1. *J Immunol* 177(11)**,** 8017-8026. doi: 10.4049/jimmunol.177.11.8017.
21. Prat, C, Haas, PJ, Bestebroer, J, de Haas, CJ, van Strijp, JA, and van Kessel, KP (2009). A homolog of formyl peptide receptor-like 1 (FPRL1) inhibitor from Staphylococcus aureus (FPRL1 inhibitory protein) that inhibits FPRL1 and FPR. *J Immunol* 183(10)**,** 6569-6578. doi: 10.4049/jimmunol.0801523.
22. Bestebroer, J, Poppelier, MJ, Ulfman, LH, Lenting, PJ, Denis, CV, van Kessel, KP, et al. (2007). Staphylococcal superantigen-like 5 binds PSGL-1 and inhibits P-selectin-mediated neutrophil rolling. *Blood* 109(7)**,** 2936-2943. doi: 10.1182/blood-2006-06-015461.
23. Fevre, C, Bestebroer, J, Mebius, MM, de Haas, CJ, van Strijp, JA, Fitzgerald, JR, et al. (2014). Staphylococcus aureus proteins SSL6 and SElX interact with neutrophil receptors as identified using secretome phage display. *Cell Microbiol* 16(11)**,** 1646-1665. doi: 10.1111/cmi.12313.
24. Rooijakkers, SH, Ruyken, M, Roos, A, Daha, MR, Presanis, JS, Sim, RB, et al. (2005). Immune evasion by a staphylococcal complement inhibitor that acts on C3 convertases. *Nat Immunol* 6(9)**,** 920-927. doi: 10.1038/ni1235.
25. Forsgren, A, and Sjoquist, J (1966). "Protein A" from S. aureus. I. Pseudo-immune reaction with human gamma-globulin. *J Immunol* 97(6)**,** 822-827.
26. Kronvall, G, Grey, HM, and Williams, RC, Jr. (1970). Protein A reactivity with mouse immunoglobulins. Structural relationship between some mouse and human immunoglobulins. *J Immunol* 105(5)**,** 1116-1123.
27. Sjodahl, J (1977). Structural studies on the four repetitive Fc-binding regions in protein A from Staphylococcus aureus. *Eur J Biochem* 78(2)**,** 471-490. doi: 10.1111/j.1432-1033.1977.tb11760.x.
28. Langley, R, Wines, B, Willoughby, N, Basu, I, Proft, T, and Fraser, JD (2005). The staphylococcal superantigen-like protein 7 binds IgA and complement C5 and inhibits IgA-Fc alpha RI binding and serum killing of bacteria. *J Immunol* 174(5)**,** 2926-2933. doi: 10.4049/jimmunol.174.5.2926.
29. Smith, EJ, Visai, L, Kerrigan, SW, Speziale, P, and Foster, TJ (2011). The Sbi protein is a multifunctional immune evasion factor of Staphylococcus aureus. *Infect Immun* 79(9)**,** 3801-3809. doi: 10.1128/IAI.05075-11.
30. Lu, T, Porter, AR, Kennedy, AD, Kobayashi, SD, and DeLeo, FR (2014). Phagocytosis and killing of Staphylococcus aureus by human neutrophils. *J Innate Immun* 6(5)**,** 639-649. doi: 10.1159/000360478.
31. Peschel, A, Otto, M, Jack, RW, Kalbacher, H, Jung, G, and Gotz, F (1999). Inactivation of the dlt operon in Staphylococcus aureus confers sensitivity to defensins, protegrins, and other antimicrobial peptides. *J Biol Chem* 274(13)**,** 8405-8410. doi: 10.1074/jbc.274.13.8405.
32. Collins, LV, Kristian, SA, Weidenmaier, C, Faigle, M, Van Kessel, KP, Van Strijp, JA, et al. (2002). Staphylococcus aureus strains lacking D-alanine modifications of teichoic acids

are highly susceptible to human neutrophil killing and are virulence attenuated in mice. *J Infect Dis* 186(2)**,** 214-219. doi: 10.1086/341454.
33. Peschel, A, Jack, RW, Otto, M, Collins, LV, Staubitz, P, Nicholson, G, et al. (2001). Staphylococcus aureus resistance to human defensins and evasion of neutrophil killing via the novel virulence factor MprF is based on modification of membrane lipids with l-lysine. *J Exp Med* 193(9)**,** 1067-1076. doi: 10.1084/jem.193.9.1067.
34. Jin, T, Bokarewa, M, Foster, T, Mitchell, J, Higgins, J, and Tarkowski, A (2004). Staphylococcus aureus resists human defensins by production of staphylokinase, a novel bacterial evasion mechanism. *J Immunol* 172(2)**,** 1169-1176. doi: 10.4049/jimmunol.172.2.1169.
35. Stapels, DA, Ramyar, KX, Bischoff, M, von Kockritz-Blickwede, M, Milder, FJ, Ruyken, M, et al. (2014). Staphylococcus aureus secretes a unique class of neutrophil serine protease inhibitors. *Proc Natl Acad Sci U S A* 111(36)**,** 13187-13192. doi: 10.1073/pnas.1407616111.
36. Karavolos, MH, Horsburgh, MJ, Ingham, E, and Foster, SJ (2003). Role and regulation of the superoxide dismutases of Staphylococcus aureus. *Microbiology* 149(Pt 10)**,** 2749-2758. doi: 10.1099/mic.0.26353-0.
37. Liu, GY, Essex, A, Buchanan, JT, Datta, V, Hoffman, HM, Bastian, JF, et al. (2005). Staphylococcus aureus golden pigment impairs neutrophil killing and promotes virulence through its antioxidant activity. *J Exp Med* 202(2)**,** 209-215. doi: 10.1084/jem.20050846.
38. Singh, VK, Vaish, M, Johansson, TR, Baum, KR, Ring, RP, Singh, S, et al. (2015). Significance of four methionine sulfoxide reductases in Staphylococcus aureus. *PLoS One* 10(2)**,** e0117594. doi: 10.1371/journal.pone.0117594.
39. Guerra, FE, Addison, CB, de Jong, NW, Azzolino, J, Pallister, KB, van Strijp, JA, et al. (2016). Staphylococcus aureus SaeR/S-regulated factors reduce human neutrophil reactive oxygen species production. *J Leukoc Biol* 100(5)**,** 1005-1010. doi: 10.1189/jlb.4VMAB0316-100RR.
40. Buvelot, H, Posfay-Barbe, KM, Linder, P, Schrenzel, J, and Krause, KH (2017). Staphylococcus aureus, phagocyte NADPH oxidase and chronic granulomatous disease. *FEMS Microbiol Rev* 41(2)**,** 139-157. doi: 10.1093/femsre/fuw042.
41. Gresham, HD, Lowrance, JH, Caver, TE, Wilson, BS, Cheung, AL, and Lindberg, FP (2000). Survival of Staphylococcus aureus inside neutrophils contributes to infection. *J Immunol* 164(7)**,** 3713-3722. doi: 10.4049/jimmunol.164.7.3713.
42. McLoughlin, RM, Lee, JC, Kasper, DL, and Tzianabos, AO (2008). IFN-gamma regulated chemokine production determines the outcome of Staphylococcus aureus infection. *J Immunol* 181(2)**,** 1323-1332. doi: 10.4049/jimmunol.181.2.1323.
43. Berends, ET, Horswill, AR, Haste, NM, Monestier, M, Nizet, V, and von Kockritz-Blickwede, M (2010). Nuclease expression by Staphylococcus aureus facilitates escape from neutrophil extracellular traps. *J Innate Immun* 2(6)**,** 576-586. doi: 10.1159/000319909.
44. Thammavongsa, V, Missiakas, DM, and Schneewind, O (2013). Staphylococcus aureus degrades neutrophil extracellular traps to promote immune cell death. *Science* 342(6160)**,** 863-866. doi: 10.1126/science.1242255.
45. Greenlee-Wacker, MC, Rigby, KM, Kobayashi, SD, Porter, AR, DeLeo, FR, and Nauseef, WM (2014). Phagocytosis of Staphylococcus aureus by human neutrophils prevents macrophage efferocytosis and induces programmed necrosis. *J Immunol* 192(10)**,** 4709-4717. doi: 10.4049/jimmunol.1302692.
46. Flannagan, RS, Cosio, G, and Grinstein, S (2009). Antimicrobial mechanisms of phagocytes and bacterial evasion strategies. *Nat Rev Microbiol* 7(5)**,** 355-366. doi: 10.1038/nrmicro2128.

47. Flannagan, RS, Kuiack, RC, McGavin, MJ, and Heinrichs, DE (2018). Staphylococcus aureus Uses the GraXRS Regulatory System To Sense and Adapt to the Acidified Phagolysosome in Macrophages. *mBio* 9(4). doi: 10.1128/mBio.01143-18.
48. Surewaard, BG, Deniset, JF, Zemp, FJ, Amrein, M, Otto, M, Conly, J, et al. (2016). Identification and treatment of the Staphylococcus aureus reservoir in vivo. *J Exp Med* 213(7)**,** 1141-1151. doi: 10.1084/jem.20160334.
49. Fournier, B (2012). The function of TLR2 during staphylococcal diseases. *Front Cell Infect Microbiol* 2**,** 167. doi: 10.3389/fcimb.2012.00167.
50. Takeuchi, O, Hoshino, K, and Akira, S (2000). Cutting edge: TLR2-deficient and MyD88-deficient mice are highly susceptible to Staphylococcus aureus infection. *J Immunol* 165(10)**,** 5392-5396. doi: 10.4049/jimmunol.165.10.5392.
51. Miller, LS, O'Connell, RM, Gutierrez, MA, Pietras, EM, Shahangian, A, Gross, CE, et al. (2006). MyD88 mediates neutrophil recruitment initiated by IL-1R but not TLR2 activation in immunity against Staphylococcus aureus. *Immunity* 24(1)**,** 79-91. doi: 10.1016/j.immuni.2005.11.011.
52. Miller, LS, Pietras, EM, Uricchio, LH, Hirano, K, Rao, S, Lin, H, et al. (2007). Inflammasome-mediated production of IL-1beta is required for neutrophil recruitment against Staphylococcus aureus in vivo. *J Immunol* 179(10)**,** 6933-6942. doi: 10.4049/jimmunol.179.10.6933.
53. Jann, NJ, Schmaler, M, Ferracin, F, and Landmann, R (2011). TLR2 enhances NADPH oxidase activity and killing of Staphylococcus aureus by PMN. *Immunol Lett* 135(1-2)**,** 17-23. doi: 10.1016/j.imlet.2010.09.007.
54. Koymans, KJ, Feitsma, LJ, Brondijk, TH, Aerts, PC, Lukkien, E, Lossl, P, et al. (2015). Structural basis for inhibition of TLR2 by staphylococcal superantigen-like protein 3 (SSL3). *Proc Natl Acad Sci U S A* 112(35)**,** 11018-11023. doi: 10.1073/pnas.1502026112.
55. Deshmukh, HS, Hamburger, JB, Ahn, SH, McCafferty, DG, Yang, SR, and Fowler, VG, Jr. (2009). Critical role of NOD2 in regulating the immune response to Staphylococcus aureus. *Infect Immun* 77(4)**,** 1376-1382. doi: 10.1128/IAI.00940-08.
56. Schaffler, H, Demircioglu, DD, Kuhner, D, Menz, S, Bender, A, Autenrieth, IB, et al. (2014). NOD2 stimulation by Staphylococcus aureus-derived peptidoglycan is boosted by Toll-like receptor 2 costimulation with lipoproteins in dendritic cells. *Infect Immun* 82(11)**,** 4681-4688. doi: 10.1128/IAI.02043-14.
57. Hruz, P, Zinkernagel, AS, Jenikova, G, Botwin, GJ, Hugot, JP, Karin, M, et al. (2009). NOD2 contributes to cutaneous defense against Staphylococcus aureus through alpha-toxin-dependent innate immune activation. *Proc Natl Acad Sci U S A* 106(31)**,** 12873-12878. doi: 10.1073/pnas.0904958106.
58. Gjertsson, I, Hultgren, OH, Stenson, M, Holmdahl, R, and Tarkowski, A (2000). Are B lymphocytes of importance in severe Staphylococcus aureus infections? *Infect Immun* 68(5)**,** 2431-2434. doi: 10.1128/iai.68.5.2431-2434.2000.
59. Fritz, SA, Tiemann, KM, Hogan, PG, Epplin, EK, Rodriguez, M, Al-Zubeidi, DN, et al. (2013). A serologic correlate of protective immunity against community-onset Staphylococcus aureus infection. *Clin Infect Dis* 56(11)**,** 1554-1561. doi: 10.1093/cid/cit123.
60. Adhikari, RP, Ajao, AO, Aman, MJ, Karauzum, H, Sarwar, J, Lydecker, AD, et al. (2012). Lower antibody levels to Staphylococcus aureus exotoxins are associated with sepsis in hospitalized adults with invasive S. aureus infections. *J Infect Dis* 206(6)**,** 915-923. doi: 10.1093/infdis/jis462.
61. Pelzek, AJ, Shopsin, B, Radke, EE, Tam, K, Ueberheide, BM, Fenyo, D, et al. (2018). Human Memory B Cells Targeting Staphylococcus aureus Exotoxins Are Prevalent with Skin and Soft Tissue Infection. *mBio* 9(2). doi: 10.1128/mBio.02125-17.

62. Falugi, F, Kim, HK, Missiakas, DM, and Schneewind, O (2013). Role of protein A in the evasion of host adaptive immune responses by Staphylococcus aureus. *mBio* 4(5)**,** e00575-00513. doi: 10.1128/mBio.00575-13.
63. Ulloa-Morales, AJ, Goodyear, CS, and Silverman, GJ (2018). Essential Domain-Dependent Roles Within Soluble IgG for in vivo Superantigen Properties of Staphylococcal Protein A: Resolving the B-Cell Superantigen Paradox. *Front Immunol* 9**,** 2011. doi: 10.3389/fimmu.2018.02011.
64. Yoong, P, and Pier, GB (2010). Antibody-mediated enhancement of community-acquired methicillin-resistant Staphylococcus aureus infection. *Proc Natl Acad Sci U S A* 107(5)**,** 2241-2246. doi: 10.1073/pnas.0910344107.
65. Skurnik, D, Merighi, M, Grout, M, Gadjeva, M, Maira-Litran, T, Ericsson, M, et al. (2010). Animal and human antibodies to distinct Staphylococcus aureus antigens mutually neutralize opsonic killing and protection in mice. *J Clin Invest* 120(9)**,** 3220-3233. doi: 10.1172/JCI42748.
66. Fattom, AI, Sarwar, J, Ortiz, A, and Naso, R (1996). A Staphylococcus aureus capsular polysaccharide (CP) vaccine and CP-specific antibodies protect mice against bacterial challenge. *Infect Immun* 64(5)**,** 1659-1665. doi: 10.1128/IAI.64.5.1659-1665.1996.
67. Lee, JC, Park, JS, Shepherd, SE, Carey, V, and Fattom, A (1997). Protective efficacy of antibodies to the Staphylococcus aureus type 5 capsular polysaccharide in a modified model of endocarditis in rats. *Infect Immun* 65(10)**,** 4146-4151. doi: 10.1128/IAI.65.10.4146-4151.1997.
68. Fattom, A, Fuller, S, Propst, M, Winston, S, Muenz, L, He, D, et al. (2004). Safety and immunogenicity of a booster dose of Staphylococcus aureus types 5 and 8 capsular polysaccharide conjugate vaccine (StaphVAX) in hemodialysis patients. *Vaccine* 23(5)**,** 656-663. doi: 10.1016/j.vaccine.2004.06.043.
69. Fattom, A, Matalon, A, Buerkert, J, Taylor, K, Damaso, S, and Boutriau, D (2015). Efficacy profile of a bivalent Staphylococcus aureus glycoconjugated vaccine in adults on hemodialysis: Phase III randomized study. *Hum Vaccin Immunother* 11(3)**,** 632-641. doi: 10.4161/hv.34414.
70. Kuklin, NA, Clark, DJ, Secore, S, Cook, J, Cope, LD, McNeely, T, et al. (2006). A novel Staphylococcus aureus vaccine: iron surface determinant B induces rapid antibody responses in rhesus macaques and specific increased survival in a murine S. aureus sepsis model. *Infect Immun* 74(4)**,** 2215-2223. doi: 10.1128/IAI.74.4.2215-2223.2006.
71. Fowler, VG, Allen, KB, Moreira, ED, Moustafa, M, Isgro, F, Boucher, HW, et al. (2013). Effect of an investigational vaccine for preventing Staphylococcus aureus infections after cardiothoracic surgery: a randomized trial. *JAMA* 309(13)**,** 1368-1378. doi: 10.1001/jama.2013.3010.
72. McNeely, TB, Shah, NA, Fridman, A, Joshi, A, Hartzel, JS, Keshari, RS, et al. (2014). Mortality among recipients of the Merck V710 Staphylococcus aureus vaccine after postoperative S. aureus infections: an analysis of possible contributing host factors. *Hum Vaccin Immunother* 10(12)**,** 3513-3516. doi: 10.4161/hv.34407.
73. Gurtman, A, Begier, E, Mohamed, N, Baber, J, Sabharwal, C, Haupt, RM, et al. (2019). The development of a staphylococcus aureus four antigen vaccine for use prior to elective orthopedic surgery. *Hum Vaccin Immunother* 15(2)**,** 358-370. doi: 10.1080/21645515.2018.1523093.
74. Narita, K, Hu, DL, Mori, F, Wakabayashi, K, Iwakura, Y, and Nakane, A (2010). Role of interleukin-17A in cell-mediated protection against Staphylococcus aureus infection in mice immunized with the fibrinogen-binding domain of clumping factor A. *Infect Immun* 78(10)**,** 4234-4242. doi: 10.1128/IAI.00447-10.
75. Creech, CB, Frenck, RW, Fiquet, A, Feldman, R, Kankam, MK, Pathirana, S, et al. (2020). Persistence of Immune Responses Through 36 Months in Healthy Adults After

Vaccination With a Novel Staphylococcus aureus 4-Antigen Vaccine (SA4Ag). *Open Forum Infect Dis* 7(1), ofz532. doi: 10.1093/ofid/ofz532.
76. Roetzer, A, Jilma, B, and Eibl, MM (2017). Vaccine against toxic shock syndrome in a first-in-man clinical trial. *Expert Rev Vaccines* 16(2), 81-83. doi: 10.1080/14760584.2017.1268921.
77. Chen, WH, Pasetti, MF, Adhikari, RP, Baughman, H, Douglas, R, El-Khorazaty, J, et al. (2016). Safety and Immunogenicity of a Parenterally Administered, Structure-Based Rationally Modified Recombinant Staphylococcal Enterotoxin B Protein Vaccine, STEBVax. *Clin Vaccine Immunol* 23(12), 918-925. doi: 10.1128/CVI.00399-16.
78. Landrum, ML, Lalani, T, Niknian, M, Maguire, JD, Hospenthal, DR, Fattom, A, et al. (2017). Safety and immunogenicity of a recombinant Staphylococcus aureus alpha-toxoid and a recombinant Panton-Valentine leukocidin subunit, in healthy adults. *Hum Vaccin Immunother* 13(4), 791-801. doi: 10.1080/21645515.2016.1248326.
79. Redi, D, Raffaelli, CS, Rossetti, B, De Luca, A, and Montagnani, F (2018). Staphylococcus aureus vaccine preclinical and clinical development: current state of the art. *New Microbiol* 41(3), 208-213.
80. Laupland, KB, Ross, T, and Gregson, DB (2008). Staphylococcus aureus bloodstream infections: risk factors, outcomes, and the influence of methicillin resistance in Calgary, Canada, 2000-2006. *J Infect Dis* 198(3), 336-343. doi: 10.1086/589717.
81. Wiese, L, Mejer, N, Schonheyder, HC, Westh, H, Jensen, AG, Larsen, AR, et al. (2013). A nationwide study of comorbidity and risk of reinfection after Staphylococcus aureus bacteraemia. *J Infect* 67(3), 199-205. doi: 10.1016/j.jinf.2013.04.018.
82. Chandesris, MO, Melki, I, Natividad, A, Puel, A, Fieschi, C, Yun, L, et al. (2012). Autosomal dominant STAT3 deficiency and hyper-IgE syndrome: molecular, cellular, and clinical features from a French national survey. *Medicine (Baltimore)* 91(4), e1-19. doi: 10.1097/MD.0b013e31825f95b9.
83. Fleischer, B, and Schrezenmeier, H (1988). T cell stimulation by staphylococcal enterotoxins. Clonally variable response and requirement for major histocompatibility complex class II molecules on accessory or target cells. *J Exp Med* 167(5), 1697-1707. doi: 10.1084/jem.167.5.1697.
84. Broker, BM, Mrochen, D, and Peton, V (2016). The T Cell Response to Staphylococcus aureus. *Pathogens* 5(1). doi: 10.3390/pathogens5010031.
85. Archer, NK, Harro, JM, and Shirtliff, ME (2013). Clearance of Staphylococcus aureus nasal carriage is T cell dependent and mediated through interleukin-17A expression and neutrophil influx. *Infect Immun* 81(6), 2070-2075. doi: 10.1128/IAI.00084-13.
86. Lin, L, Ibrahim, AS, Xu, X, Farber, JM, Avanesian, V, Baquir, B, et al. (2009). Th1-Th17 cells mediate protective adaptive immunity against Staphylococcus aureus and Candida albicans infection in mice. *PLoS Pathog* 5(12), e1000703. doi: 10.1371/journal.ppat.1000703.
87. Ishigame, H, Kakuta, S, Nagai, T, Kadoki, M, Nambu, A, Komiyama, Y, et al. (2009). Differential roles of interleukin-17A and -17F in host defense against mucoepithelial bacterial infection and allergic responses. *Immunity* 30(1), 108-119. doi: 10.1016/j.immuni.2008.11.009.
88. Brown, AF, Murphy, AG, Lalor, SJ, Leech, JM, O'Keeffe, KM, Mac Aogain, M, et al. (2015). Memory Th1 Cells Are Protective in Invasive Staphylococcus aureus Infection. *PLoS Pathog* 11(11), e1005226. doi: 10.1371/journal.ppat.1005226.
89. Karauzum, H, Haudenschild, CC, Moore, IN, Mahmoudieh, M, Barber, DL, and Datta, SK (2017). Lethal CD4 T Cell Responses Induced by Vaccination Against Staphylococcus aureus Bacteremia. *J Infect Dis* 215(8), 1231-1239. doi: 10.1093/infdis/jix096.

90. Parker, D, Ryan, CL, Alonzo, F, 3rd, Torres, VJ, Planet, PJ, and Prince, AS (2015). CD4+ T cells promote the pathogenesis of Staphylococcus aureus pneumonia. *J Infect Dis* 211(5), 835-845. doi: 10.1093/infdis/jiu525.
91. Wilke, GA, and Bubeck Wardenburg, J (2010). Role of a disintegrin and metalloprotease 10 in Staphylococcus aureus alpha-hemolysin-mediated cellular injury. *Proc Natl Acad Sci U S A* 107(30), 13473-13478. doi: 10.1073/pnas.1001815107.
92. Alonzo, F, 3rd, Kozhaya, L, Rawlings, SA, Reyes-Robles, T, DuMont, AL, Myszka, DG, et al. (2013). CCR5 is a receptor for Staphylococcus aureus leukotoxin ED. *Nature* 493(7430), 51-55. doi: 10.1038/nature11724.
93. Grumann, D, Nubel, U, and Broker, BM (2014). Staphylococcus aureus toxins--their functions and genetics. *Infect Genet Evol* 21, 583-592. doi: 10.1016/j.meegid.2013.03.013.
94. Tuffs, SW, Haeryfar, SMM, and McCormick, JK (2018). Manipulation of Innate and Adaptive Immunity by Staphylococcal Superantigens. *Pathogens* 7(2). doi: 10.3390/pathogens7020053.
95. DeVries, AS, Lesher, L, Schlievert, PM, Rogers, T, Villaume, LG, Danila, R, et al. (2011). Staphylococcal toxic shock syndrome 2000-2006: epidemiology, clinical features, and molecular characteristics. *PLoS One* 6(8), e22997. doi: 10.1371/journal.pone.0022997.
96. Holtfreter, S, Roschack, K, Eichler, P, Eske, K, Holtfreter, B, Kohler, C, et al. (2006). Staphylococcus aureus carriers neutralize superantigens by antibodies specific for their colonizing strain: a potential explanation for their improved prognosis in severe sepsis. *J Infect Dis* 193(9), 1275-1278. doi: 10.1086/503048.
97. Frodermann, V, Chau, TA, Sayedyahossein, S, Toth, JM, Heinrichs, DE, and Madrenas, J (2011). A modulatory interleukin-10 response to staphylococcal peptidoglycan prevents Th1/Th17 adaptive immunity to Staphylococcus aureus. *J Infect Dis* 204(2), 253-262. doi: 10.1093/infdis/jir276.
98. Schreiner, J, Kretschmer, D, Klenk, J, Otto, M, Buhring, HJ, Stevanovic, S, et al. (2013). Staphylococcus aureus phenol-soluble modulin peptides modulate dendritic cell functions and increase in vitro priming of regulatory T cells. *J Immunol* 190(7), 3417-3426. doi: 10.4049/jimmunol.1202563.
99. Cho, JS, Pietras, EM, Garcia, NC, Ramos, RI, Farzam, DM, Monroe, HR, et al. (2010). IL-17 is essential for host defense against cutaneous Staphylococcus aureus infection in mice. *J Clin Invest* 120(5), 1762-1773. doi: 10.1172/JCI40891.
100. Marchitto, MC, Dillen, CA, Liu, H, Miller, RJ, Archer, NK, Ortines, RV, et al. (2019). Clonal Vgamma6(+)Vdelta4(+) T cells promote IL-17-mediated immunity against Staphylococcus aureus skin infection. *Proc Natl Acad Sci U S A* 116(22), 10917-10926. doi: 10.1073/pnas.1818256116.
101. Dillen, CA, Pinsker, BL, Marusina, AI, Merleev, AA, Farber, ON, Liu, H, et al. (2018). Clonally expanded gammadelta T cells protect against Staphylococcus aureus skin reinfection. *J Clin Invest* 128(3), 1026-1042. doi: 10.1172/JCI96481.
102. Maher, BM, Mulcahy, ME, Murphy, AG, Wilk, M, O'Keeffe, KM, Geoghegan, JA, et al. (2013). Nlrp-3-driven interleukin 17 production by gammadeltaT cells controls infection outcomes during Staphylococcus aureus surgical site infection. *Infect Immun* 81(12), 4478-4489. doi: 10.1128/IAI.01026-13.
103. Murphy, AG, O'Keeffe, KM, Lalor, SJ, Maher, BM, Mills, KH, and McLoughlin, RM (2014). Staphylococcus aureus infection of mice expands a population of memory gammadelta T cells that are protective against subsequent infection. *J Immunol* 192(8), 3697-3708. doi: 10.4049/jimmunol.1303420.
104. Cheng, P, Liu, T, Zhou, WY, Zhuang, Y, Peng, LS, Zhang, JY, et al. (2012). Role of gamma-delta T cells in host response against Staphylococcus aureus-induced pneumonia. *BMC Immunol* 13, 38. doi: 10.1186/1471-2172-13-38.

105. Perez-Bosque, A, Miro, L, Polo, J, Russell, L, Campbell, J, Weaver, E, et al. (2008). Dietary plasma proteins modulate the immune response of diffuse gut-associated lymphoid tissue in rats challenged with Staphylococcus aureus enterotoxin B. *J Nutr* 138(3)**,** 533-537. doi: 10.1093/jn/138.3.533.
106. Kumar, S, Colpitts, SL, Menoret, A, Budelsky, AL, Lefrancois, L, and Vella, AT (2013). Rapid alphabeta T-cell responses orchestrate innate immunity in response to Staphylococcal enterotoxin A. *Mucosal Immunol* 6(5)**,** 1006-1015. doi: 10.1038/mi.2012.138.
107. Morita, CT, Li, H, Lamphear, JG, Rich, RR, Fraser, JD, Mariuzza, RA, et al. (2001). Superantigen recognition by gammadelta T cells: SEA recognition site for human Vgamma2 T cell receptors. *Immunity* 14(3)**,** 331-344. doi: 10.1016/s1074-7613(01)00113-3.
108. Barral, DC, and Brenner, MB (2007). CD1 antigen presentation: how it works. *Nat Rev Immunol* 7(12)**,** 929-941. doi: 10.1038/nri2191.
109. Kwiecinski, J, Rhost, S, Lofbom, L, Blomqvist, M, Mansson, JE, Cardell, SL, et al. (2013). Sulfatide attenuates experimental Staphylococcus aureus sepsis through a CD1d-dependent pathway. *Infect Immun* 81(4)**,** 1114-1120. doi: 10.1128/IAI.01334-12.
110. Hayworth, JL, Mazzuca, DM, Maleki Vareki, S, Welch, I, McCormick, JK, and Haeryfar, SM (2012). CD1d-independent activation of mouse and human iNKT cells by bacterial superantigens. *Immunol Cell Biol* 90(7)**,** 699-709. doi: 10.1038/icb.2011.90.
111. Szabo, PA, Rudak, PT, Choi, J, Xu, SX, Schaub, R, Singh, B, et al. (2017). Invariant Natural Killer T Cells Are Pathogenic in the HLA-DR4-Transgenic Humanized Mouse Model of Toxic Shock Syndrome and Can Be Targeted to Reduce Morbidity. *J Infect Dis* 215(5)**,** 824-829. doi: 10.1093/infdis/jiw646.
112. Doisne, JM, Soulard, V, Becourt, C, Amniai, L, Henrot, P, Havenar-Daughton, C, et al. (2011). Cutting edge: crucial role of IL-1 and IL-23 in the innate IL-17 response of peripheral lymph node NK1.1- invariant NKT cells to bacteria. *J Immunol* 186(2)**,** 662-666. doi: 10.4049/jimmunol.1002725.
113. King, JM, Kulhankova, K, Stach, CS, Vu, BG, and Salgado-Pabon, W (2016). Phenotypes and Virulence among Staphylococcus aureus USA100, USA200, USA300, USA400, and USA600 Clonal Lineages. *mSphere* 1(3). doi: 10.1128/mSphere.00071-16.
114. Van Rhijn, I, van Berlo, T, Hilmenyuk, T, Cheng, TY, Wolf, BJ, Tatituri, RV, et al. (2016). Human autoreactive T cells recognize CD1b and phospholipids. *Proc Natl Acad Sci U S A* 113(2)**,** 380-385. doi: 10.1073/pnas.1520947112.
115. Visvabharathy, L, Genardi, S, Cao, L, He, Y, Alonzo, F, 3rd, Berdyshev, E, et al. (2020). Group 1 CD1-restricted T cells contribute to control of systemic Staphylococcus aureus infection. *PLoS Pathog* 16(4)**,** e1008443. doi: 10.1371/journal.ppat.1008443.
116. Kolata, J, Bode, LG, Holtfreter, S, Steil, L, Kusch, H, Holtfreter, B, et al. (2011). Distinctive patterns in the human antibody response to Staphylococcus aureus bacteremia in carriers and non-carriers. *Proteomics* 11(19)**,** 3914-3927. doi: 10.1002/pmic.201000760.
117. Kolata, JB, Kuhbandner, I, Link, C, Normann, N, Vu, CH, Steil, L, et al. (2015). The Fall of a Dogma? Unexpected High T-Cell Memory Response to Staphylococcus aureus in Humans. *J Infect Dis* 212(5)**,** 830-838. doi: 10.1093/infdis/jiv128.
118. Rossjohn, J, Pellicci, DG, Patel, O, Gapin, L, and Godfrey, DI (2012). Recognition of CD1d-restricted antigens by natural killer T cells. *Nat Rev Immunol* 12(12)**,** 845-857. doi: 10.1038/nri3328.
119. Park, SH, Weiss, A, Benlagha, K, Kyin, T, Teyton, L, and Bendelac, A (2001). The mouse CD1d-restricted repertoire is dominated by a few autoreactive T cell receptor families. *J Exp Med* 193(8)**,** 893-904. doi: 10.1084/jem.193.8.893.
120. Fowlkes, BJ, Kruisbeek, AM, Ton-That, H, Weston, MA, Coligan, JE, Schwartz, RH, et al. (1987). A novel population of T-cell receptor alpha beta-bearing thymocytes which

predominantly expresses a single V beta gene family. *Nature* 329(6136), 251-254. doi: 10.1038/329251a0.
121. Sykes, M (1990). Unusual T cell populations in adult murine bone marrow. Prevalence of CD3+CD4-CD8- and alpha beta TCR+NK1.1+ cells. *J Immunol* 145(10), 3209-3215.
122. Levitsky, HI, Golumbek, PT, and Pardoll, DM (1991). The fate of CD4-8- T cell receptor-alpha beta+ thymocytes. *J Immunol* 146(4), 1113-1117.
123. Zlotnik, A, Godfrey, DI, Fischer, M, and Suda, T (1992). Cytokine production by mature and immature CD4-CD8- T cells. Alpha beta-T cell receptor+ CD4-CD8- T cells produce IL-4. *J Immunol* 149(4), 1211-1215.
124. Koseki, H, Imai, K, Nakayama, F, Sado, T, Moriwaki, K, and Taniguchi, M (1990). Homogenous junctional sequence of the V14+ T-cell antigen receptor alpha chain expanded in unprimed mice. *Proc Natl Acad Sci U S A* 87(14), 5248-5252. doi: 10.1073/pnas.87.14.5248.
125. Lantz, O, and Bendelac, A (1994). An invariant T cell receptor alpha chain is used by a unique subset of major histocompatibility complex class I-specific CD4+ and CD4-8- T cells in mice and humans. *J Exp Med* 180(3), 1097-1106. doi: 10.1084/jem.180.3.1097.
126. Adachi, Y, Koseki, H, Zijlstra, M, and Taniguchi, M (1995). Positive selection of invariant V alpha 14+ T cells by non-major histocompatibility complex-encoded class I-like molecules expressed on bone marrow-derived cells. *Proc Natl Acad Sci U S A* 92(4), 1200-1204. doi: 10.1073/pnas.92.4.1200.
127. Bendelac, A, Lantz, O, Quimby, ME, Yewdell, JW, Bennink, JR, and Brutkiewicz, RR (1995). CD1 recognition by mouse NK1+ T lymphocytes. *Science* 268(5212), 863-865. doi: 10.1126/science.7538697.
128. Roark, JH, Park, SH, Jayawardena, J, Kavita, U, Shannon, M, and Bendelac, A (1998). CD1.1 expression by mouse antigen-presenting cells and marginal zone B cells. *J Immunol* 160(7), 3121-3127.
129. Kawano, T, Cui, J, Koezuka, Y, Toura, I, Kaneko, Y, Motoki, K, et al. (1997). CD1d-restricted and TCR-mediated activation of valpha14 NKT cells by glycosylceramides. *Science* 278(5343), 1626-1629. doi: 10.1126/science.278.5343.1626.
130. Benlagha, K, Weiss, A, Beavis, A, Teyton, L, and Bendelac, A (2000). In vivo identification of glycolipid antigen-specific T cells using fluorescent CD1d tetramers. *J Exp Med* 191(11), 1895-1903. doi: 10.1084/jem.191.11.1895.
131. Matsuda, JL, Naidenko, OV, Gapin, L, Nakayama, T, Taniguchi, M, Wang, CR, et al. (2000). Tracking the response of natural killer T cells to a glycolipid antigen using CD1d tetramers. *J Exp Med* 192(5), 741-754. doi: 10.1084/jem.192.5.741.
132. Benlagha, K, Wei, DG, Veiga, J, Teyton, L, and Bendelac, A (2005). Characterization of the early stages of thymic NKT cell development. *J Exp Med* 202(4), 485-492. doi: 10.1084/jem.20050456.
133. Griewank, K, Borowski, C, Rietdijk, S, Wang, N, Julien, A, Wei, DG, et al. (2007). Homotypic interactions mediated by Slamf1 and Slamf6 receptors control NKT cell lineage development. *Immunity* 27(5), 751-762. doi: 10.1016/j.immuni.2007.08.020.
134. Dutta, M, Kraus, ZJ, Gomez-Rodriguez, J, Hwang, SH, Cannons, JL, Cheng, J, et al. (2013). A role for Ly108 in the induction of promyelocytic zinc finger transcription factor in developing thymocytes. *J Immunol* 190(5), 2121-2128. doi: 10.4049/jimmunol.1202145.
135. Benlagha, K, Kyin, T, Beavis, A, Teyton, L, and Bendelac, A (2002). A thymic precursor to the NK T cell lineage. *Science* 296(5567), 553-555.
136. Berzins, SP, McNab, FW, Jones, CM, Smyth, MJ, and Godfrey, DI (2006). Long-term retention of mature NK1.1+ NKT cells in the thymus. *J Immunol* 176(7), 4059-4065. doi: 10.4049/jimmunol.176.7.4059.

137. Kovalovsky, D, Uche, OU, Eladad, S, Hobbs, RM, Yi, W, Alonzo, E, et al. (2008). The BTB-zinc finger transcriptional regulator PLZF controls the development of invariant natural killer T cell effector functions. *Nat Immunol* 9(9)**,** 1055-1064. doi: 10.1038/ni.1641.
138. Raphael, I, Nalawade, S, Eagar, TN, and Forsthuber, TG (2015). T cell subsets and their signature cytokines in autoimmune and inflammatory diseases. *Cytokine* 74(1)**,** 5-17. doi: 10.1016/j.cyto.2014.09.011.
139. Lee, YJ, Holzapfel, KL, Zhu, J, Jameson, SC, and Hogquist, KA (2013). Steady-state production of IL-4 modulates immunity in mouse strains and is determined by lineage diversity of iNKT cells. *Nat Immunol* 14(11)**,** 1146-1154. doi: 10.1038/ni.2731.
140. Lynch, L, Michelet, X, Zhang, S, Brennan, PJ, Moseman, A, Lester, C, et al. (2015). Regulatory iNKT cells lack expression of the transcription factor PLZF and control the homeostasis of T(reg) cells and macrophages in adipose tissue. *Nat Immunol* 16(1)**,** 85-95. doi: 10.1038/ni.3047.
141. Chang, PP, Barral, P, Fitch, J, Pratama, A, Ma, CS, Kallies, A, et al. (2011). Identification of Bcl-6-dependent follicular helper NKT cells that provide cognate help for B cell responses. *Nat Immunol* 13(1)**,** 35-43. doi: 10.1038/ni.2166.
142. Engel, I, Seumois, G, Chavez, L, Samaniego-Castruita, D, White, B, Chawla, A, et al. (2016). Innate-like functions of natural killer T cell subsets result from highly divergent gene programs. *Nat Immunol* 17(6)**,** 728-739. doi: 10.1038/ni.3437.
143. Cardell, S, Tangri, S, Chan, S, Kronenberg, M, Benoist, C, and Mathis, D (1995). CD1-restricted CD4+ T cells in major histocompatibility complex class II-deficient mice. *J Exp Med* 182(4)**,** 993-1004. doi: 10.1084/jem.182.4.993.
144. Skold, M, Faizunnessa, NN, Wang, CR, and Cardell, S (2000). CD1d-specific NK1.1+ T cells with a transgenic variant TCR. *J Immunol* 165(1)**,** 168-174. doi: 10.4049/jimmunol.165.1.168.
145. Stetson, DB, Mohrs, M, Reinhardt, RL, Baron, JL, Wang, ZE, Gapin, L, et al. (2003). Constitutive cytokine mRNAs mark natural killer (NK) and NK T cells poised for rapid effector function. *J Exp Med* 198(7)**,** 1069-1076. doi: 10.1084/jem.20030630.
146. Zhao, J, Weng, X, Bagchi, S, and Wang, CR (2014). Polyclonal type II natural killer T cells require PLZF and SAP for their development and contribute to CpG-mediated antitumor response. *Proc Natl Acad Sci U S A* 111(7)**,** 2674-2679. doi: 10.1073/pnas.1323845111.
147. Girardi, E, and Zajonc, DM (2012). Molecular basis of lipid antigen presentation by CD1d and recognition by natural killer T cells. *Immunol Rev* 250(1)**,** 167-179. doi: 10.1111/j.1600-065X.2012.01166.x.
148. Chancellor, A, Gadola, SD, and Mansour, S (2018). The versatility of the CD1 lipid antigen presentation pathway. *Immunology* 154(2)**,** 196-203. doi: 10.1111/imm.12912.
149. de la Salle, H, Mariotti, S, Angenieux, C, Gilleron, M, Garcia-Alles, LF, Malm, D, et al. (2005). Assistance of microbial glycolipid antigen processing by CD1e. *Science* 310(5752)**,** 1321-1324. doi: 10.1126/science.1115301.
150. Cox, D, Fox, L, Tian, R, Bardet, W, Skaley, M, Mojsilovic, D, et al. (2009). Determination of cellular lipids bound to human CD1d molecules. *PLoS One* 4(5)**,** e5325. doi: 10.1371/journal.pone.0005325.
151. Fox, LM, Cox, DG, Lockridge, JL, Wang, X, Chen, X, Scharf, L, et al. (2009). Recognition of lyso-phospholipids by human natural killer T lymphocytes. *PLoS Biol* 7(10)**,** e1000228. doi: 10.1371/journal.pbio.1000228.
152. Haig, NA, Guan, Z, Li, D, McMichael, A, Raetz, CR, and Xu, XN (2011). Identification of self-lipids presented by CD1c and CD1d proteins. *J Biol Chem* 286(43)**,** 37692-37701. doi: 10.1074/jbc.M111.267948.
153. Moody, DB, and Cotton, RN (2017). Four pathways of CD1 antigen presentation to T cells. *Curr Opin Immunol* 46**,** 127-133. doi: 10.1016/j.coi.2017.07.013.

154. Cernadas, M, Sugita, M, van der Wel, N, Cao, X, Gumperz, JE, Maltsev, S, et al. (2003). Lysosomal localization of murine CD1d mediated by AP-3 is necessary for NK T cell development. *J Immunol* 171(8)**,** 4149-4155. doi: 10.4049/jimmunol.171.8.4149.
155. van den Elzen, P, Garg, S, Leon, L, Brigl, M, Leadbetter, EA, Gumperz, JE, et al. (2005). Apolipoprotein-mediated pathways of lipid antigen presentation. *Nature* 437(7060)**,** 906-910. doi: 10.1038/nature04001.
156. Kang, SJ, and Cresswell, P (2004). Saposins facilitate CD1d-restricted presentation of an exogenous lipid antigen to T cells. *Nat Immunol* 5(2)**,** 175-181. doi: 10.1038/ni1034.
157. Borg, NA, Wun, KS, Kjer-Nielsen, L, Wilce, MC, Pellicci, DG, Koh, R, et al. (2007). CD1d-lipid-antigen recognition by the semi-invariant NKT T-cell receptor. *Nature* 448(7149)**,** 44-49. doi: 10.1038/nature05907.
158. McCarthy, C, Shepherd, D, Fleire, S, Stronge, VS, Koch, M, Illarionov, PA, et al. (2007). The length of lipids bound to human CD1d molecules modulates the affinity of NKT cell TCR and the threshold of NKT cell activation. *J Exp Med* 204(5)**,** 1131-1144. doi: 10.1084/jem.20062342.
159. Van Kaer, L, Parekh, VV, and Wu, L (2015). The Response of CD1d-Restricted Invariant NKT Cells to Microbial Pathogens and Their Products. *Front Immunol* 6**,** 226. doi: 10.3389/fimmu.2015.00226.
160. Kinjo, Y, Wu, D, Kim, G, Xing, GW, Poles, MA, Ho, DD, et al. (2005). Recognition of bacterial glycosphingolipids by natural killer T cells. *Nature* 434(7032)**,** 520-525. doi: 10.1038/nature03407.
161. Kinjo, Y, Tupin, E, Wu, D, Fujio, M, Garcia-Navarro, R, Benhnia, MR, et al. (2006). Natural killer T cells recognize diacylglycerol antigens from pathogenic bacteria. *Nat Immunol* 7(9)**,** 978-986. doi: 10.1038/ni1380.
162. Fischer, K, Scotet, E, Niemeyer, M, Koebernick, H, Zerrahn, J, Maillet, S, et al. (2004). Mycobacterial phosphatidylinositol mannoside is a natural antigen for CD1d-restricted T cells. *Proc Natl Acad Sci U S A* 101(29)**,** 10685-10690. doi: 10.1073/pnas.0403787101.
163. Chang, YJ, Kim, HY, Albacker, LA, Lee, HH, Baumgarth, N, Akira, S, et al. (2011). Influenza infection in suckling mice expands an NKT cell subset that protects against airway hyperreactivity. *J Clin Invest* 121(1)**,** 57-69. doi: 10.1172/JCI44845.
164. Wieland Brown, LC, Penaranda, C, Kashyap, PC, Williams, BB, Clardy, J, Kronenberg, M, et al. (2013). Production of alpha-galactosylceramide by a prominent member of the human gut microbiota. *PLoS Biol* 11(7)**,** e1001610. doi: 10.1371/journal.pbio.1001610.
165. Amprey, JL, Im, JS, Turco, SJ, Murray, HW, Illarionov, PA, Besra, GS, et al. (2004). A subset of liver NK T cells is activated during Leishmania donovani infection by CD1d-bound lipophosphoglycan. *J Exp Med* 200(7)**,** 895-904. doi: 10.1084/jem.20040704.
166. Kitamura, H, Iwakabe, K, Yahata, T, Nishimura, S, Ohta, A, Ohmi, Y, et al. (1999). The natural killer T (NKT) cell ligand alpha-galactosylceramide demonstrates its immunopotentiating effect by inducing interleukin (IL)-12 production by dendritic cells and IL-12 receptor expression on NKT cells. *J Exp Med* 189(7)**,** 1121-1128. doi: 10.1084/jem.189.7.1121.
167. Leite-De-Moraes, MC, Hameg, A, Arnould, A, Machavoine, F, Koezuka, Y, Schneider, E, et al. (1999). A distinct IL-18-induced pathway to fully activate NK T lymphocytes independently from TCR engagement. *J Immunol* 163(11)**,** 5871-5876.
168. Brigl, M, Bry, L, Kent, SC, Gumperz, JE, and Brenner, MB (2003). Mechanism of CD1d-restricted natural killer T cell activation during microbial infection. *Nat Immunol* 4(12)**,** 1230-1237. doi: 10.1038/ni1002.
169. Cohen, NR, Tatituri, RV, Rivera, A, Watts, GF, Kim, EY, Chiba, A, et al. (2011). Innate recognition of cell wall beta-glucans drives invariant natural killer T cell responses against fungi. *Cell Host Microbe* 10(5)**,** 437-450. doi: 10.1016/j.chom.2011.09.011.

170. Paget, C, Mallevaey, T, Speak, AO, Torres, D, Fontaine, J, Sheehan, KC, et al. (2007). Activation of invariant NKT cells by toll-like receptor 9-stimulated dendritic cells requires type I interferon and charged glycosphingolipids. *Immunity* 27(4)**,** 597-609. doi: 10.1016/j.immuni.2007.08.017.
171. Lotter, H, Gonzalez-Roldan, N, Lindner, B, Winau, F, Isibasi, A, Moreno-Lafont, M, et al. (2009). Natural killer T cells activated by a lipopeptidophosphoglycan from Entamoeba histolytica are critically important to control amebic liver abscess. *PLoS Pathog* 5(5)**,** e1000434. doi: 10.1371/journal.ppat.1000434.
172. Nagarajan, NA, and Kronenberg, M (2007). Invariant NKT cells amplify the innate immune response to lipopolysaccharide. *J Immunol* 178(5)**,** 2706-2713. doi: 10.4049/jimmunol.178.5.2706.
173. Brigl, M, Tatituri, RV, Watts, GF, Bhowruth, V, Leadbetter, EA, Barton, N, et al. (2011). Innate and cytokine-driven signals, rather than microbial antigens, dominate in natural killer T cell activation during microbial infection. *J Exp Med* 208(6)**,** 1163-1177. doi: 10.1084/jem.20102555.
174. Jahng, A, Maricic, I, Aguilera, C, Cardell, S, Halder, RC, and Kumar, V (2004). Prevention of autoimmunity by targeting a distinct, noninvariant CD1d-reactive T cell population reactive to sulfatide. *J Exp Med* 199(7)**,** 947-957. doi: 10.1084/jem.20031389.
175. Blomqvist, M, Rhost, S, Teneberg, S, Lofbom, L, Osterbye, T, Brigl, M, et al. (2009). Multiple tissue-specific isoforms of sulfatide activate CD1d-restricted type II NKT cells. *Eur J Immunol* 39(7)**,** 1726-1735. doi: 10.1002/eji.200839001.
176. Arrenberg, P, Halder, R, Dai, Y, Maricic, I, and Kumar, V (2010). Oligoclonality and innate-like features in the TCR repertoire of type II NKT cells reactive to a beta-linked self-glycolipid. *Proc Natl Acad Sci U S A* 107(24)**,** 10984-10989. doi: 10.1073/pnas.1000576107.
177. Nair, S, Boddupalli, CS, Verma, R, Liu, J, Yang, R, Pastores, GM, et al. (2015). Type II NKT-TFH cells against Gaucher lipids regulate B-cell immunity and inflammation. *Blood* 125(8)**,** 1256-1271. doi: 10.1182/blood-2014-09-600270.
178. Maricic, I, Girardi, E, Zajonc, DM, and Kumar, V (2014). Recognition of lysophosphatidylcholine by type II NKT cells and protection from an inflammatory liver disease. *J Immunol* 193(9)**,** 4580-4589. doi: 10.4049/jimmunol.1400699.
179. Tatituri, RV, Watts, GF, Bhowruth, V, Barton, N, Rothchild, A, Hsu, FF, et al. (2013). Recognition of microbial and mammalian phospholipid antigens by NKT cells with diverse TCRs. *Proc Natl Acad Sci U S A* 110(5)**,** 1827-1832. doi: 10.1073/pnas.1220601110.
180. Wolf, BJ, Tatituri, RV, Almeida, CF, Le Nours, J, Bhowruth, V, Johnson, D, et al. (2015). Identification of a Potent Microbial Lipid Antigen for Diverse NKT Cells. *J Immunol* 195(6)**,** 2540-2551. doi: 10.4049/jimmunol.1501019.
181. Tripathi, P, Sedimbi, SK, Singh, AK, Lofbom, L, Issazadeh-Navikas, S, Weiss, S, et al. (2019). Innate and adaptive stimulation of murine diverse NKT cells result in distinct cellular responses. *Eur J Immunol* 49(3)**,** 443-453. doi: 10.1002/eji.201847647.
182. Akbari, O, Stock, P, Meyer, EH, Freeman, GJ, Sharpe, AH, Umetsu, DT, et al. (2008). ICOS/ICOSL interaction is required for CD4+ invariant NKT cell function and homeostatic survival. *J Immunol* 180(8)**,** 5448-5456. doi: 10.4049/jimmunol.180.8.5448.
183. Wilson, MT, Johansson, C, Olivares-Villagomez, D, Singh, AK, Stanic, AK, Wang, CR, et al. (2003). The response of natural killer T cells to glycolipid antigens is characterized by surface receptor down-modulation and expansion. *Proc Natl Acad Sci U S A* 100(19)**,** 10913-10918. doi: 10.1073/pnas.1833166100.
184. Uldrich, AP, Crowe, NY, Kyparissoudis, K, Pellicci, DG, Zhan, Y, Lew, AM, et al. (2005). NKT cell stimulation with glycolipid antigen in vivo: costimulation-dependent expansion,

Bim-dependent contraction, and hyporesponsiveness to further antigenic challenge. *J Immunol* 175(5), 3092-3101. doi: 10.4049/jimmunol.175.5.3092.
185. Parekh, VV, Wilson, MT, Olivares-Villagomez, D, Singh, AK, Wu, L, Wang, CR, et al. (2005). Glycolipid antigen induces long-term natural killer T cell anergy in mice. *J Clin Invest* 115(9), 2572-2583. doi: 10.1172/JCI24762.
186. Chiba, A, Dascher, CC, Besra, GS, and Brenner, MB (2008). Rapid NKT cell responses are self-terminating during the course of microbial infection. *J Immunol* 181(4), 2292-2302. doi: 10.4049/jimmunol.181.4.2292.
187. Choi, HJ, Xu, H, Geng, Y, Colmone, A, Cho, H, and Wang, CR (2008). Bacterial infection alters the kinetics and function of iNKT cell responses. *J Leukoc Biol* 84(6), 1462-1471. doi: 10.1189/jlb.0108038.
188. Kim, S, Lalani, S, Parekh, VV, Vincent, TL, Wu, L, and Van Kaer, L (2008). Impact of bacteria on the phenotype, functions, and therapeutic activities of invariant NKT cells in mice. *J Clin Invest* 118(6), 2301-2315. doi: 10.1172/JCI33071.
189. Minagawa, M, Deng, Q, Liu, ZX, Tsukamoto, H, and Dennert, G (2004). Activated natural killer T cells induce liver injury by Fas and tumor necrosis factor-alpha during alcohol consumption. *Gastroenterology* 126(5), 1387-1399. doi: 10.1053/j.gastro.2004.01.022.
190. Getz, GS, and Reardon, CA (2017). Natural killer T cells in atherosclerosis. *Nat Rev Cardiol* 14(5), 304-314. doi: 10.1038/nrcardio.2017.2.
191. Duarte, N, Stenstrom, M, Campino, S, Bergman, ML, Lundholm, M, Holmberg, D, et al. (2004). Prevention of diabetes in nonobese diabetic mice mediated by CD1d-restricted nonclassical NKT cells. *J Immunol* 173(5), 3112-3118. doi: 10.4049/jimmunol.173.5.3112.
192. Kadri, N, Korpos, E, Gupta, S, Briet, C, Lofbom, L, Yagita, H, et al. (2012). CD4(+) type II NKT cells mediate ICOS and programmed death-1-dependent regulation of type 1 diabetes. *J Immunol* 188(7), 3138-3149. doi: 10.4049/jimmunol.1101390.
193. Maricic, I, Sheng, H, Marrero, I, Seki, E, Kisseleva, T, Chaturvedi, S, et al. (2015). Inhibition of type I natural killer T cells by retinoids or following sulfatide-mediated activation of type II natural killer T cells attenuates alcoholic liver disease in mice. *Hepatology* 61(4), 1357-1369. doi: 10.1002/hep.27632.
194. Arrenberg, P, Maricic, I, and Kumar, V (2011). Sulfatide-mediated activation of type II natural killer T cells prevents hepatic ischemic reperfusion injury in mice. *Gastroenterology* 140(2), 646-655. doi: 10.1053/j.gastro.2010.10.003.
195. Liao, CM, Zimmer, MI, Shanmuganad, S, Yu, HT, Cardell, SL, and Wang, CR (2012). dysregulation of CD1d-restricted type ii natural killer T cells leads to spontaneous development of colitis in mice. *Gastroenterology* 142(2), 326-334 e321-322. doi: 10.1053/j.gastro.2011.10.030.
196. Singh, AK, Tripathi, P, and Cardell, SL (2018). Type II NKT Cells: An Elusive Population With Immunoregulatory Properties. *Front Immunol* 9, 1969. doi: 10.3389/fimmu.2018.01969.
197. Arrunategui-Correa, V, and Kim, HS (2004). The role of CD1d in the immune response against Listeria infection. *Cell Immunol* 227(2), 109-120. doi: 10.1016/j.cellimm.2004.02.003.
198. Ranson, T, Bregenholt, S, Lehuen, A, Gaillot, O, Leite-de-Moraes, MC, Herbelin, A, et al. (2005). Invariant V alpha 14+ NKT cells participate in the early response to enteric Listeria monocytogenes infection. *J Immunol* 175(2), 1137-1144. doi: 10.4049/jimmunol.175.2.1137.
199. Dieli, F, Taniguchi, M, Kronenberg, M, Sidobre, S, Ivanyi, J, Fattorini, L, et al. (2003). An anti-inflammatory role for V alpha 14 NK T cells in Mycobacterium bovis bacillus Calmette-Guerin-infected mice. *J Immunol* 171(4), 1961-1968. doi: 10.4049/jimmunol.171.4.1961.

200. Tupin, E, Benhnia, MR, Kinjo, Y, Patsey, R, Lena, CJ, Haller, MC, et al. (2008). NKT cells prevent chronic joint inflammation after infection with Borrelia burgdorferi. *Proc Natl Acad Sci U S A* 105(50), 19863-19868. doi: 10.1073/pnas.0810519105.
201. Olson, CM, Jr., Bates, TC, Izadi, H, Radolf, JD, Huber, SA, Boyson, JE, et al. (2009). Local production of IFN-gamma by invariant NKT cells modulates acute Lyme carditis. *J Immunol* 182(6), 3728-3734. doi: 10.4049/jimmunol.0804111.
202. Kawakami, K, Kinjo, Y, Uezu, K, Yara, S, Miyagi, K, Koguchi, Y, et al. (2001). Monocyte chemoattractant protein-1-dependent increase of V alpha 14 NKT cells in lungs and their roles in Th1 response and host defense in cryptococcal infection. *J Immunol* 167(11), 6525-6532. doi: 10.4049/jimmunol.167.11.6525.
203. Kawakami, K, Yamamoto, N, Kinjo, Y, Miyagi, K, Nakasone, C, Uezu, K, et al. (2003). Critical role of Valpha14+ natural killer T cells in the innate phase of host protection against Streptococcus pneumoniae infection. *Eur J Immunol* 33(12), 3322-3330. doi: 10.1002/eji.200324254.
204. Thanabalasuriar, A, Neupane, AS, Wang, J, Krummel, MF, and Kubes, P (2016). iNKT Cell Emigration out of the Lung Vasculature Requires Neutrophils and Monocyte-Derived Dendritic Cells in Inflammation. *Cell Rep* 16(12), 3260-3272. doi: 10.1016/j.celrep.2016.07.052.
205. Nakamatsu, M, Yamamoto, N, Hatta, M, Nakasone, C, Kinjo, T, Miyagi, K, et al. (2007). Role of interferon-gamma in Valpha14+ natural killer T cell-mediated host defense against Streptococcus pneumoniae infection in murine lungs. *Microbes Infect* 9(3), 364-374. doi: 10.1016/j.micinf.2006.12.003.
206. Nieuwenhuis, EE, Matsumoto, T, Exley, M, Schleipman, RA, Glickman, J, Bailey, DT, et al. (2002). CD1d-dependent macrophage-mediated clearance of Pseudomonas aeruginosa from lung. *Nat Med* 8(6), 588-593. doi: 10.1038/nm0602-588.
207. Hill, TM, Gilchuk, P, Cicek, BB, Osina, MA, Boyd, KL, Durrant, DM, et al. (2015). Border Patrol Gone Awry: Lung NKT Cell Activation by Francisella tularensis Exacerbates Tularemia-Like Disease. *PLoS Pathog* 11(6), e1004975. doi: 10.1371/journal.ppat.1004975.
208. Emoto, M, Yoshizawa, I, Emoto, Y, Miamoto, M, Hurwitz, R, and Kaufmann, SH (2006). Rapid development of a gamma interferon-secreting glycolipid/CD1d-specific Valpha14+ NK1.1- T-cell subset after bacterial infection. *Infect Immun* 74(10), 5903-5913. doi: 10.1128/IAI.00311-06.
209. Deignan, T, Curry, MP, Doherty, DG, Golden-Mason, L, Volkov, Y, Norris, S, et al. (2002). Decrease in hepatic CD56(+) T cells and V alpha 24(+) natural killer T cells in chronic hepatitis C viral infection. *J Hepatol* 37(1), 101-108. doi: 10.1016/s0168-8278(02)00072-7.
210. Lucas, M, Gadola, S, Meier, U, Young, NT, Harcourt, G, Karadimitris, A, et al. (2003). Frequency and phenotype of circulating Valpha24/Vbeta11 double-positive natural killer T cells during hepatitis C virus infection. *J Virol* 77(3), 2251-2257. doi: 10.1128/jvi.77.3.2251-2257.2003.
211. Miyaki, E, Hiraga, N, Imamura, M, Uchida, T, Kan, H, Tsuge, M, et al. (2017). Interferon alpha treatment stimulates interferon gamma expression in type I NKT cells and enhances their antiviral effect against hepatitis C virus. *PLoS One* 12(3), e0172412. doi: 10.1371/journal.pone.0172412.
212. Jiang, X, Zhang, M, Lai, Q, Huang, X, Li, Y, Sun, J, et al. (2011). Restored circulating invariant NKT cells are associated with viral control in patients with chronic hepatitis B. *PLoS One* 6(12), e28871. doi: 10.1371/journal.pone.0028871.
213. Zeissig, S, Murata, K, Sweet, L, Publicover, J, Hu, Z, Kaser, A, et al. (2012). Hepatitis B virus-induced lipid alterations contribute to natural killer T cell-dependent protective immunity. *Nat Med* 18(7), 1060-1068. doi: 10.1038/nm.2811.

214. De Santo, C, Salio, M, Masri, SH, Lee, LY, Dong, T, Speak, AO, et al. (2008). Invariant NKT cells reduce the immunosuppressive activity of influenza A virus-induced myeloid-derived suppressor cells in mice and humans. *J Clin Invest* 118(12)**,** 4036-4048. doi: 10.1172/JCI36264.
215. Kok, WL, Denney, L, Benam, K, Cole, S, Clelland, C, McMichael, AJ, et al. (2012). Pivotal Advance: Invariant NKT cells reduce accumulation of inflammatory monocytes in the lungs and decrease immune-pathology during severe influenza A virus infection. *J Leukoc Biol* 91(3)**,** 357-368. doi: 10.1189/jlb.0411184.
216. Paget, C, Ivanov, S, Fontaine, J, Blanc, F, Pichavant, M, Renneson, J, et al. (2011). Potential role of invariant NKT cells in the control of pulmonary inflammation and CD8+ T cell response during acute influenza A virus H3N2 pneumonia. *J Immunol* 186(10)**,** 5590-5602. doi: 10.4049/jimmunol.1002348.
217. Paget, C, Ivanov, S, Fontaine, J, Renneson, J, Blanc, F, Pichavant, M, et al. (2012). Interleukin-22 is produced by invariant natural killer T lymphocytes during influenza A virus infection: potential role in protection against lung epithelial damages. *J Biol Chem* 287(12)**,** 8816-8829. doi: 10.1074/jbc.M111.304758.
218. Ronet, C, Darche, S, Leite de Moraes, M, Miyake, S, Yamamura, T, Louis, JA, et al. (2005). NKT cells are critical for the initiation of an inflammatory bowel response against Toxoplasma gondii. *J Immunol* 175(2)**,** 899-908. doi: 10.4049/jimmunol.175.2.899.
219. Soulard, V, Roland, J, Sellier, C, Gruner, AC, Leite-de-Moraes, M, Franetich, JF, et al. (2007). Primary infection of C57BL/6 mice with Plasmodium yoelii induces a heterogeneous response of NKT cells. *Infect Immun* 75(5)**,** 2511-2522. doi: 10.1128/IAI.01818-06.
220. Duthie, MS, Kahn, M, White, M, Kapur, RP, and Kahn, SJ (2005). Critical proinflammatory and anti-inflammatory functions of different subsets of CD1d-restricted natural killer T cells during Trypanosoma cruzi infection. *Infect Immun* 73(1)**,** 181-192. doi: 10.1128/IAI.73.1.181-192.2005.
221. Mallevaey, T, Fontaine, J, Breuilh, L, Paget, C, Castro-Keller, A, Vendeville, C, et al. (2007). Invariant and noninvariant natural killer T cells exert opposite regulatory functions on the immune response during murine schistosomiasis. *Infect Immun* 75(5)**,** 2171-2180. doi: 10.1128/IAI.01178-06.
222. Krishack, PA, Louviere, TJ, Decker, TS, Kuzel, TG, Greenberg, JA, Camacho, DF, et al. (2019). Protection against Staphylococcus aureus bacteremia-induced mortality depends on ILC2s and eosinophils. *JCI Insight* 4(6). doi: 10.1172/jci.insight.124168.
223. White, DC, and Frerman, FE (1967). Extraction, characterization, and cellular localization of the lipids of Staphylococcus aureus. *J Bacteriol* 94(6)**,** 1854-1867. doi: 10.1128/JB.94.6.1854-1867.1967.
224. Hewelt-Belka, W, Nakonieczna, J, Belka, M, Baczek, T, Namiesnik, J, and Kot-Wasik, A (2014). Comprehensive methodology for Staphylococcus aureus lipidomics by liquid chromatography and quadrupole time-of-flight mass spectrometry. *J Chromatogr A* 1362**,** 62-74. doi: 10.1016/j.chroma.2014.08.020.
225. Rieder, SA, Nagarkatti, P, and Nagarkatti, M (2011). CD1d-independent activation of invariant natural killer T cells by staphylococcal enterotoxin B through major histocompatibility complex class II/T cell receptor interaction results in acute lung injury. *Infect Immun* 79(8)**,** 3141-3148. doi: 10.1128/IAI.00177-11.
226. See, I, Mu, Y, Albrecht, V, Karlsson, M, Dumyati, G, Hardy, DJ, et al. (2020). Trends in Incidence of Methicillin-resistant Staphylococcus aureus Bloodstream Infections Differ by Strain Type and Healthcare Exposure, United States, 2005-2013. *Clin Infect Dis* 70(1)**,** 19-25. doi: 10.1093/cid/ciz158.

227. Godfrey, DI, Koay, HF, McCluskey, J, and Gherardin, NA (2019). The biology and functional importance of MAIT cells. *Nat Immunol* 20(9), 1110-1128. doi: 10.1038/s41590-019-0444-8.
228. Treiner, E, Duban, L, Bahram, S, Radosavljevic, M, Wanner, V, Tilloy, F, et al. (2003). Selection of evolutionarily conserved mucosal-associated invariant T cells by MR1. *Nature* 422(6928), 164-169. doi: 10.1038/nature01433.
229. Kjer-Nielsen, L, Patel, O, Corbett, AJ, Le Nours, J, Meehan, B, Liu, L, et al. (2012). MR1 presents microbial vitamin B metabolites to MAIT cells. *Nature* 491(7426), 717-723. doi: 10.1038/nature11605.
230. Porcelli, S, Yockey, CE, Brenner, MB, and Balk, SP (1993). Analysis of T cell antigen receptor (TCR) expression by human peripheral blood CD4-8- alpha/beta T cells demonstrates preferential use of several V beta genes and an invariant TCR alpha chain. *J Exp Med* 178(1), 1-16. doi: 10.1084/jem.178.1.1.
231. Tilloy, F, Treiner, E, Park, SH, Garcia, C, Lemonnier, F, de la Salle, H, et al. (1999). An invariant T cell receptor alpha chain defines a novel TAP-independent major histocompatibility complex class Ib-restricted alpha/beta T cell subpopulation in mammals. *J Exp Med* 189(12), 1907-1921. doi: 10.1084/jem.189.12.1907.
232. Gold, MC, Cerri, S, Smyk-Pearson, S, Cansler, ME, Vogt, TM, Delepine, J, et al. (2010). Human mucosal associated invariant T cells detect bacterially infected cells. *PLoS Biol* 8(6), e1000407. doi: 10.1371/journal.pbio.1000407.
233. Le Bourhis, L, Martin, E, Peguillet, I, Guihot, A, Froux, N, Core, M, et al. (2010). Antimicrobial activity of mucosal-associated invariant T cells. *Nat Immunol* 11(8), 701-708. doi: 10.1038/ni.1890.
234. Corbett, AJ, Eckle, SB, Birkinshaw, RW, Liu, L, Patel, O, Mahony, J, et al. (2014). T-cell activation by transitory neo-antigens derived from distinct microbial pathways. *Nature* 509(7500), 361-365. doi: 10.1038/nature13160.
235. Rahimpour, A, Koay, HF, Enders, A, Clanchy, R, Eckle, SB, Meehan, B, et al. (2015). Identification of phenotypically and functionally heterogeneous mouse mucosal-associated invariant T cells using MR1 tetramers. *J Exp Med* 212(7), 1095-1108. doi: 10.1084/jem.20142110.
236. Seach, N, Guerri, L, Le Bourhis, L, Mburu, Y, Cui, Y, Bessoles, S, et al. (2013). Double-positive thymocytes select mucosal-associated invariant T cells. *J Immunol* 191(12), 6002-6009. doi: 10.4049/jimmunol.1301212.
237. Koay, HF, Gherardin, NA, Enders, A, Loh, L, Mackay, LK, Almeida, CF, et al. (2016). A three-stage intrathymic development pathway for the mucosal-associated invariant T cell lineage. *Nat Immunol* 17(11), 1300-1311. doi: 10.1038/ni.3565.
238. Winter, SJ, Kunze-Schumacher, H, Imelmann, E, Grewers, Z, Osthues, T, and Krueger, A (2019). MicroRNA miR-181a/b-1 controls MAIT cell development. *Immunol Cell Biol* 97(2), 190-202. doi: 10.1111/imcb.12211.
239. Reantragoon, R, Corbett, AJ, Sakala, IG, Gherardin, NA, Furness, JB, Chen, Z, et al. (2013). Antigen-loaded MR1 tetramers define T cell receptor heterogeneity in mucosal-associated invariant T cells. *J Exp Med* 210(11), 2305-2320. doi: 10.1084/jem.20130958.
240. Meermeier, EW, Laugel, BF, Sewell, AK, Corbett, AJ, Rossjohn, J, McCluskey, J, et al. (2016). Human TRAV1-2-negative MR1-restricted T cells detect S. pyogenes and alternatives to MAIT riboflavin-based antigens. *Nat Commun* 7, 12506. doi: 10.1038/ncomms12506.
241. Koay, HF, Gherardin, NA, Xu, C, Seneviratna, R, Zhao, Z, Chen, Z, et al. (2019). Diverse MR1-restricted T cells in mice and humans. *Nat Commun* 10(1), 2243. doi: 10.1038/s41467-019-10198-w.

242. Kurioka, A, Jahun, AS, Hannaway, RF, Walker, LJ, Fergusson, JR, Sverremark-Ekstrom, E, et al. (2017). Shared and Distinct Phenotypes and Functions of Human CD161++ Valpha7.2+ T Cell Subsets. *Front Immunol* 8**,** 1031. doi: 10.3389/fimmu.2017.01031.
243. Carolan, E, Tobin, LM, Mangan, BA, Corrigan, M, Gaoatswe, G, Byrne, G, et al. (2015). Altered distribution and increased IL-17 production by mucosal-associated invariant T cells in adult and childhood obesity. *J Immunol* 194(12)**,** 5775-5780. doi: 10.4049/jimmunol.1402945.
244. Chen, Z, Wang, H, D'Souza, C, Sun, S, Kostenko, L, Eckle, SB, et al. (2017). Mucosal-associated invariant T-cell activation and accumulation after in vivo infection depends on microbial riboflavin synthesis and co-stimulatory signals. *Mucosal Immunol* 10(1)**,** 58-68. doi: 10.1038/mi.2016.39.
245. Wang, H, D'Souza, C, Lim, XY, Kostenko, L, Pediongco, TJ, Eckle, SBG, et al. (2018). MAIT cells protect against pulmonary Legionella longbeachae infection. *Nat Commun* 9(1)**,** 3350. doi: 10.1038/s41467-018-05202-8.
246. Slichter, CK, McDavid, A, Miller, HW, Finak, G, Seymour, BJ, McNevin, JP, et al. (2016). Distinct activation thresholds of human conventional and innate-like memory T cells. *JCI Insight* 1(8). doi: 10.1172/jci.insight.86292.
247. van Wilgenburg, B, Scherwitzl, I, Hutchinson, EC, Leng, T, Kurioka, A, Kulicke, C, et al. (2016). MAIT cells are activated during human viral infections. *Nat Commun* 7**,** 11653. doi: 10.1038/ncomms11653.
248. Leeansyah, E, Svard, J, Dias, J, Buggert, M, Nystrom, J, Quigley, MF, et al. (2015). Arming of MAIT Cell Cytolytic Antimicrobial Activity Is Induced by IL-7 and Defective in HIV-1 Infection. *PLoS Pathog* 11(8)**,** e1005072. doi: 10.1371/journal.ppat.1005072.
249. Salio, M, Gasser, O, Gonzalez-Lopez, C, Martens, A, Veerapen, N, Gileadi, U, et al. (2017). Activation of Human Mucosal-Associated Invariant T Cells Induces CD40L-Dependent Maturation of Monocyte-Derived and Primary Dendritic Cells. *J Immunol* 199(8)**,** 2631-2638. doi: 10.4049/jimmunol.1700615.
250. Georgel, P, Radosavljevic, M, Macquin, C, and Bahram, S (2011). The non-conventional MHC class I MR1 molecule controls infection by Klebsiella pneumoniae in mice. *Mol Immunol* 48(5)**,** 769-775. doi: 10.1016/j.molimm.2010.12.002.
251. Meierovics, A, Yankelevich, WJ, and Cowley, SC (2013). MAIT cells are critical for optimal mucosal immune responses during in vivo pulmonary bacterial infection. *Proc Natl Acad Sci U S A* 110(33)**,** E3119-3128. doi: 10.1073/pnas.1302799110.
252. Meierovics, AI, and Cowley, SC (2016). MAIT cells promote inflammatory monocyte differentiation into dendritic cells during pulmonary intracellular infection. *J Exp Med* 213(12)**,** 2793-2809. doi: 10.1084/jem.20160637.
253. Chua, WJ, Truscott, SM, Eickhoff, CS, Blazevic, A, Hoft, DF, and Hansen, TH (2012). Polyclonal mucosa-associated invariant T cells have unique innate functions in bacterial infection. *Infect Immun* 80(9)**,** 3256-3267. doi: 10.1128/IAI.00279-12.
254. Vorkas, CK, Levy, O, Skular, M, Li, K, Aube, J, and Glickman, MS (2020). Efficient 5-OP-RU-induced enrichment of Mucosal-associated invariant T cells in the murine lung does not enhance control of aerosol Mycobacterium tuberculosis infection. *Infect Immun*. doi: 10.1128/IAI.00524-20.
255. D'Souza, C, Pediongco, T, Wang, H, Scheerlinck, JY, Kostenko, L, Esterbauer, R, et al. (2018). Mucosal-Associated Invariant T Cells Augment Immunopathology and Gastritis in Chronic Helicobacter pylori Infection. *J Immunol* 200(5)**,** 1901-1916. doi: 10.4049/jimmunol.1701512.
256. Jahreis, S, Bottcher, S, Hartung, S, Rachow, T, Rummler, S, Dietl, AM, et al. (2018). Human MAIT cells are rapidly activated by Aspergillus spp. in an APC-dependent manner. *Eur J Immunol* 48(10)**,** 1698-1706. doi: 10.1002/eji.201747312.

257. van Wilgenburg, B, Loh, L, Chen, Z, Pediongco, TJ, Wang, H, Shi, M, et al. (2018). MAIT cells contribute to protection against lethal influenza infection in vivo. *Nat Commun* 9(1)**,** 4706. doi: 10.1038/s41467-018-07207-9.
258. Mpina, M, Maurice, NJ, Yajima, M, Slichter, CK, Miller, HW, Dutta, M, et al. (2017). Controlled Human Malaria Infection Leads to Long-Lasting Changes in Innate and Innate-like Lymphocyte Populations. *J Immunol* 199(1)**,** 107-118. doi: 10.4049/jimmunol.1601989.
259. Johansson, MA, Bjorkander, S, Mata Forsberg, M, Qazi, KR, Salvany Celades, M, Bittmann, J, et al. (2016). Probiotic Lactobacilli Modulate Staphylococcus aureus-Induced Activation of Conventional and Unconventional T cells and NK Cells. *Front Immunol* 7**,** 273. doi: 10.3389/fimmu.2016.00273.
260. Shaler, CR, Choi, J, Rudak, PT, Memarnejadian, A, Szabo, PA, Tun-Abraham, ME, et al. (2017). MAIT cells launch a rapid, robust and distinct hyperinflammatory response to bacterial superantigens and quickly acquire an anergic phenotype that impedes their cognate antimicrobial function: Defining a novel mechanism of superantigen-induced immunopathology and immunosuppression. *PLoS Biol* 15(6)**,** e2001930. doi: 10.1371/journal.pbio.2001930.
261. Zhang, J, Bedel, R, Krovi, SH, Tuttle, KD, Zhang, B, Gross, J, et al. (2016). Mutation of the Traj18 gene segment using TALENs to generate Natural Killer T cell deficient mice. *Sci Rep* 6**,** 27375. doi: 10.1038/srep27375.
262. Bedel, R, Matsuda, JL, Brigl, M, White, J, Kappler, J, Marrack, P, et al. (2012). Lower TCR repertoire diversity in Traj18-deficient mice. *Nat Immunol* 13(8)**,** 705-706. doi: 10.1038/ni.2347.
263. Chen, YH, Chiu, NM, Mandal, M, Wang, N, and Wang, CR (1997). Impaired NK1+ T cell development and early IL-4 production in CD1-deficient mice. *Immunity* 6(4)**,** 459-467. doi: 10.1016/s1074-7613(00)80289-7.
264. Bligh, EG, and Dyer, WJ (1959). A rapid method of total lipid extraction and purification. *Can J Biochem Physiol* 37(8)**,** 911-917. doi: 10.1139/o59-099.
265. Vaskovsky, VE, Kostetsky, EY, and Vasendin, IM (1975). A universal reagent for phospholipid analysis. *J Chromatogr* 114(1)**,** 129-141. doi: 10.1016/s0021-9673(00)85249-8.
266. Exley, MA, Tahir, SM, Cheng, O, Shaulov, A, Joyce, R, Avigan, D, et al. (2001). A major fraction of human bone marrow lymphocytes are Th2-like CD1d-reactive T cells that can suppress mixed lymphocyte responses. *J Immunol* 167(10)**,** 5531-5534. doi: 10.4049/jimmunol.167.10.5531.
267. Salou, M, Franciszkiewicz, K, and Lantz, O (2017). MAIT cells in infectious diseases. *Curr Opin Immunol* 48**,** 7-14. doi: 10.1016/j.coi.2017.07.009.
268. Li, M, Diep, BA, Villaruz, AE, Braughton, KR, Jiang, X, DeLeo, FR, et al. (2009). Evolution of virulence in epidemic community-associated methicillin-resistant Staphylococcus aureus. *Proc Natl Acad Sci U S A* 106(14)**,** 5883-5888. doi: 10.1073/pnas.0900743106.
269. Kinjo, Y, Illarionov, P, Vela, JL, Pei, B, Girardi, E, Li, X, et al. (2011). Invariant natural killer T cells recognize glycolipids from pathogenic Gram-positive bacteria. *Nat Immunol* 12(10)**,** 966-974. doi: 10.1038/ni.2096.
270. Selvanantham, T, Escalante, NK, Cruz Tleugabulova, M, Fieve, S, Girardin, SE, Philpott, DJ, et al. (2013). Nod1 and Nod2 enhance TLR-mediated invariant NKT cell activation during bacterial infection. *J Immunol* 191(11)**,** 5646-5654. doi: 10.4049/jimmunol.1301412.
271. Fergusson, JR, Smith, KE, Fleming, VM, Rajoriya, N, Newell, EW, Simmons, R, et al. (2014). CD161 defines a transcriptional and functional phenotype across distinct human T cell lineages. *Cell Rep* 9(3)**,** 1075-1088. doi: 10.1016/j.celrep.2014.09.045.

272. Zhao, YX, Nilsson, IM, and Tarkowski, A (1998). The dual role of interferon-gamma in experimental Staphylococcus aureus septicaemia versus arthritis. *Immunology* 93(1), 80-85. doi: 10.1046/j.1365-2567.1998.00407.x.
273. Halder, RC, Aguilera, C, Maricic, I, and Kumar, V (2007). Type II NKT cell-mediated anergy induction in type I NKT cells prevents inflammatory liver disease. *J Clin Invest* 117(8), 2302-2312. doi: 10.1172/JCI31602.
274. Macho-Fernandez, E, and Brigl, M (2015). The Extended Family of CD1d-Restricted NKT Cells: Sifting through a Mixed Bag of TCRs, Antigens, and Functions. *Front Immunol* 6, 362. doi: 10.3389/fimmu.2015.00362.
275. Mallevaey, T, and Selvanantham, T (2012). Strategy of lipid recognition by invariant natural killer T cells: 'one for all and all for one'. *Immunology* 136(3), 273-282. doi: 10.1111/j.1365-2567.2012.03580.x.
276. Wang, J, Li, Y, Kinjo, Y, Mac, TT, Gibson, D, Painter, GF, et al. (2010). Lipid binding orientation within CD1d affects recognition of Borrelia burgorferi antigens by NKT cells. *Proc Natl Acad Sci U S A* 107(4), 1535-1540. doi: 10.1073/pnas.0909479107.
277. Gumperz, JE, Roy, C, Makowska, A, Lum, D, Sugita, M, Podrebarac, T, et al. (2000). Murine CD1d-restricted T cell recognition of cellular lipids. *Immunity* 12(2), 211-221. doi: 10.1016/s1074-7613(00)80174-0.
278. DeMaria, TF, and Kapral, FA (1978). Pulmonary infection of mice with Staphylococcus aureus. *Infect Immun* 21(1), 114-123. doi: 10.1128/IAI.21.1.114-123.1978.
279. Snyder-Cappione, JE, Nixon, DF, Loo, CP, Chapman, JM, Meiklejohn, DA, Melo, FF, et al. (2007). Individuals with pulmonary tuberculosis have lower levels of circulating CD1d-restricted NKT cells. *J Infect Dis* 195(9), 1361-1364. doi: 10.1086/513567.
280. Kadivar, M, Petersson, J, Svensson, L, and Marsal, J (2016). CD8alphabeta+ gammadelta T Cells: A Novel T Cell Subset with a Potential Role in Inflammatory Bowel Disease. *J Immunol* 197(12), 4584-4592. doi: 10.4049/jimmunol.1601146.
281. Chang, DH, Deng, H, Matthews, P, Krasovsky, J, Ragupathi, G, Spisek, R, et al. (2008). Inflammation-associated lysophospholipids as ligands for CD1d-restricted T cells in human cancer. *Blood* 112(4), 1308-1316. doi: 10.1182/blood-2008-04-149831.
282. Paquin-Proulx, D, Greenspun, BC, Pasquet, L, Strunz, B, Aleman, S, Falconer, K, et al. (2018). IL13Ralpha2 expression identifies tissue-resident IL-22-producing PLZF(+) innate T cells in the human liver. *Eur J Immunol* 48(8), 1329-1335. doi: 10.1002/eji.201747334.
283. Siddiqui, S, Visvabharathy, L, and Wang, CR (2015). Role of Group 1 CD1-Restricted T Cells in Infectious Disease. *Front Immunol* 6, 337. doi: 10.3389/fimmu.2015.00337.
284. Pereira, CS, and Macedo, MF (2016). CD1-Restricted T Cells at the Crossroad of Innate and Adaptive Immunity. *J Immunol Res* 2016, 2876275. doi: 10.1155/2016/2876275.
285. Felio, K, Nguyen, H, Dascher, CC, Choi, HJ, Li, S, Zimmer, MI, et al. (2009). CD1-restricted adaptive immune responses to Mycobacteria in human group 1 CD1 transgenic mice. *J Exp Med* 206(11), 2497-2509. doi: 10.1084/jem.20090898.
286. Shang, S, Kats, D, Cao, L, Morgun, E, Velluto, D, He, Y, et al. (2018). Induction of Mycobacterium Tuberculosis Lipid-Specific T Cell Responses by Pulmonary Delivery of Mycolic Acid-Loaded Polymeric Micellar Nanocarriers. *Front Immunol* 9, 2709. doi: 10.3389/fimmu.2018.02709.
287. Shimizu, K, Sato, Y, Shinga, J, Watanabe, T, Endo, T, Asakura, M, et al. (2014). KLRG+ invariant natural killer T cells are long-lived effectors. *Proc Natl Acad Sci U S A* 111(34), 12474-12479. doi: 10.1073/pnas.1406240111.
288. Wen, X, Rao, P, Carreno, LJ, Kim, S, Lawrenczyk, A, Porcelli, SA, et al. (2013). Human CD1d knock-in mouse model demonstrates potent antitumor potential of human CD1d-restricted invariant natural killer T cells. *Proc Natl Acad Sci U S A* 110(8), 2963-2968. doi: 10.1073/pnas.1300200110.

289. Zhou, L, Adrianto, I, Wang, J, Wu, X, Datta, I, and Mi, QS (2020). Single-Cell RNA-Seq Analysis Uncovers Distinct Functional Human NKT Cell Sub-Populations in Peripheral Blood. *Front Cell Dev Biol* 8**,** 384. doi: 10.3389/fcell.2020.00384.
290. Li, L, Han, J, Wang, Z, Liu, J, Wei, J, Xiong, S, et al. (2014). Mass spectrometry methodology in lipid analysis. *Int J Mol Sci* 15(6)**,** 10492-10507. doi: 10.3390/ijms150610492.

Appendix

List of Publications

1. **Genardi S**, Visvabharathy L, Cao L, Morgun E, Cui Y, Qi C, Chen Y-H, Gapin L, Berdyshev E, Wang CR. Type II natural killer T cells contribute to protection in systemic methicillin-resistant *Staphylococcus aureus* infection. Front Immunol (2020) 11: 1-16.
2. Visvabharathy L, **Genardi S**, Cao L, He Y, Alonzo F, Berdyshev E, Wang CR. Group 1 CD1-restricted T cells contribute to control of systemic *Staphylococcus aureus* infection. PLOS Pathogens (2020) 16; (4): e1008443.
3. Zhang Y, Wang Y, Gao B, Sun Y, Cao L, **Genardi S**, Wang CR, Zhaolin Sun HL, Yang Y, Fang D. USP22 controls iNKT immunity through MED1 suppression of histone H2A monoubiquitination. JEM (2020) 217; (5): 1-14.
4. Bagchi S, **Genardi S**, Wang CR. Linking CD1-restricted T cells with autoimmunity and dyslipidemia: lipid levels matter. Front Immunol (2018) 9; (1616): 1-12.